MERCURY STABLE ISOTOPE GEOCHEMISTRY AS A TOOL FOR TRACING SOURCES AND CHEMICAL TRANSFORMATIONS IN THE ENVIRONMENT

BY

GIDEON BARTOV

DISSERTATION

Submitted in partial fulfillment of the requirements
for the degree of Doctor of Philosophy in Geology
in the Graduate College of the
University of Illinois at Urbana-Champaign, 2014

Urbana, Illinois

Doctoral Committee:

Professor Thomas M. Johnson, Chair and Director of Research
Professor Craig C. Lundstrom
Associate Professor Timothy J. Strathmann
Research Associate Professor Robert A. Sanford

ABSTRACT

Mercury (Hg) is a redox-active, global contaminant. Hg has two stable oxidation states in the environment, Hg(0) and Hg(II). Hg(0) is significantly less soluble than Hg(II) and is less reactive. Hg(II) is very soluble and highly reactive, being able to form methylmercury, a potent neurotoxin. Hg is a health concern due to its neurological effects, ability to cross the blood-brain barrier and placental barrier, and its tendency to be biomagnified. Anthropogenic inputs of Hg into the environment are dominantly due to coal burning and artisanal gold and silver mining.

Hg stable isotope ratios have been developed since the early 2000s in order to improve understanding of Hg cycling in the environment. The three studies reported in this dissertation aimed to develop Hg isotope ratios as tools for apportioning contamination sources, identifying Hg chemical transformations in contaminated environments, and understanding interactions between dissolved Hg(0) and Hg(II).

In the first study, Hg isotopes were used to apportion different Hg sources into Emory and Clinch Rivers in Tennessee, USA. Following a coal ash spill into the Emory River, elevated Hg concentrations were detected; however, known Hg contamination from another source enters the Clinch River from upstream of the spill. Hg isotope ratios were used to apportion the Hg inputs into the Emory and Clinch Rivers. The spilled coal ash samples have very negative isotopic values (δ^{202}Hg = −1.78±0.35‰), whereas the nominally uncontaminated sediments from Emory River Mile 12 had moderately negative δ^{202}Hg values (−1.17±0.35‰). The Clinch River sediments, contaminated by a different source, had near-zero values (δ^{202}Hg = −0.23±0.16‰). A fourth possible Hg source was an old paper mill on the Emory River (δ^{202}Hg = −0.47±0.04‰). The Hg isotope ratios in the sediments indicate the Emory River was affected by the coal ash and paper mill, but not affected by Clinch River sediments. The Clinch River sediments downstream of the coal ash spill were affected by the ash, but to varying degrees across its sampling sites.

The second study attempted to use Hg isotopes in order to detect and quantify natural chemical transformations of Hg in a contaminated creek. The East Fork of Poplar Creek (EFPC) is a contaminated creek that runs through the U.S. Dept. of Energy Y-12 plant in Oak Ridge, Tennessee, USA. The Y-12 plant historically used large amounts of Hg, some of which was released into the creek and the surrounding floodplain. The Hg being released from the Y-12 complex is not highly fractionated isotopically (δ^{202}Hg = 0.15±0.10‰), and is similar to a strongly contaminated sediment layer known as the "black layer" (Hg concentrations = 2380 ppm, δ^{202}Hg = −0.15±0.08‰). Sediments from reference sites chosen to represent the regional background for the EFPC exhibited very negative values (δ^{202}Hg = −6.90±0.43‰). The isotope values measured in water samples collected from the EFPC showed a slight positive trend with increasing distance downstream. However, the water samples indicated a lack of strong chemical transformations. Hg isotope measurements in fish samples from the EFPC revealed minor (up to 10%) photochemical Hg(II) reduction taking place in the EFPC waters, indicated by mass independent fractionation recorded in the odd Hg isotopes present in the fish tissue.

In the third study, laboratory experiments were conducted in order to better understand the interaction between dissolved Hg(0) and Hg(II). Hg(0) and Hg(II) species are expected to be in contact in any environment in which Hg is getting actively chemically transformed. However, no studies have looked into the isotopic exchange interaction between these two dissolved species. The results of the isotopic exchange experiments show that Hg(0) and Hg(II) have the ability to exchange isotopes very quickly. This process, will overprint previous kinetic fractionation the Hg experience, and drive the Hg species towards isotopic equilibrium. This will limit our ability to identify chemical transformations of Hg in environmental samples unless they had clear photochemical induced mass independent fractionation.

To my parents, I love you

ACKNOWLEDGMENTS

I am forever grateful for my adviser, Dr. Thomas M. Johnson, for his mentorship and patience. Thank you for challenging me, and allowing me to make mistakes and grow as a scientist and as a person. I also extend my sincerest thanks to my doctoral committee members. I would like to thank Dr. Craig Lundstrom for all his help in the lab and wonderful insight into the isotope world. I thank Dr. Rob Sanford for the use of his equipment and his constant support throughout my graduate studies. I also extend my deep gratitude to Dr. Timm Strathmann for his sharp questions and suggestions regarding my projects.

I would like to thank the geology support staff: Marilyn Whalen, Lana Holben, Shelley Campbell, Lori Baker, Jennifer Drennan, and Scott Morris; who made sure everything went smoothly every time I needed help, and were always good for a laugh. I would also like to thank the rest of the geology faculty for their mentoring and support.

I would also like to thank my fellow graduate students, both past and present: Stephanie Mager, Deep Sen, Brian Farrell, Jessica Colberg, Marissa Kelly, and Stephen Picek for getting me out of the office and just being my friends when I needed them to.

My fellow isotope lab group peers (both past and present): Amanda Raddatz, Charles Bopp, Val Finlayson, Anirban Basu, Xiangli Wang, Norbert Gajos, Ted Grimm, Elizabeth Armstrong, Alyssa Shiel, Nick Huggett, Kelsey Kehoe, and Katelyn Zatwarnicki for their help and support. Thank you for all the great times outside the office.

I thank my friends—Seth Kelter, Bryan Mendes, Liz Pritchard, Frances Rickard, Max Schoenoff, Will Schoenoff, Charles and Dannette Tucker—for always being so accommodating and willing to help at a moment's notice. Thank you for all the intellectually challenging debates, and the less intellectual laughs.

Yoni Zilberman, my friend since childhood, deserves a special mention in these acknowledgments. Your friendship and constant support has made my life so much more colorful and amazing.

Finally, I would like to thank my number one fans, my family. To my siblings—Daniel, Tamar, Anat, and Yael—thank you for your unwavering belief in me and your constant encouragement. Last but not least, I would like to thank my heroes, my parents, Sergio and Judith, for being there for me through it all, and for loving me unconditionally.

TABLE OF CONTENTS

CHAPTER 1

Introduction

GENERAL BACKGROUND

General geochemistry of Hg. Mercury (Hg) is a transition metal occurring in group 6 of the periodic table. Hg is a rare element in the earth, comprising, on average, 0.02 ppm in the crust (Ehmann and Lovering, 1967). In ore deposits, it is generally found in its HgS form (cinnabar). Hg is naturally introduced into the environment via outgassing from volcanoes, biomass, and the oceans (Driscoll et al., 2013). Under surface conditions, Hg is present in two major valences; Hg(0) and Hg(II). Hg(0) is a metallic liquid that is sparingly soluble in water, and somewhat volatile. It is less toxic than Hg(II). Hg(II), by comparison, is highly soluble, highly reactive, and strongly interactive with multiple ligands and solid surfaces (Morel et al., 1998; Wang et al., 2004). Hg(II) can also be chemically transformed into the most toxic form of Hg, methylmercury (MeHg), a potent neurotoxin. MeHg has the ability to bioaccumulate in aquatic systems (U.S. Environmental Protection Agency, 1997; Hsu-Kim et al., 2013) (Figure 1.1).

Hg is a globally circulating contaminant (U.S. Environmental Protection Agency, 1997; U.S. Environmental Protection Agency, 2006). In the U.S. alone, Hg accounts for over 4700 impaired water bodies (U.S. Environmental Protection Agency, 2014). Mercury enters the environment through natural geogenic sources such as degassing from volcanoes, weathering of mineral deposits and biomass burning (Wang et al., 2004; Streets et al., 2009), and anthropogenic sources such as coal burning, gold mining, and chlorine production (U.S. Environmental Protection

Agency, 1997; Streets et al., 2011). Due to anthropogenic inputs, the total influx of Hg into the environment has doubled (Yin et al., 2010).

Hg contamination is of major environmental concern due to its high toxicity. Elevated levels of Hg have been shown to adversely affect the reproductive success and thyroidal hormone levels of fish and birds (Wada et al., 2009; Mulder et al., 2012; Wiener, 2013), and the physical and cognitive performance of chicks and rats (Heinz and Hoffman, 2003; Piedrafita et al., 2008; Kenow et al., 2010; Felipo, 2012).

Studies of the effects of elevated Hg levels in humans have also shown adverse effects of cognitive and physiological effects (Clarkson and Magos, 2006; Gallagher and Meliker, 2012; Syversen and Kaur, 2012; Shigeru et al., 2014). Two famous cases of mass Hg poisoning, in Minamata Bay, Japan, and in rural Iraq have been well documented. The Minamata Bay episode occurred from the late 1940s, when a chemical factory released MeHg as a byproduct of its acetaldehyde production into Minamata Bay, exposing 200,000 people to contaminated fish. The Iraq epidemic occurred in rural Iraq in 1971 and 1972; 40,000 people were exposed to Hg-contaminated bread due to seed grain being treated with organic mercury (MeHg and ethylmercury) (Syversen and Kaur, 2012). The U.S. Environmental Protection Agency issues multiple fish advisories in order to reduce the exposure of people, specifically pregnant women, to high levels of Hg (U.S. Environmental Protection Agency, 2011).

In order for us to mitigate these risks associated with Hg, we need to understand how Hg behaves in the environment. That means we need to be able to 1) identify different sources of Hg into the environment, and 2) be able to track redox transformations that greatly affect its mobility and environmental impact. Reduction, oxidation, and methylation are extremely important processes to understand since they control Hg mobility and bioavailability. In order to do that, we are

beginning to use stable isotope geochemistry in order to have a direct measure of Hg sources and chemical transformations in the environment.

Isotope geochemistry of Hg. Mercury has 7 stable isotopes: ^{196}Hg, ^{198}Hg, ^{199}Hg, ^{200}Hg, ^{201}Hg, ^{202}Hg, and ^{204}Hg. Their natural abundances are 0.15%, 10.03%, 16.94%, 23.14%, 13.17%, 29.75%, and 6.82%, respectively. The relative abundances of these ratios are expressed using delta notation (δ) as defined by:

$$\delta^{xxx}\mathrm{Hg} = \left(\frac{R^{xxx}_{sample}}{R^{xxx}_{standard}} - 1\right) * 1000‰ \quad (1)$$

Where R^{xxx}_{sample} and $R^{xxx}_{standard}$ are the ^{xxx}Hg/^{198}Hg ratios of the sample and an interlaboratory standard (NIST SRM 3133), respectively. The ^{196}Hg/^{198}Hg and ^{204}Hg/^{198}Hg ratios are generally not used due to analytical difficulties resulting from the low abundances of ^{196}Hg and ^{204}Hg (Blum and Bergquist, 2007).

Studies have shown that different sources of Hg (cinnabar, coal, plants, igneous rocks, etc.) may contain different and distinct ^{202}Hg/^{198}Hg ratios (Biswas et al., 2008; Foucher et al., 2009; Yin et al., 2010; Gehrke et al., 2011; Lefticariu et al., 2011). However, Hg isotope ratio variations can be induced by mass-dependent isotopic fractionation (MDF) during microbial reduction of Hg(II) to Hg(0) (Kritee et al., 2007; Kritee et al., 2008) and abiotic reduction of Hg(II) to Hg(0) (Bergquist and Blum, 2007), microbial demethylation (Kritee et al., 2009) and abiotic demethylation (Bergquist and Blum, 2007), microbial methylation (Rodríguez-González et al., 2009) and abiotic methylation (Jiménez-Moreno et al., 2013), evaporation (Estrade et al., 2009), and equilibration between aqueous and adsorbed species (Wiederhold et al., 2010; Jiskra et al., 2012). Generally, the lighter isotopes of Hg react faster than the heavy Hg isotopes. This causes the product to be preferentially enriched in the light isotopes of Hg. By convention, ^{202}Hg/^{198}Hg is used as the indicator of MDF, with ^{200}Hg/^{198}Hg used as a redundant quality assurance measurement.

Recently, $^{201}Hg/^{198}Hg$ and $^{199}Hg/^{198}Hg$ ratios have been observed to vary in ways that deviate from the simple pattern followed by MDF. These deviations from the predicted MDF are called mass independent fractionation (MIF). There are three known processes that cause MIF: The first is the magnetic isotopic effect (MIE). This affects only the odd isotopes, and arises from the fact that they have nuclear spins. During photochemical reactions, such as photochemical reduction of Hg(II) and photodegradation of MeHg, radical pairs are formed and exchange of spins between odd nuclei and electrons affects reactions kinetics (Bergquist and Blum, 2007; Perrot et al., 2010; Perrot et al., 2012; Tsui et al., 2012).

The second type of MIF is a subtle effect, related to the fact that most of the observed isotopic fractionation aside from magnetic isotope effects is actually caused by differences in *sizes* of nuclei, rather than masses *per se*. This effect is called the nuclear field shift or nuclear volume effect (NVE), and it arises from the interactions of certain electron orbitals and the nucleus. Interactions between these orbitals and the nucleus depend on the nuclear size, and thus, the various Hg isotopes have slightly different electron orbital energies and bonding energies. Accordingly, the differing nuclear sizes among the Hg isotopes cause them to differ thermodynamically and react slightly differently, causing NVE-driven isotopic fractionation. Because nuclear volume closely correlates with nuclear mass, NVE effects are very similar to MDF. However, the odd Hg isotopes are anomalously small (Angeli, 2004; Angeli and Marinova, 2013). Therefore, processes that cause strong MDF will also induce slight MIF detectable in the odd isotopes because of the slight deviation of NVE from the relationships expected for MDF (Schauble, 2007). Nuclear volume-related MIF has been detected in evaporation (Zheng et al., 2007; Estrade et al., 2009; Ghosh et al., 2013), precipitation (Gratz et al., 2010; Chen et al., 2012), and dark abiotic reduction of Hg(II) (Zheng and Hintelmann, 2010b).

The third, and final, MIF effect is a very rare effect called "self-shielding" (Mead et al., 2013). Under certain circumstances when gaseous Hg is affected by ultraviolet radiation (e.g., inside a fluorescent lamp), it is possible that Hg atoms "shield" other Hg atoms from photochemical reactions by absorbing UV energy. Each isotope has a slightly different UV absorption wavelength, and for each wavelength, the shielding effect is proportional to the abundance of the isotope. Accordingly, reactions are stronger for the poorly shielded rare isotopes, causing a mass independent signature. Large amounts of MIF have been observed in compact fluorescent bulbs (Mead et al., 2013). Notably, δ^{200}Hg deviates from the MDF pattern; to date, self-shielding is the only mechanism proposed for such deviations. Small deviations have been observed in precipitation (Gratz et al., 2010; Chen et al., 2012); and contamination from fluorescent devices has been proposed as one explanation (Mead et al., 2013).

Mass independent fractionation is quantified as the per mil difference between a measured δ-value (δ^{199}Hg, δ^{200}Hg, or δ^{201}Hg) and the predicted values for MDF-only fractionation, based on the measured δ^{202}Hg value. The predicted MDF-only δ^{199}Hg, δ^{200}Hg, and δ^{201}Hg values are determined from the measured δ^{202}Hg using an exponential isotopic fractionation law that closely approximates MDF (Blum and Bergquist, 2007). Therefore, the Δ^{199}Hg, Δ^{200}Hg, and Δ^{201}Hg are calculated as follows:

$$\Delta^{199}\mathrm{Hg} = 1000 * \left(\left[\ln\left(\left(\delta^{199}\mathrm{Hg}/1000\right)+1\right)\right] - 0.252\left[\ln\left(\left(\delta^{202}\mathrm{Hg}/1000\right)+1\right)\right]\right) \quad (2)$$

$$\Delta^{200}\mathrm{Hg} = 1000 * \left(\left[\ln\left(\left(\delta^{200}\mathrm{Hg}/1000\right)+1\right)\right] - 0.502\left[\ln\left(\left(\delta^{202}\mathrm{Hg}/1000\right)+1\right)\right]\right) \quad (3)$$

$$\Delta^{201}\mathrm{Hg} = 1000 * \left(\left[\ln\left(\left(\delta^{201}\mathrm{Hg}/1000\right)+1\right)\right] - 0.752\left[\ln\left(\left(\delta^{202}\mathrm{Hg}/1000\right)+1\right)\right]\right) \quad (4)$$

Table 1.1 shows our current knowledge of Hg isotopic shifts during its chemical transformations. Using this knowledge, we have been able to use Hg isotopes to track Hg in river sediments (Foucher et al., 2009; Gehrke et al., 2011; Liu et al., 2011; Bartov et al., 2013; Foucher et al.,

2013), identify coastal proximity and trophic level effects in aquatic organisms (Senn et al., 2010; Perrot et al., 2012), and identify different Hg sources into artisanal gold miners (Laffont et al., 2009; Laffont et al., 2011).

GOALS OF THE STUDY

The goals of this study are to determine: 1) the ability of Hg isotope data to distinguish different Hg point sources into the environment, 2) the magnitude of isotopic fractionation of industrial Hg used in electrochemical processes, 3) the extent of natural chemical transformation of industrial Hg in a contaminated river system, and 4) the magnitude and rate at which Hg(II) and Hg(0) equilibrate isotopically. I conducted field studies and controlled laboratory experiments in order to achieve each of these goals. In this dissertation, I present the findings of each study in three chapters.

The first chapter addresses the first goal. I use Hg isotopes as tracers of different sources into a contaminated river system. On December 22, 2008, a coal ash dredge cell failed and released approximately 4.1 million cubic meters of ash into the Emory, Clinch, and Tennessee Rivers (Dewan, 2008). Hg isotopes provided a tool for determining the varying contributions of regional background Hg, paper mill Hg, historical Hg from the Y-12 plant complex at the Oak Ridge Reservation, and ash. This is the first study to apportion 4 sources into a river system. The study was published in Environmental Science & Technology in 2013.

The second chapter addresses the second and third goals. I used Hg isotope ratios to elucidate whether electrochemical processes in the Y-12 complex at Oak Ridge imparted detectable isotopic fractionation and whether the Hg present in the contaminated fresh water creek, East Fork Poplar Creek, goes through any detectable natural chemical transformations. The Y-12 plant complex was involved in thermonuclear weapons production, which requires large amounts of Hg. Over the life

of the plant, large amounts of Hg were spilled into the local environment. This study is the first to use Hg isotopes in an attempt to better understand Hg cycling in contaminated freshwater systems. This study is nearly ready for submission to Chemical Geology.

The fourth chapter addresses the last goal. If Hg(II) and Hg(0) are in contact together in the environment, it is possible that they might exchange isotopes with each other and evolve towards isotopic equilibrium. It is very important to know whether this isotopic exchange is fast enough, and large enough to overprint isotopic compositions previously set by kinetic isotope effects. In order to measure both the isotopic exchange rate and the final equilibrium fractionation factor, laboratory experiments were run in anoxic conditions, with Hg(0) and Hg(II) both dissolved, in order to understand the interaction between Hg(0) and Hg(II) in the presence of each other. This manuscript is being prepared for submission to Geochimica et Cosmochimica Acta.

FIGURES AND TABLES

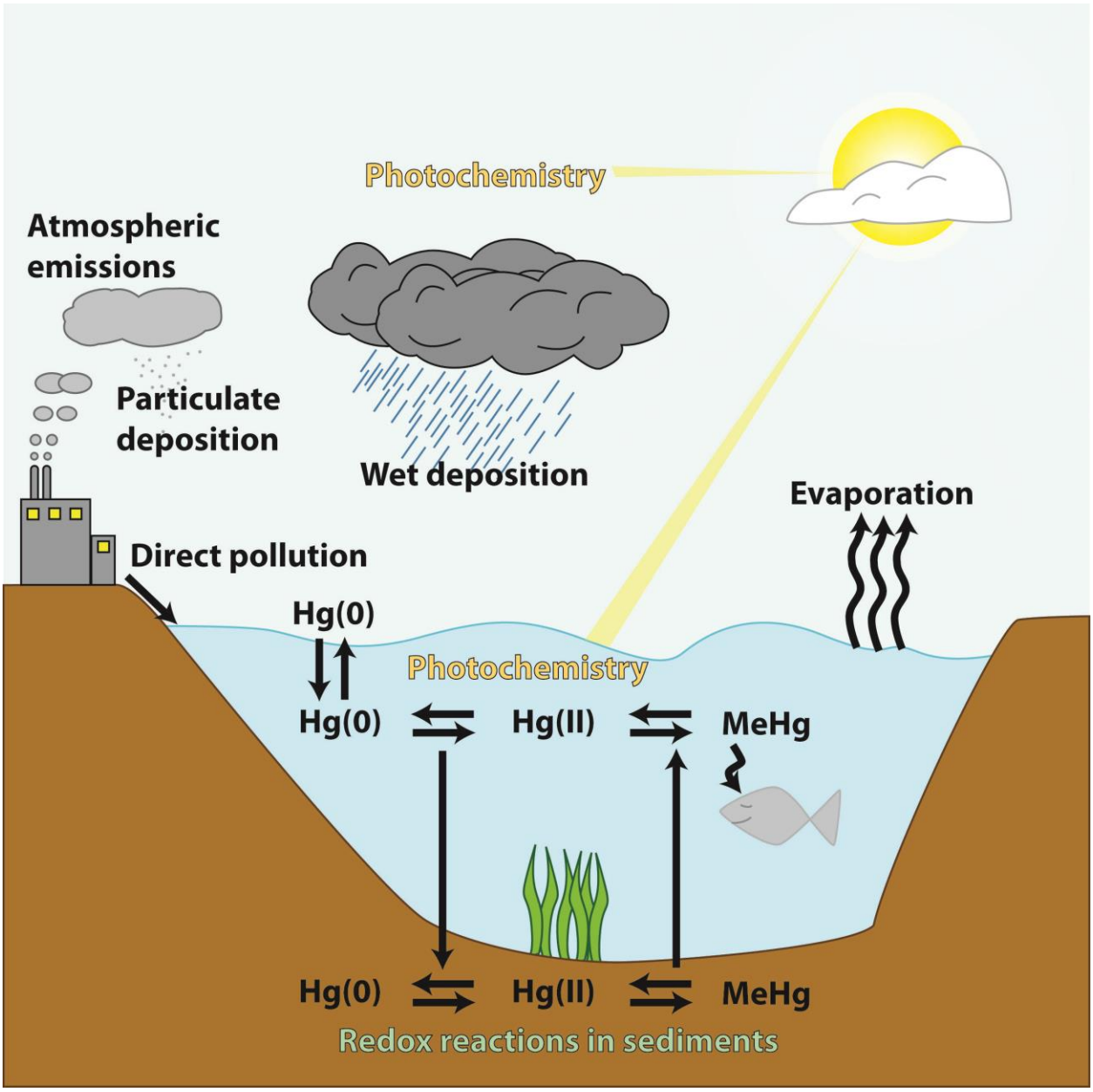

Figure 1.1. Generalized Hg cycle after being emitted to the environment. Not shown are natural emission sources such as volcanoes and biomass.

Table 1.1. Isotopic shifts (reactant relative to product flux) induced by Hg transformations. Units are per mil (‰; parts per thousand)

Transformation	Mechanism	Magnitude of MDF (ordinary kinetic isotope effect)[a]	Magnitude of MIE (magnetic isotope effect)[b]	Reference
Hg(II) to Hg(0)	Photochemical	0.6‰	2.5‰	(Bergquist and Blum, 2007)
Hg(II) to Hg(0)	Photochemical, variable DOC	0.72–1.71‰	0.26–5.63‰	(Zheng and Hintelmann, 2009; 2010a)
Hg(II) to Hg(0)	Abiotic, non-photochemical	1.2–1.8‰	0.0‰	(Bergquist and Blum, 2007; Zheng and Hintelmann, 2010b)
Hg(II) to Hg(0)	Microbial	1.3–2.0‰	0.0‰	(Kritee et al., 2007; 2008)
Methyl-Hg breakdown	Photochemical	1.3‰	1.7‰	(Bergquist and Blum, 2007)
Methyl-Hg breakdown	Microbial	0.4‰	0.0‰	(Kritee et al., 2009)
Methylation	Microbial	2.6‰	0.0‰	(Rodríguez-González et al., 2009)
Methylation	Abiotic	4.0‰	0.0‰	(Jiménez-Moreno et al., 2013)
Hg(0) volatilization from solution	Diffusion	0.5–1.3‰	0.0‰	(Zheng et al., 2007; Ghosh et al., 2013)

[a]Isotopic fractionation driven by mass and nuclear volume difference; variation in the $^{202}Hg/^{198}Hg$ ratio.

[b]Additional isotopic fractionation effecting odd isotopes only; revealed in $^{199}Hg/^{198}Hg$ and $^{201}Hg/^{198}Hg$ ratios.

REFERENCES

Angeli, I., 2004. A consistent set of nuclear rms charge radii: properties of the radius surface R(N,Z). Atomic Data and Nuclear Data Tables, 87.

Angeli, I., Marinova, K.P., 2013. Table of experimental nuclear ground state charge radii: An update. Atomic Data and Nuclear Data Tables, 99.

Bartov, G. et al., 2013. Environmental Impacts of the Tennessee Valley Authority Kingston Coal Ash Spill. 1. Source Apportionment Using Mercury Stable Isotopes. Environmental Science & Technology, 47(4): 2092-2099.

Bergquist, B., Blum, J., 2007. Mass-dependent and -independent fractionation of Hg isotopes by photoreduction in aquatic systems. Science (New York, N.Y.), 318: 417-437.

Biswas, A., Blum, J., Bergquist, B., Keeler, G., Xie, Z., 2008. Natural mercury isotope variation in coal deposits and organic soils. Environmental Science & Technology, 42: 8303-8312.

Blum, J., Bergquist, B., 2007. Reporting of variations in the natural isotopic composition of mercury. Analytical and Bioanalytical Chemistry, 388: 353-362.

Chen, J., Hintelmann, H., Feng, X., Dimock, B., 2012. Unusual fractionation of both odd and even mercury isotopes in precipitation from Peterborough, ON, Canada. Geochimica et Cosmochimica Acta, 90.

Clarkson, T., Magos, L., 2006. The toxicology of mercury and its chemical compounds. Critical reviews in toxicology, 36(8): 609-662.

Dewan, S., 2008. Water supplies tested after Tennessee spill, The New York Times. The New York Times Company, New York, NY.

Driscoll, C.T., Mason, R.P., Chan, H.M., Jacob, D.J., Pirrone, N., 2013. Mercury as a Global Pollutant: Sources, Pathways, and Effects. Environmental science & technology.

Ehmann, W.D., Lovering, J.F., 1967. The abundance of mercury in meteorites and rocks by neutron activation analysis. Geochimica et Cosmochimica Acta.

Estrade, N., Carignan, J., Sonke, J.E., Donard, O.F.X., 2009. Mercury isotope fractionation during liquid–vapor evaporation experiments. Geochimica et Cosmochimica Acta, 73.

Felipo, V., 2012. Methylmercury during development impairs the glutamate-NO-cGMP pathway and learning. Toxicology Letters, 211.

Foucher, D., Hintelmann, H., Al, T.A., MacQuarrie, K.T., 2013. Mercury isotope fractionation in waters and sediments of the Murray Brook mine watershed (New Brunswick, Canada): Tracing mercury contamination and transformation. Chemical Geology, 336(0): 87-95.

Foucher, D., Ogrinc, Hintelmann, H., 2009. Tracing Mercury Contamination from the Idrija Mining Region (Slovenia) to the Gulf of Trieste Using Hg Isotope Ratio Measurements. Environmental Science & Technology, 43.

Gallagher, C., Meliker, J., 2012. Mercury and thyroid autoantibodies in U.S. women, NHANES 2007-2008. Environment international, 40: 39-43.

Gehrke, G.E., Blum, J.D., Marvin-DiPasquale, M., 2011. Sources of mercury to San Francisco Bay surface sediment as revealed by mercury stable isotopes. Geochimica et Cosmochimica Acta, 75.

Ghosh, S., Schauble, E.A., Couloume, G.L., Blum, J.D., Bergquist, B.A., 2013. Estimation of nuclear volume dependent fractionation of mercury isotopes in equilibrium liquid–vapor evaporation experiments. Chemical Geology, 336.

Gratz, L., Keeler, G., Blum, J., Sherman, L., 2010. Isotopic composition and fractionation of mercury in Great Lakes precipitation and ambient air. Environmental science & technology, 44(20): 7764-7770.

Heinz, G., Hoffman, D., 2003. Embryotoxic thresholds of mercury: estimates from individual mallard eggs. Archives of environmental contamination and toxicology, 44(2): 257-264.

Hsu-Kim, H., Kucharzyk, K., Zhang, T., Deshusses, M., 2013. Mechanisms regulating mercury bioavailability for methylating microorganisms in the aquatic environment: a critical review. Environmental science & technology, 47(6): 2441-2456.

Jiménez-Moreno, M., Perrot, V., Vladimir, N.E., Monperrus, M., Amouroux, D., 2013. Chemical kinetic isotope fractionation of mercury during abiotic methylation of Hg(II) by methylcobalamin in aqueous chloride media. Chemical Geology, 336: 26-36.

Jiskra, M., Wiederhold, J., Bourdon, B., Kretzschmar, R., 2012. Solution Speciation Controls Mercury Isotope Fractionation of Hg(II) Sorption to Goethite. Environmental science & technology, 46: 6654-6716.

Kenow, K., Hines, R., Meyer, M., Suarez, S., Gray, B., 2010. Effects of methylmercury exposure on the behavior of captive-reared common loon (*Gavia immer*) chicks. Ecotoxicology (London, England), 19(5): 933-944.

Kritee, K., Barkay, T., Blum, J.D., 2009. Mass dependent stable isotope fractionation of mercury during *mer* mediated microbial degradation of monomethylmercury. Geochimica et Cosmochimica Acta.

Kritee, K., Blum, J., Barkay, T., 2008. Mercury stable isotope fractionation during reduction of Hg(II) by different microbial pathways. Environmental Science & Technology, 42: 9171-9178.

Kritee, K., Blum, J., Johnson, M., Bergquist, B., Barkay, T., 2007. Mercury stable isotope fractionation during reduction of Hg(II) to Hg(0) by mercury resistant microorganisms. Environmental Science & Technology, 41: 1889-1984.

Laffont, L. et al., 2009. Anomalous mercury isotopic compositions of fish and human hair in the Bolivian Amazon. Environmental science & technology, 43(23): 8985-8990.

Laffont, L. et al., 2011. Hg speciation and stable isotope signatures in human hair as a tracer for dietary and occupational exposure to mercury. Environmental science & technology, 45: 9910-9916.

Lefticariu, L., Blum, J., Gleason, J., 2011. Mercury Isotopic Evidence for Multiple Mercury Sources in Coal from the Illinois Basin. Environmental Science & Technology, 45: 1724–1729.

Liu, J., Feng, X., Yin, R., Zhu, W., Li, Z., 2011. Mercury distributions and mercury isotope signatures in sediments of Dongjiang, the Pearl River Delta, China. Chemical Geology, 287.

Mead, C., Lyons, J., Johnson, T., Anbar, A., 2013. Unique Hg stable isotope signatures of compact fluorescent lamp-sourced Hg. Environmental Science & Technology, 47(6): 2542-2547.

Morel, F.M.M., Kraepiel, A.M.L., Amyot, M., 1998. The chemical cycle and bioaccumulation of mercury. Annual Review of Ecology and Systematics.

Mulder, P. et al., 2012. Mercury in Molar Excess of Selenium Interferes with Thyroid Hormone Function in Free-Ranging Freshwater Fish. Environmental science & technology.

Perrot, V. et al., 2010. Tracing sources and bioaccumulation of mercury in fish of Lake Baikal--Angara River using Hg isotopic composition. Environmental Science & Technology, 44: 8030-8037.

Perrot, V. et al., 2012. Higher mass-independent isotope fractionation of methylmercury in the pelagic food web of lake baikal (Russia). Environmental science & technology, 46(11): 5902-5911.

Piedrafita, B., Erceg, S., Cauli, O., Felipo, V., 2008. Developmental exposure to polychlorinated biphenyls or methylmercury, but not to its combination, impairs the glutamate-nitric oxide-cyclic GMP pathway and learning in 3-month-old rats. Neuroscience, 154(4): 1408-1416.

Rodríguez-González, P. et al., 2009. Species-specific stable isotope fractionation of mercury during Hg(II) methylation by an anaerobic bacteria (*Desulfobulbus propionicus*) under dark conditions. Environmental Science & Technology, 43: 9183-9191.

Schauble, E., 2007. Role of nuclear volume in driving equilibrium stable isotope fractionation of mercury, thallium, and other very heavy elements. Geochimica et Cosmochimica Acta, 71: 2170-2189.

Senn, D. et al., 2010. Stable isotope (N, C, Hg) study of methylmercury sources and trophic transfer in the northern gulf of Mexico. Environmental science & technology, 44(5): 1630-1637.

Shigeru, T. et al., 2014. Signs and symptoms of methylmercury contamination in a First Nations community in Northwestern Ontario, Canada. Science of The Total Environment, 468-469.

Streets, D. et al., 2011. All-time releases of mercury to the atmosphere from human activities. Environmental science & technology, 45(24): 10485-10491.

Streets, D., Zhang, Q., Wu, Y., 2009. Projections of global mercury emissions in 2050. Environmental science & technology, 43(8): 2983-2988.

Syversen, T., Kaur, P., 2012. The toxicology of mercury and its compounds. Journal of trace elements in medicine and biology : organ of the Society for Minerals and Trace Elements (GMS), 26(4): 215-226.

Tsui, M. et al., 2012. Sources and transfers of methylmercury in adjacent river and forest food webs. Environmental science & technology, 46(20): 10957-10964.

U.S. Environmental Protection Agency, 1997. Mercury study report to Congress 2. EPA-452/R-97-003, Office of Air Quality and Planning and Standards, Office of Research and Development, U.S. Environmental Protection Agency, Washington, DC.

U.S. Environmental Protection Agency, 2006. EPA's roadmap for mercury. EPA-HQ-OPPT-2005-0013, U.S. Environmental Protection Agency, Washington, DC.

U.S. Environmental Protection Agency, 2011. 2010 Biennial National Listing of Fish Advisories. EPA-820-F-11-014.

U.S. Environmental Protection Agency, 2014. National Summary of Impaired Waters and TMDL Information.

Wada, H., Cristol, D., McNabb, F., Hopkins, W., 2009. Suppressed adrenocortical responses and thyroid hormone levels in birds near a mercury-contaminated river. Environmental science & technology, 43(15): 6031-6038.

Wang, Q., Kim, D., Dionysiou, D., Sorial, G., Timberlake, D., 2004. Sources and remediation for mercury contamination in aquatic systems--a literature review. Environmental Pollution (Barking, Essex : 1987), 131: 323-359.

Wiederhold, J.G. et al., 2010. Equilibrium mercury isotope fractionation between dissolved Hg (II) species and thiol-bound Hg. Environmental Science & Technology, 44: 4191-4197.

Wiener, J., 2013. Mercury exposed: advances in environmental analysis and ecotoxicology of a highly toxic metal. Environmental toxicology and chemistry / SETAC, 32(10): 2175-2178.

Yin, R., Feng, X., Shi, W., 2010. Application of the stable-isotope system to the study of sources and fate of Hg in the environment: A review. Applied Geochemistry, 25.

Zheng, W., Foucher, D., Hintelmann, H., 2007. Mercury isotope fractionation during volatilization of Hg (0) from solution into the gas phase. Journal of Analytical Atomic Spectrometry, 22(9): 1097-1104.

Zheng, W., Hintelmann, H., 2009. Mercury isotope fractionation during photoreduction in natural water is controlled by its Hg/DOC ratio. Geochimica et Cosmochimica Acta, 73.

Zheng, W., Hintelmann, H., 2010a. Isotope fractionation of mercury during its photochemical reduction by low-molecular-weight organic compounds. The journal of physical chemistry. A, 114(12): 4246-4253.

Zheng, W., Hintelmann, H., 2010b. Nuclear field shift effect in isotope fractionation of mercury during abiotic reduction in the absence of light. The journal of physical chemistry. A, 114(12): 4238-4245.

CHAPTER 2

Environmental impacts of the Tennessee Valley Authority Kingston coal ash spill. 1. Source apportionment using mercury stable isotopes

Gideon Bartov[¥], Amrika Deonarine[‡1], Thomas M. Johnson[¥], Laura Ruhl[+], Avner Vengosh[+], and Heileen Hsu-Kim[‡]*

[¥] Department of Geology, 208 Natural History Building, University of Illinois at Urbana-Champaign, Urbana, Illinois 61801.

[‡] Department of Civil and Environmental Engineering, 121 Hudson Hall, Box 90287, Duke University, Durham, North Carolina 27708.

[+] Division of Earth and Ocean Sciences, Nicholas School of the Environment, 205 Old Chemistry Building, Box 90227, Duke University, Durham, North Carolina 27708

[1] Current affiliation: U.S. Geological Survey, Reston, VA

This chapter had been previously published in Environmental Science & Technology. Supporting information for this article is provided in Appendix A.

ABSTRACT

Mercury stable isotope abundances were used to trace transport of Hg-impacted river sediment near a coal ash spill at Harriman, Tennessee, USA. δ^{202}Hg values for Kingston coal ash released into the Emory River in 2008 are significantly negative (−1.78±0.35‰), whereas sediments of the Clinch River, into which the Emory River flows, are contaminated by an additional Hg source (potentially from Y-12 complex near Oak Ridge, Tennessee) with near-zero values (−0.23±0.16‰). Nominally uncontaminated Emory River sediments (12 miles upstream from the confluence with the Clinch) have intermediate values (−1.17±0.13‰) and contain lower Hg concentrations. Emory River mile 10 sediments, possibly impacted by an old paper mill (δ^{202}Hg values of −0.47±0.04‰). A mixing model, using δ^{202}Hg values and Hg concentrations, yielded estimates of the relative contributions of coal ash, Clinch River, and Emory River sediments for a suite of 71 sediment samples taken over a 30 month time period from 13 locations. Emory River samples, with two exceptions, are unaffected by Clinch River sediment, despite occasional upstream flow from the Clinch River. As expected, Clinch River sediment below its confluence with the Emory River are affected by Kingston coal ash; however, the relative contribution of the coal ash varies among sampling sites.

INTRODUCTION

Mercury contamination. Mercury (Hg) is a widespread contaminant (U.S. Environmental Protection Agency, 1997; U.S. Environmental Protection Agency, 2006). Industrialization has increased total Hg input into the environment by as much as a factor of two (Yin et al., 2010). The main anthropogenic inputs of Hg into the environment are coal burning and losses from gold mining operations (U.S. Environmental Protection Agency, 1997), though many other sources and pathways have been reported. For example, point sources of Hg contamination have been reported

from the Idrija region in Slovenia to the Brazilian Amazon (Fréry et al., 2001; Harada et al., 2001; Foucher et al., 2009; Feng et al., 2010; Perrot et al., 2010; Estrade et al., 2011; Gehrke et al., 2011; Liu et al., 2011; Sherman et al., 2012). Studies have also shown that Hg cycles through the atmosphere and can get deposited far from point sources (Wang et al., 2004; Fitzgerald et al., 2005; Yang et al., 2010a; Yang et al., 2010b) and accumulate in biota (St Louis et al., 2011; Guigueno et al., 2012; Nicolardi et al., 2012).

The chemistry of Hg plays a major role in evaluation of Hg mobility, bioavailability, and biological impacts. The dominant inorganic valences of Hg in nature are Hg(0) and Hg(II); Hg(0) is sparingly soluble and generally a less reactive volatile species, while Hg(II) is soluble but highly reactive, forming many aqueous complexes with various ligands and surface complexes on solids, and forming solids like HgS and HgSe (Yudovich and Ketris, 2005). The ability of Hg(II) to adsorb onto sediments allows it to remain sequestered in solid materials for long periods of time. Hg also has various organic forms, the most important of which is methylmercury, a deadly neurotoxin that bioaccumulates in biota and causes most of Hg's biological impact.

Coal-fired power plants release Hg into the environment both through smokestack emissions and releases of coal ash, which contains elevated levels of Hg and other contaminants (U.S. Environmental Protection Agency, 2009). According to the EPA, there are at least 240 coal ash storage facilities containing various coal combustion residuals (fly-ash, bottom ash, coal slag, and flue gas desulfurization residue) across the United States. As of August 2009, 30 facilities and 49 surface impoundments are considered to have a high hazard potential, which is defined as a high probability for significant economic and human life loss if an impoundment failure were to occur (U.S. Environmental Protection Agency, 2009).

On December 22, 2008, a coal ash dredge cell failed at the Tennessee Valley Authority (TVA) Kingston coal-fired power plant at Harriman, TN, releasing approximately 4.1 million cubic meters of coal ash into the Emory and Clinch Rivers in Tennessee. Measurements of Hg in the sediment, ash, and fish samples taken after the spill have shown that Hg is above its toxicological screening threshold for benthic organisms (0.18 mg/kg dry weight) and over the human health screening values in the fish (0.0406 mg/kg) (Tennessee Valley Authority, 2009b; Tennessee Valley Authority, 2011a). These high concentrations of Hg are of concern because Hg bioaccumulates and poses a risk to humans and wildlife.

Mercury geochemistry. Hg stable isotope measurements have grown as a tool for examining sources and chemical transformations of Hg in the environment (Biswas et al., 2008; Foucher et al., 2009; Stetson et al., 2009; Feng et al., 2010; Perrot et al., 2010; Estrade et al., 2011; Gehrke et al., 2011; Lefticariu et al., 2011; Liu et al., 2011; Day et al., 2012; Sherman et al., 2012). Hg has 7 stable isotopes with nominal masses 196, 198, 199, 200, 201, 202, and 204 amu. Variations in their relative abundance are measured as variations in the $^{199}Hg/^{198}Hg$, $^{200}Hg/^{198}Hg$, $^{201}Hg/^{198}Hg$, and $^{202}Hg/^{198}Hg$ isotopes ratios (the other two ratios are usually not used because of analytical issues (Blum and Bergquist, 2007). These variations are reported in permil (‰) deviations from NIST Standard Reference Material 3133. For example, $^{202}Hg/^{198}Hg$ ratio variations are expressed using

$$\delta^{xxx}Hg = \left(\frac{R^{xxx}_{sample}}{R^{xxx}_{standard}} - 1\right) * 1000‰ \quad (1)$$

Where R^{xxx}_{sample} and $R^{xxx}_{standard}$ are the $^{xxx}Hg/^{198}Hg$ ratios of the sample and an interlaboratory standard (NIST SRM 3133), respectively.

Hg isotope ratio variations can be induced by mass-dependent isotopic fractionation (MDF). During reduction of Hg(II) to Hg(0) (microbial (Kritee et al., 2007; Kritee et al., 2008) and abiotic

(Bergquist and Blum, 2007)), lighter isotopes react at a slightly greater rate, causing enrichment of lighter isotopes in reaction products and enrichment of heavier isotopes in the reactant pool. Other MDF reactions include methylation (Rodríguez-González et al., 2009), evaporation (Estrade et al., 2009), and equilibration between aqueous and adsorbed species (Wiederhold et al., 2010; Jiskra et al., 2012). Blum and Bergquist (2007) give a good summary of how to report isotope ratios. Mass-dependent isotopic variations are determined by measuring δ^{202}Hg, with δ^{200}Hg serving to confirm results. Recent studies have found δ^{200}Hg can vary from the predicted mass dependent calculations (Gratz et al., 2010; Chen et al., 2012); however, no studies exist showing δ^{200}Hg varying from the predicted mass dependent calculations in sediments or ash.

The odd isotopes of Hg (^{199}Hg and ^{201}Hg) have been shown to vary by other processes in addition to those causing mass-dependent fractionation. These phenomena are known as mass independent fractionation (MIF). The dominant cause of MIF appears to be photochemical transformations (Bergquist and Blum, 2007), though other, smaller MIF effects have been reported (Estrade et al., 2009; Zheng and Hintelmann, 2010). MIF is reported as the per mil deviation of the measured $\delta^{199/198}$Hg and $\delta^{201/198}$Hg values from the expected mass-dependent fractionation derived from the measured δ^{202}Hg of the same sample. These are calculated as Δ^{199}Hg and Δ^{201}Hg, respectively (Blum and Bergquist, 2007).

The Hg isotope ratios of various sources of Hg in the environment differ due to MDF and/or MIF (Biswas et al., 2008; Stetson et al., 2009; Gehrke et al., 2011; Lefticariu et al., 2011). These variations provide the potential to determine the source(s) of Hg in systems where multiple sources of contamination exist, or to distinguish contaminant Hg sources from the natural background. Multiple studies have used Hg isotopes in order to trace Hg contamination and sources through natural systems, e.g., studies in the Idrija region in Slovenia (Foucher et al., 2009), Lake Baikal

(Perrot et al., 2010), northern France (Estrade et al., 2011), San Francisco Bay, California (Gehrke et al., 2011), and China (Feng et al., 2010; Liu et al., 2011; Yin et al., 2012b). However, the Hg isotope ratios of the sources are not necessarily immutable "signatures"; tracing of sources can be disrupted by isotopic shifts resulting from chemical reactions.

In this study, we present an extensive Hg isotope data set for river sediments near the Kingston, TN coal ash spill. The river system also contains historical Hg from the Y-12 plant complex at the Oak Ridge Reservation (Tennessee Valley Authority, 2009b; Tennessee Valley Authority, 2011a). The objectives of this study are 1) determine whether the Hg isotopic values of the four different sources (coal ash, Y-12 Hg, paper mill impacted sediments, and natural background) are distinct from each other; and 2) to estimate the relative contributions of these three sources and the regional Hg background to the sediments' Hg contents at various locations. In order to achieve this, we determined the isotopic compositions of the various Hg sources into the system and developed evidence that these compositions are not greatly changing over time. The resulting Hg sourcing information is used in a companion paper (Deonarine et al., 2013) to determine if the availability of Hg for methylation is greater for the recent coal ash-derived Hg, relative to older Hg in the system, or whether the other elements found in the coal ash act as nutrients that increase methylation rates for existing Hg in the sediments.

METHODS AND MATERIALS

Field setting and sampling procedures. The Kingston coal fired power plant is located at the confluence of the Emory and Clinch Rivers in Tennessee, USA (Figure 2.1). Water flow is to the south and west on the Emory and Clinch Rivers, respectively. Under normal conditions, the Emory River discharge is exceeded by that of the Clinch (Tennessee Valley Authority, 2010a). During normal plant operations, cooling water is drawn from the Emory River, which can sometimes cause

the Clinch River water to flow upstream in the Emory for ~2 miles to the plant intake (Tennessee Valley Authority, 2010b).

Ash from the 2008 spill was found mainly between Emory River Mile 1 (ERM 1; one mile upstream from its confluence with the Clinch River) to ERM 5.5, with a one mile stretch containing an ash layer up to 30 feet thick. Ash traveled upstream to ERM 6, up the Clinch River to Clinch River Mile (CRM) 5, and was found as far downstream as Tennessee River Mile 563 (Tennessee Valley Authority, 2009a; Tennessee Valley Authority, 2011a). Dredging in the Emory River from 2009 to 2010 removed 65% of the 4.1 million cubic meters of spilled ash (Zeller, 2011). Ash samples were collected from the dredge cell from early to late 2009. A cove across from the dredge cell (but on the same side of the river) was completely filled with ash during the spill. Sediments from this cove were sampled in late 2009.

Three river locations were chosen to provide sediments uncontaminated by the ash spill. Emory River Mile 12 (Figure 2.1) samples have relatively low Hg concentrations and were unaffected by the ash spill because they are located several miles upstream. There are no known point sources of Hg upstream of ERM 12, and we thus assume the observed Hg is some combination of atmospheric deposition, mostly derived from coal-fired power plants, and natural Hg derived from rock weathering. Thus, analyses of the six ERM 12 results serve as a proxy for the regional Hg background. Emory River Mile 10 is located one mile downstream of a former paper mill with known presence of Hg in its surrounding sediments (Tennessee Department of Environment and Conservation, 2011). ERM 10 is, therefore, assumed to represent a mixture of background sediments and sediments affected by the paper mill Hg. Clinch River sediments are known to be contaminated by Hg released from activities at the U.S. Dept. of Energy Y-12 plant near Oak-Ridge, TN decades ago (Tennessee Valley Authority, 2009b; Brooks and Southworth, 2011;

Tennessee Valley Authority, 2011a). Our analyses of sediment from Clinch River Mile 5.5, which was not affected by the 2008 ash spill, were used to represent the composition of Clinch River sediments prior to any mixing with the ash.

Sediments from the river bottom were collected using a Wildco box corer (up to 25cm depth) (Ruhl et al., 2010). Samples were generally obtained close to the river channel midpoints. Samples were homogenized by hand and kept at 4°C (for about 1-3 days) until transport to the lab, where they were frozen upon arrival (-20°C). Samples were kept frozen until use.

Analytical methods. Samples for Hg isotope measurements were thawed and up to 0.1g (wet weight) of sediments were weighed into 30ml glass tubes. The sediment samples were then digested overnight in 4ml aqua regia (3:1 HCl:HNO_3) at 95°C. Sediments containing Hg concentrations $\leq$ 2 mg kg^{-1} were pre-concentrated after digestion using an anion exchange step adapted from Malinovsky et al. (2008). The anion exchange resin (0.4ml bed volume) was washed with 5% (m/v) thiourea, conditioned with 2M HCl, and samples were eluted using 4ml 5% thiourea solution. Fresh thiourea solutions were made immediately prior to each ion exchange session. Final Hg concentrations of sample solutions used for mass spectrometry were 1–3 ng g^{-1}.

Mass spectrometry followed the methods of Mead and Johnson (2010). Samples were spiked with a calibrated double isotope tracer solution containing ^{196}Hg and ^{204}Hg and allowed to chemically equilibrate overnight. Spiking was done after digestion and prior to any further chemical processing. Isotopic compositions were measured on a Nu Plasma HR multi-collector inductively coupled plasma mass spectrometer at the University of Illinois at Urbana-Champaign. Hg was introduced into the instrument via a cold-vapor generation device using a $SnCl_2$ reductant. For samples prepared using ion exchange, the reductant solution was made strongly basic; this weakens thiourea-Hg complexes and enables the $SnCl_2$ to reduce the Hg(II). Sample uptake rate

was 0.5 ml min^{-1}. The instrument's mass-bias was corrected using the measured $^{204}Hg/^{196}Hg$ ratio and a previously described double-spike data reduction routine[37]. Isobaric interferences were monitored by measuring $^{194}Pt^{+}$, $^{203}Tl^{+}$, $^{206}Pb^{+}$, and $^{196}HgH^{+}$; and corrected for the HgH^{+} interferences.

The long term precision of the isotopic method was evaluated by preparing and analyzing 12 samples multiple times, on different days, for a total of 27 replicate samples. The root mean square of the $\delta^{202}Hg$ difference is 0.06‰; we thus estimate our 95% confidence precision to be ±0.12‰. The 95% confidence precision for $\Delta^{199}Hg$ and $\Delta^{201}Hg$ are ±0.07‰ and ±0.06‰, respectively. Blanks were also prepared with each digestion batch and averaged 95 pg Hg, whereas the minimum Hg mass per sample was 4 ng. Concentrations of Hg in the sediments were calculated using isotope dilution; the double-spike concentration is calibrated against a concentration standard (TCLP Hg standard, Ricca Chemical Co.).

Mixing Calculations. Standard equations were used to calculate the isotope ratios and concentrations of sediment mixtures derived from variable proportions of upstream Clinch River sediment, background Emory River sediment, and fly ash. Compositions of these three components, or "end-members" were represented by average compositions of multiple analyses of CRM 5.5, ERM 12, ERM 10 and fly ash, respectively. The series of equations required is:

$$\delta^{202}Hg_{Mixture} = \frac{f_{Ash}\delta_{Ash}C_{Ash}+f_{ERM10}\delta_{ERM10}C_{ERM10}+f_{ERM12/CRM5.5}\delta_{ERM12/CRM5.5}C_{ERM12/CRM5.5}}{f_{Ash}C_{Ash}+f_{ERM10}C_{ERM10}+f_{ERM12/CRM5.5}C_{ERM12/CRM5.5}} \quad (2)$$

$$C_{Mixture} = f_{Ash}C_{Ash} + f_{ERM10}C_{ERM10} + f_{ERM12/CRM5.5}C_{ERM12/CRM5.5} \quad (3)$$

$$1 = f_{Ash} + f_{ERM10} + f_{ERM12/CRM5.5} \quad (4)$$

Where ERM 12 is used to calculate the mixture for the Emory River samples (with the exception of 2 samples), and CRM 5.5 is used in the Clinch River samples' mixing model. Variable f

represents the mass fraction of each end-member present in the mixture, and δ and C give the measured δ^{202}Hg value and concentration of the mixture and each end-member. In order to determine the fraction of each end-member in each measured mixture, the equations were rearranged and solved iteratively for the f values as a function of the samples' δ and C values.

RESULTS

Coal-ash and upstream sediments from the Emory and Clinch Rivers. Sediments collected from the upstream Emory River (site ERM 12) yielded the lowest Hg concentrations (0.014–0.033 mg kg^{-1}), about 38 times lower than the Clinch River Mile 5.5 sediments (0.49–1.2 mg kg^{-1}), and the largest variability (~38% RSD). Emory River Mile 10 sediments contained higher concentrations of Hg (0.024–0.043 mg kg^{-1}) and very consistent δ^{202}Hg values (−0.47±0.04‰). In contrast, the four coal-ash samples exhibited higher Hg concentrations (0.099–0.15 mg kg^{-1}) and substantial variability of δ^{202}Hg values, ranging from -1.40‰ to −2.23‰ (Table 2.1, Figure 2.2). The ERM 12 and CRM 5.5 locations were remarkably consistent in δ^{202}Hg (−1.17±0.13‰ and −0.23±0.16‰, respectively) considering they were sampled over 5 (ERM 12) and 11 (CRM 5.5) month periods (Figure 2.2). The Δ^{199}Hg and Δ^{201}Hg also remained consistent over time. The MIF signatures also clustered such that Clinch River samples were distinct from the Emory and Ash samples – which were indistinguishable from each other (Figure 2.3, Table 2.2).

River sediments. Table 2.2 gives mean values of the various river locations aside from those used as end-members for the various Hg sources. Complete analytical results are reported in Tables S1–S3 in supplementary material. Figure 2.2 presents results from individual samples, along with curves delineating calculated mixing models (δ^{202}Hg vs. inverse concentration in supplementary material). Six samples from the cove area plot with the ash samples. This is expected since the cove was completely filled with ash from the spill.

Nearly all Emory River samples are consistent with being mixtures of ash and Emory River sediments, without any Clinch River influence. Two exceptions are one ERM 1 sample and one ERM 2 sample, which plot in the Clinch River mixing field. We also note that some ERM 1 and ERM 2 samples, and one ERM 3 sample, fall within the field defined by the cove and ash samples, indicating the former locations are at times dominated by ash-derived Hg. In contrast, none of the samples from the ERM 4 location, the farthest upstream of the spill-contaminated locations sampled, plot within that field (Figure 2.2).

Data from the Clinch River sediments below the confluence are more complex. Some locations on the Clinch appear to be dominated by Emory River sediments at certain times, but sediments at these locations also vary with time and are sometimes dominated by coal ash. On the other hand, all CRM 2 samples, with the exception of one, plot within the field defined by the upstream CRM 5.5 location, indicating limited Emory influence (Figure 2.2).

Mass independent fractionation of ^{199}Hg and ^{201}Hg provides a second, independent isotopic difference between the Clinch River sediments and those from the upstream Emory River and the Kingston Coal Ash (Figure 2.3). The Clinch River Mile 5.5 sediments have significantly greater Δ^{199}Hg and Δ^{201}Hg than the Emory River upstream samples and the ash. The mean Δ^{199}Hg and Δ^{201}Hg of the Clinch River sediments are −0.06±0.03‰ (2 SD) and −0.07±0.04‰ (2 SD), respectively, while the means for the ERM 12 and coal ash are −0.21±0.09‰ (2 SD) and −0.15±0.09‰ (2 SD), respectively, and ERM 10 are −0.15±0.06 (2 SD) and −0.13±0.02 (2 SD), respectively (SI Tables S1–S3).

DISCUSSION

Evidence for stability of Hg isotope ratios in sediments over time. Previous studies have demonstrated that Hg isotope ratios may differ among Hg sources in sediments of natural systems,

and suggested that the relative contributions of each source can be estimated at various locations by using the Hg isotopic systematics (Foucher et al., 2009; Feng et al., 2010; Perrot et al., 2010; Estrade et al., 2011; Gehrke et al., 2011; Liu et al., 2011; Yin et al., 2012b). However, these studies implicitly assume that the isotopic ratios of sediment from each source do not change over time. If this assumption is incorrect, spatial variations in the ratios may be attributable to modifications of the isotopic ratios of the sediments rather than source differences, thus it would be impossible to calculate the percent contribution of each Hg source with confidence.

A recent study employing sequential extraction out of the Kingston coal ash has shown that most (roughly 93%) of the Hg is strongly complexed in the ash (Matsumoto et al., 2011). Recent studies looking into the interaction of Hg and organic matter have shown that Hg complexes very strongly with dissolved organic matter (DOM) (Haitzer et al., 2003; Dong et al., 2011; Gu et al., 2011). Isotopically, Hg bound by thiol groups is up to 0.63‰ lighter than its dissolved species (Wiederhold et al., 2010); however, Jiskra et al. (2012) found that the sorption process does not impart any isotopic fractionation on Hg when sorbing onto goethite. Given the strong interaction of Hg with DOM and the lack of fractionation associated with sorption processes off of goethite, it is very unlikely that the Hg isotopic composition is changing over time.

Loss of labile Hg from the sediments has the potential to cause a shift in its Hg isotopic ratios (Wiederhold et al., 2010; Gu et al., 2011; Delphine et al., 2012; Yin et al., 2012a). For example, reduction of Hg(II) to Hg(0), and subsequent loss of isotopically light Hg(0) vapor could result in an increase of the remaining δ^{202}Hg. It is important to note that a significant fraction of the Hg must release from the sediments in order to cause a detectable isotopic shift. Chemical alteration of Hg having no contact with the environment – trapped inside a sediment grain, for example – will not affect the isotopic values. Similarly, loss of Hg with an isotopic composition matching

that of the average sediment Hg will not cause a shift in the isotopes. On the other hand, it is very likely there are multiple forms of Hg within the sediments, and that these forms are isotopically distinct. A preferential loss of one of those forms will shift the measured values in the sediments.

The data from the present study provide evidence that sediments in this system have stable Hg isotope ratios that do not change significantly with time. We observe that CRM 5.5 and ERM 12 isotopic values scatter over narrow ranges (0.40‰ and 0.36‰, respectively). The Clinch River is known to have been affected by Hg released from the U.S. Dept. of Energy Y-12 plant near Oak Ridge, TN since the 1950's (Tennessee Valley Authority, 2009b). If the Hg isotope ratios of the Clinch River sediment have been evolving over time, we would expect the chemical reactions or other processes would cause a variable isotopic shift in space. Our data require that either the sediments have no major shift in their original isotopic values, or they have all shifted precisely the same amount. The latter scenario is highly unlikely. Similarly, the nominally uncontaminated background Emory River sediments show little variation and, it is thus, unlikely that major Hg isotope shifts occur as sediments age in the river. Given this evidence, we suggest the Hg does not change isotopically over time in this system, and therefore can treat the measured Hg isotope ratios as semi-permanent "signatures".

Estimates of sediment contributions from the three sources. The relative contributions of the two Hg contaminant sources (Y-12 Hg and TVA ash) to the sediments at various points in the system is of great importance as the region recovers from the spill. Using the data from this study, we are able to estimate the amounts of sediment sourced from the Clinch River, the Emory River, and the coal ash spill, even though the sediments might not have an obvious visual indicator of contamination (i.e. distinctive sediment type). Our ability to distinguish the different contributors

of Hg into the system should be useful in tracking the Hg and efficacy of the remediation efforts (Tennessee Valley Authority, 2011a).

The Hg concentration and isotopic composition of all samples can be successfully modeled as mixtures of the TVA coal ash, upstream Clinch River sediments as represented by CRM 5.5, and Emory River sediment as represented by ERM 12 and ERM 10. We used the mean Hg isotopic and concentration values at these locations (Table 2.1) as "end-members" which then mix to produce the compositions observed in the samples (Table 2.2). The ERM 12, ERM 10, and CRM 5.5 end-members represent sediment unaffected by the coal ash spill and the limited ranges of isotopic values are taken to represent limited inherent variability in those two sources. The wider isotopic range (0.84‰) of the coal ash end-member in the model is expected because TVA imports coal from multiple locations in the United States (Tennessee Valley Authority, 2011b). Previous studies have shown that coal isotopic values may vary between, and within, regions in the United States (Biswas et al., 2008; Lefticariu et al., 2011).

In Figure 2.2, the Hg concentration and δ^{202}Hg values of all possible mixtures of the four chosen end-member sediments define two distorted triangles. The curves forming the sides of each field represent binary mixtures containing two of the four sources. The Emory River sediments plot within the three end-member mixing field delineated by ERM 12 (background), ERM 10 (paper mill), and the coal ash end-members, and do not trend towards the Clinch sediments end-member. Clinch River sediments are more complicated. Clinch River Mile 1 and all but one of the CRM 2 samples plot close to the area of zero contribution of the coal ash end-member, whereas sediments from CRM 4 and CRM 0 appear to have a coal ash component in them. This result is consistent with microscopic analysis of sediment particle characteristics along the Clinch River showing primarily native sediments at Clinch River Mile 2 and a significant coal ash component at CRM 0

(Tennessee Valley Authority, 2009a). This result can be explained by the difference in channel width between CRM 4 and CRM 0, narrowing at CRM 2 and CRM 1 and widening at CRM 4 and 0 (Scott, 2012). The microscopic analysis did not, however, distinguish between the Emory and Clinch sediments, which we were able to do using the resultant Hg isotope data.

The Hg concentration and isotopic composition of each sample, combined with the mixing model (Figure 2.2), can be used to calculate estimates of the relative contributions of the four sediment sources. These estimates carry significant uncertainties because the four end-members have variable compositions that depart from the compositions used to define the model. In order to estimate the uncertainty of the calculations, we used the most extreme values for the calculations and found that the uncertainties for the Emory and Clinch Rivers are about ±14% and ±40%, respectively (discussion in appendix A).

According to the model calculations, Clinch River sediments comprise less than 5% (and only 9% in the most extreme case as discussed above) of sampled sediment at all Emory River locations, while the Kingston coal ash was found far up the Emory River, with substantial contributions up to ERM 4 (Table 2.3). This is consistent with previous observations (Tennessee Valley Authority, 2009a; Tennessee Valley Authority, 2011a).

At a few locations in the Clinch River, about 57% of the sediments are sourced from the TVA power plant spill (Figure 2.2). However, most Clinch River samples (19 of 22) have less than 40% coal ash, according our calculations. Overall, there is no clear pattern that describes the Clinch River results; this is not surprising given the known sediment dynamics (see below).

The Δ^{199}Hg and Δ^{201}Hg data cannot be used to calculate sediment mixing proportions, because of the lack of a significant difference between the Kingston ash and ERM 12, and the small magnitude of the Clinch versus Emory/Ash difference relative to the measurement uncertainty.

However, the separate grouping of the Clinch and Emory/Ash samples supports our conclusion that Clinch River sediments comprise less than 5% of the sediments found at the Emory River locations.

The observed patterns of sediment mixing, and the variability observed, are consistent with known patterns of water flow and observed sediment dynamics. The presence of Clinch River sediment within the Emory River is caused by periodic artificial reversals of flow direction. During normal plant operation water is pumped from the Clinch/Emory confluence and flow up the Emory River approximately 2 miles into the plant intake (Figure 2.1).

Immediately following the spill, most of the ash remained in the Emory River (Tennessee Valley Authority, 2011a), and was observed to transport downstream only in distinct pulses related to flooding events (Tennessee Valley Authority, 2009c; Tennessee Valley Authority, 2011a). The most significant ash transport event occurred in May 2009 (Tennessee Valley Authority, 2009c). Accordingly, we expect spatial and temporal variability of the sediments at each sampling location downstream of the spill site; this is a potential complicating factor in attempting to define patterns of contamination using our data and similar isotopic data in other studies (Baker and Smith, 2011). For example, one sample might be derived from old, pre-spill sediments exposed in recent scour, the next sample at the same nominal location might be dominated by spill material, and another sample might be primarily recently-deposited uncontaminated sediments. This could occur either because the exact sampling location varied by a few meters or because the river's bedforms migrated or changed seasonally. It is important to note that the sediments themselves do not have different δ^{202}Hg values, but the resultant mixture can produce a different isotopic value at each sampling location.

Broader implications. The results of this study demonstrate the ability to use Hg isotopes as tracers of contaminated river sediments affected by a recent spill event. This approach enables us to distinguish between different sources without the need to have visually distinct sediment compositions (i.e. coal ash versus river sediments). Compared to other studies which apportion Hg in systems that only have chronic contamination (Foucher et al., 2009; Feng et al., 2010; Perrot et al., 2010; Estrade et al., 2011; Gehrke et al., 2011; Liu et al., 2011; Sherman et al., 2012), this study shows that Hg may be stable in some sediments to allow for immediate apportionment of sources during a single contamination event superimposed on an old, chronic contamination problem. Our ability to distinguish between sources, and estimate their contribution to the system, is a powerful tool in tracking Hg as active remediation occurs.

Determining the relative contributions of various Hg sources is useful in understanding both the transport of contaminated sediments and the potential for differing biogeochemical properties of Hg coming from those sources. In a companion paper (Deonarine et al., 2013), we use the results of the present study to determine whether Hg sourced from the coal ash is more bioavailable for methylation than the Hg already present in the system, or alternatively whether nutrients derived from the ash are responsible for increased Hg methylation.

ACKNOWLEDGMENT

The authors thank Restoration Services Inc. and Environmental Standards Inc. for their assistance with field sampling and quality oversight, respectively. This work was supported in part by a grant from the Oak Ridge Associated Universities and the Tennessee Valley Authority.

SUPPORTING INFORMATION AVAILABLE

Three tables containing individual sample concentration, isotopic composition, and calculated mixture percents; UM Almadén values; inverse concentration mixing diagram; MIF and mixing

model calculations. This information is available free of charge via the Internet at http://pubs.acs.org/

FIGURES AND TABLES

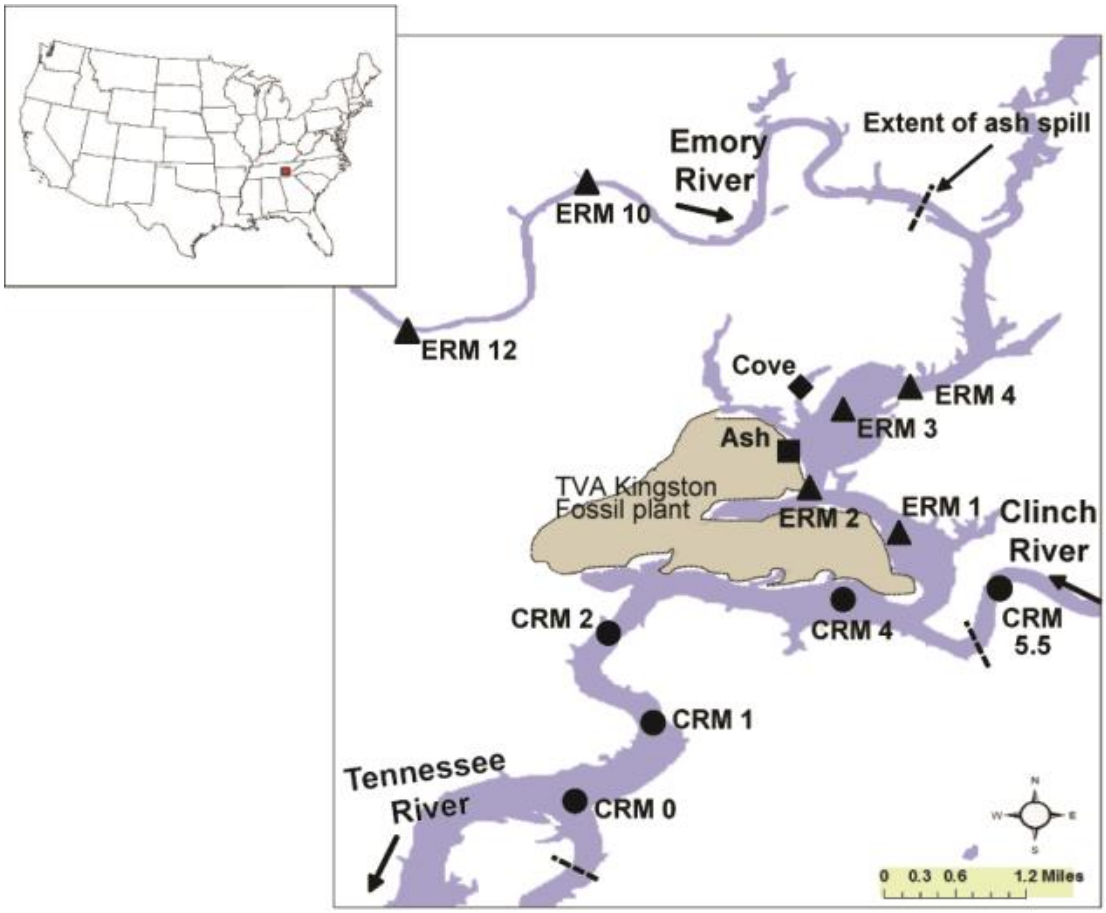

Figure 2.1. Map of Kingston power plant site showing river sampling locations (rivers are in dark blue). Emory River sampling sites are marked using triangles (Δ), Clinch River samples are marked using circles (○), and the cove samples are marked with a diamond (◊). Arrows below river names represent flow directions. Dashed lines indicate extent of ash found immediately after the spill.

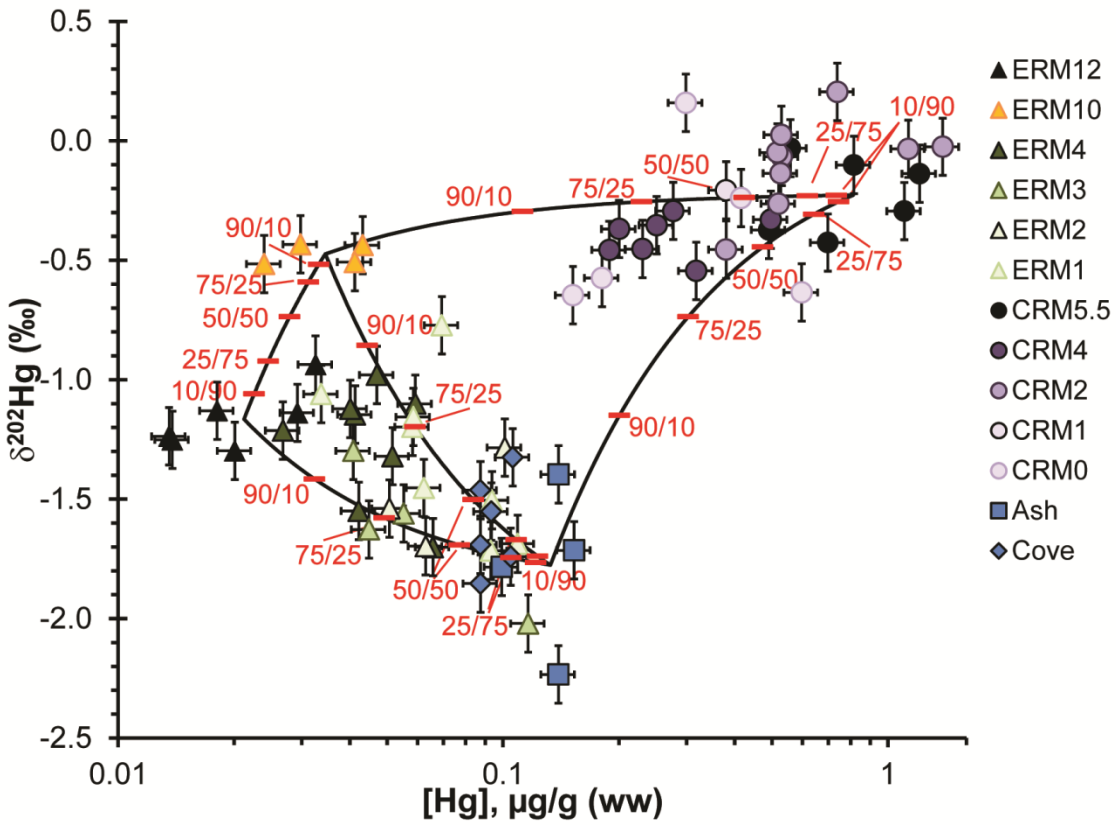

Figure 2.2. δ^{202}Hg values relative to log Hg concentration. Ash samples are blue squares (□), cove samples are blue diamonds (◊), Clinch River sediments are purple circles (○), and Emory River sediments are green and orange triangles (Δ). Lighter colors indicate sites farther downstream. The black lines indicate mixing curves between pair of the end-members, and the red tick marks give mixing proportions at various points along those lines. All Emory River sediments, except one, plot between the Emory River and ash end-members. The Clinch River sediments are more complex and vary with time. Vertical error bars represent 2SD uncertainty, horizontal error bars represent 10% uncertainty.

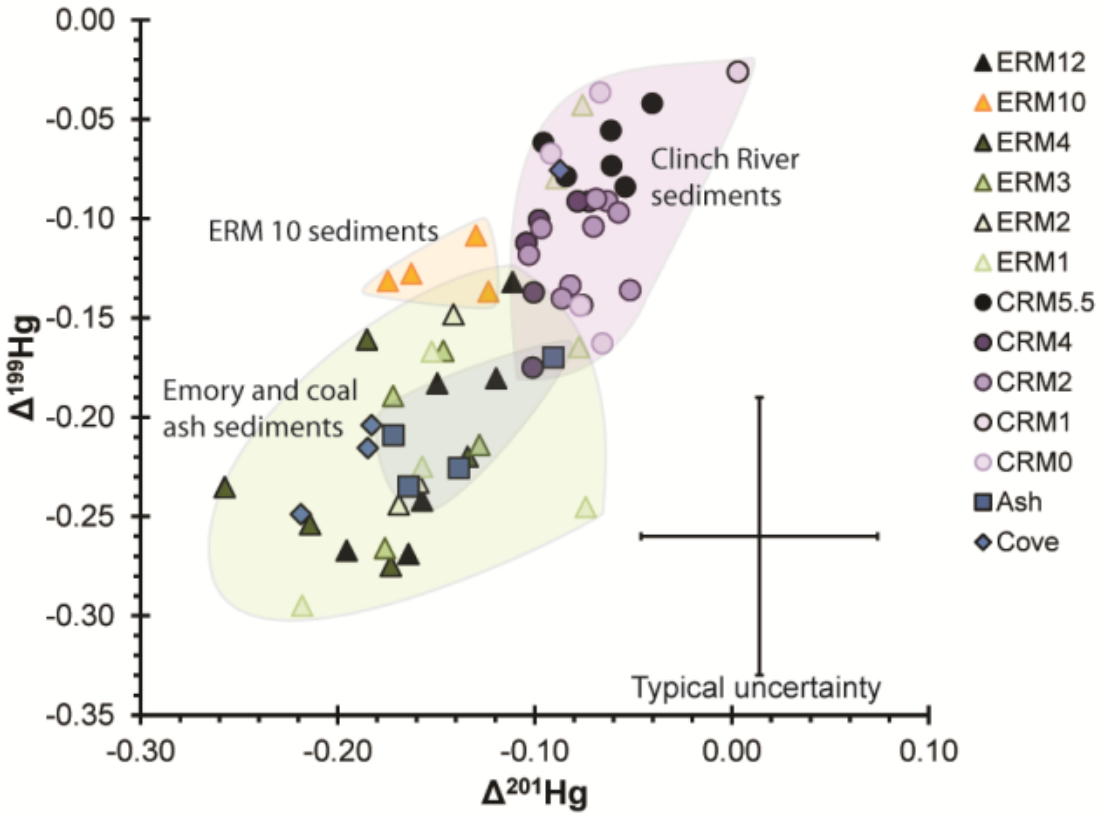

Figure 2.3. Mass independent anomalies Δ^{199}Hg plotted against Δ^{201}Hg. Ash samples are blue squares (□), cove samples are blue diamonds (◊), Clinch River sediments are purple circles (○), and Emory River sediments are green triangles (Δ). Lighter colors indicate sites farther downstream. Clinch River sediments plot in a distinct group from the Kingston ash and Emory River sediments, which are indistinguishable from each other. Error bars represent 2SD uncertainty.

Table 2.1. Mean analyses and standard deviations for the four end-member materials ± 2SD.

Material	Concentration (mg kg^{-1})	$\delta^{202}Hg$	$\Delta^{199}Hg$	$\Delta^{201}Hg$	n
Kingston Fly Ash	0.133 ± 0.023	−1.78 ± 0.35‰	−0.21 ± 0.03‰	−0.14 ± 0.04‰	4
CRM 5.5 Sediment	0.813 ± 0.219	−0.23 ± 0.16‰	−0.07 ± 0.02‰	−0.07 ± 0.02‰	6
ERM 12 Sediment	0.021 ± 0.008	−1.17 ± 0.13‰	−0.21 ± 0.06‰	−0.15 ± 0.03‰	6
ERM 10 Sediment	0.035 ± 0.009	−0.47 ± 0.04‰	−0.13 ± 0.01‰	−0.15 ± 0.02‰	4

Table 2.2. Average concentration, δ^{202}Hg, δ^{200}Hg, Δ^{199}Hg, and Δ^{201}Hg ±SD of river locations.

River location	Concentration (mg kg^{-1})	δ^{202}Hg	δ^{200}Hg	Δ^{199}Hg	Δ^{201}Hg	n
Cove	0.094±0.01	−1.60±0.19‰	−0.83±0.08‰	−0.19±0.08‰	−0.17±0.06‰	6
ERM 4	0.047±0.01	−1.27±0.24‰	−0.670±.17‰	−0.22±0.04‰	−0.15±0.08‰	7
ERM 3	0.064±0.04	−1.63±0.30‰	−0.85±0.13‰	−0.21±0.04‰	−0.16±0.02‰	4
ERM 2	0.072±0.03	−1.51±0.21‰	−0.85±0.22‰	−0.21±0.04‰	−0.16±0.01‰	3
ERM 1	0.072±0.02	−1.32±0.33‰	−0.72±0.18‰	−0.18±0.09‰	−0.12±0.06‰	7
CRM 4	0.28±0.11	−0.40±0.09‰	−0.22±0.06‰	−0.12±0.03‰	−0.09±0.01‰	7
CRM 2	0.66±0.33	−0.10±0.18‰	−0.05±0.09‰	−0.10±0.03‰	−0.07±0.03‰	9
CRM 1[a]	0.38±0.04	−0.21±0.12‰	−0.04±0.13‰	−0.03±0.07‰	0.00±0.06‰	1
CRM 0	0.33±0.18	−0.39±0.35‰	−0.24±0.21‰	−0.10±0.06‰	−0.08±0.01‰	4

[a] Uncertainty listed is 10% for concentration and 2SD external reproducibility for isotopic values

Table 2.3. Percent sediment contribution of each end-member to specific river locations.

River location	% Clinch	% Ash	% ERM 12	% ERM 10	n
ERM 4	0	4–40	0–88	0–82	7
ERM 3	0	14–85	15–79	0–26	4
ERM 2	0–3	26–48	0–67	0–50	3
ERM 1	0–4	6–76	0–56	3–91	7
CRM 4	18–36	6–57	0	16–69	7
CRM 2	39–100	0–41	0	0–31	9
CRM 1	36	0	0	64	1
CRM 0	11–57	0–28	0	0–44	4

Uncertainties are estimated to be 14% and 40% for ERM and CRM samples, respectively. Clinch end-member contribution to ERM samples does not exceed 9% (discussion in supplementary material).

REFERENCES

Baker, T., Smith, J., 2011. The complexity of reservoir benthic habitats: deciphering the effects of the Kingston fly ash release on the benthic macroinvertebrate community, TVA-Kingston Fly Ash Release Environmental Research Symposium, Harriman, Tennessee.

Bergquist, B., Blum, J., 2007. Mass-dependent and -independent fractionation of Hg isotopes by photoreduction in aquatic systems. Science (New York, N.Y.), 318: 417-437.

Biswas, A., Blum, J., Bergquist, B., Keeler, G., Xie, Z., 2008. Natural mercury isotope variation in coal deposits and organic soils. Environmental Science & Technology, 42: 8303-8312.

Blum, J., Bergquist, B., 2007. Reporting of variations in the natural isotopic composition of mercury. Analytical and Bioanalytical Chemistry, 388: 353-362.

Brooks, S., Southworth, G., 2011. History of mercury use and environmental contamination at the Oak Ridge Y-12 Plant. Environmental pollution (Barking, Essex : 1987), 159: 219-247.

Chen, J., Hintelmann, H., Feng, X., Dimock, B., 2012. Unusual fractionation of both odd and even mercury isotopes in precipitation from Peterborough, ON, Canada. Geochimica et Cosmochimica Acta, 90.

Day, R. et al., 2012. Mercury stable isotopes in seabird eggs reflect a gradient from terrestrial geogenic to oceanic mercury reservoirs. Environmental Science & Technology, 46: 5327-5362.

Delphine, F., Holger, H., Tom, A.A., Kerry, T.M., 2012. Mercury isotope fractionation in waters and sediments of the Murray Brook mine watershed (New Brunswick, Canada): Tracing mercury contamination and transformation. Chemical Geology.

Deonarine, A. et al., 2013. Environmental Impacts of the Tennessee Valley Authority Kingston Coal Ash Spill. 2. Effect of Coal Ash on Methylmercury in Historically Contaminated River Sediments. Environmental Science & Technology, 47(4): 2100-2108.

Dong, W., Bian, Y., Liang, L., Gu, B., 2011. Binding constants of mercury and dissolved organic matter determined by a modified ion exchange technique. Environmental science & technology, 45(8): 3576-3583.

Estrade, N., Carignan, J., Donard, O., 2011. Tracing and Quantifying Anthropogenic Mercury Sources in Soils of Northern France Using Isotopic Signatures. Environmental science & technology, 45: 1235–1242.

Estrade, N., Carignan, J., Sonke, J.E., Donard, O.F.X., 2009. Mercury isotope fractionation during liquid–vapor evaporation experiments. Geochimica et Cosmochimica Acta, 73.

Feng, X. et al., 2010. Tracing mercury contamination sources in sediments using mercury isotope compositions. Environmental Science & Technology, 44: 3363-3371.

Fitzgerald, W. et al., 2005. Modern and historic atmospheric mercury fluxes in northern Alaska: Global sources and Arctic depletion. Environmental Science & Technology, 39: 557-625.

Foucher, D., Ogrinc, Hintelmann, H., 2009. Tracing Mercury Contamination from the Idrija Mining Region (Slovenia) to the Gulf of Trieste Using Hg Isotope Ratio Measurements. Environmental Science & Technology, 43.

Fréry, N. et al., 2001. Gold-mining activities and mercury contamination of native amerindian communities in French Guiana: key role of fish in dietary uptake. Environmental Health Perspectives, 109: 449-505.

Gehrke, G.E., Blum, J.D., Marvin-DiPasquale, M., 2011. Sources of mercury to San Francisco Bay surface sediment as revealed by mercury stable isotopes. Geochimica et Cosmochimica Acta, 75.

Gratz, L., Keeler, G., Blum, J., Sherman, L., 2010. Isotopic composition and fractionation of mercury in Great Lakes precipitation and ambient air. Environmental science & technology, 44(20): 7764-7770.

Gu, B. et al., 2011. Mercury reduction and complexation by natural organic matter in anoxic environments. Proceedings of the National Academy of Sciences of the United States of America, 108: 1479-1562.

Guigueno, M., Elliott, K., Levac, J., Wayland, M., Elliott, J., 2012. Differential exposure of alpine ospreys to mercury: melting glaciers, hydrology or deposition patterns? Environment international, 40: 24-56.

Haitzer, M., Aiken, G., Ryan, J., 2003. Binding of mercury(II) to aquatic humic substances: influence of pH and source of humic substances. Environmental science & technology, 37(11): 2436-2441.

Harada, M. et al., 2001. Mercury pollution in the Tapajos River basin, Amazon: mercury level of head hair and health effects. Environment International, 27: 285-375.

Jiskra, M., Wiederhold, J., Bourdon, B., Kretzschmar, R., 2012. Solution Speciation Controls Mercury Isotope Fractionation of Hg(II) Sorption to Goethite. Environmental science & technology, 46: 6654-6716.

Kritee, K., Blum, J., Barkay, T., 2008. Mercury stable isotope fractionation during reduction of Hg(II) by different microbial pathways. Environmental Science & Technology, 42: 9171-9178.

Kritee, K., Blum, J., Johnson, M., Bergquist, B., Barkay, T., 2007. Mercury stable isotope fractionation during reduction of Hg(II) to Hg(0) by mercury resistant microorganisms. Environmental Science & Technology, 41: 1889-1984.

Lefticariu, L., Blum, J., Gleason, J., 2011. Mercury Isotopic Evidence for Multiple Mercury Sources in Coal from the Illinois Basin. Environmental Science & Technology, 45: 1724–1729.

Liu, J., Feng, X., Yin, R., Zhu, W., Li, Z., 2011. Mercury distributions and mercury isotope signatures in sediments of Dongjiang, the Pearl River Delta, China. Chemical Geology, 287.

Malinovsky, D., Sturgeon, R., Yang, L., 2008. Anion-exchange chromatographic separation of Hg for isotope ratio measurements by multicollector ICPMS. Analytical Chemistry, 80: 2548-2603.

Matsumoto, A., Schwartz, G.E., Deonarine, A., Hsu-Kim, H., 2011. Assessment of mercury speciation in coal ash by sequential extractions, 2011 GSA Annual Meeting, Minneapolis, Minnesota, pp. 418.

Mead, C., Johnson, T., 2010. Hg stable isotope analysis by the double-spike method. Analytical and Bioanalytical Chemistry, 397: 1529-1567.

Nicolardi, V. et al., 2012. The adaptive response of lichens to mercury exposure involves changes in the photosynthetic machinery. Environmental pollution (Barking, Essex : 1987), 160: 1-11.

Perrot, V. et al., 2010. Tracing sources and bioaccumulation of mercury in fish of Lake Baikal--Angara River using Hg isotopic composition. Environmental Science & Technology, 44: 8030-8037.

Rodríguez-González, P. et al., 2009. Species-specific stable isotope fractionation of mercury during Hg(II) methylation by an anaerobic bacteria (*Desulfobulbus propionicus*) under dark conditions. Environmental Science & Technology, 43: 9183-9191.

Ruhl, L., Vengosh, A., Dwyer, G., Hsu-Kim, H., Deonarine, A., 2010. Environmental impacts of the coal ash spill in Kingston, Tennessee: an 18-month survey. Environmental Science & Technology, 44: 9272-9280.

Scott, S.H., 2012. Long term simulation of residual fly ash transport and fate in the Watts Bar Reservoir System, Coastal and Hydraulics Laboratory U.S. Army Engineering Research and Development Center at Waterways Experimentation Station.

Sherman, L., Blum, J., Keeler, G., Demers, J., Dvonch, J., 2012. Investigation of local mercury deposition from a coal-fired power plant using mercury isotopes. Environmental science & technology, 46: 382-472.

St Louis, V. et al., 2011. Differences in mercury bioaccumulation between polar bears (Ursus maritimus) from the Canadian high- and sub-Arctic. Environmental science & technology, 45: 5922-5930.

Stetson, S., Gray, J., Wanty, R., Macalady, D., 2009. Isotopic variability of mercury in ore, mine-waste calcine, and leachates of mine-waste calcine from areas mined for mercury. Environmental Science & Technology, 43: 7331-7337.

Tennessee Department of Environment and Conservation, 2011. Expanded Site Investigation Report Potential Hazardous Waste Site Clinch River Corporation, Tennessee Department of Environment and Conservation Division of Remediation - Knoxville Field Office, Knoxville, Tennessee.

Tennessee Valley Authority, 2009a. Continuing investigation of the nature and extent of ash in the Emory, Clinch and Tennessee River bottoms, Tennessee Valley Authority, Knoxville, Tennessee.

Tennessee Valley Authority, 2009b. Kingston ash incident evaluation of potential legacy contamination in local sediments, Tennessee Valley Authority, Knoxville, Tennessee.

Tennessee Valley Authority, 2009c. Kingston ash release Emory River high-flow event of May 4, 2009.

Tennessee Valley Authority, 2010a. Kingston ash recovery project weekly report October 25-31, 2010, Tennessee Valley Authority, Knoxville, Tennessee.

Tennessee Valley Authority, 2010b. TVA community involvement plan for the Kingston Ash Recovery Project, Tennessee Valley Authority,, Knoxville, Tennessee.

Tennessee Valley Authority, 2011a. TVA Kingston fossil fuel plant release sito on-scene coordinator report for the time-critical removal action May 11, 2009 through December 2010, Harriman, Roane County, Tennessee. EPA-AO-030, Tennessee Valley Authority, Knoxville, Tennessee.

Tennessee Valley Authority, 2011b. The TVA power system, Environmental impact statement of TVA's integrated resource plan TVA's environmental & energy future, Knoxville, Tennessee, pp. 39-55.

U.S. Environmental Protection Agency, 1997. Mercury study report to Congress 2. EPA-452/R-97-003, Office of Air Quality and Planning and Standards, Office of Research and Development, U.S. Environmental Protection Agency, Washington, DC.

U.S. Environmental Protection Agency, 2006. EPA's roadmap for mercury. EPA-HQ-OPPT-2005-0013, U.S. Environmental Protection Agency, Washington, DC.

U.S. Environmental Protection Agency, 2009. Coal Combustion Residues (CCR): Surface Impoundments with High Hazard Potential Rating Fact Sheet EPA530-F-09-006, U.S. Environmental Protection Agency.

Wang, Q., Kim, D., Dionysiou, D., Sorial, G., Timberlake, D., 2004. Sources and remediation for mercury contamination in aquatic systems--a literature review. Environmental Pollution (Barking, Essex : 1987), 131: 323-359.

Wiederhold, J.G. et al., 2010. Equilibrium mercury isotope fractionation between dissolved Hg (II) species and thiol-bound Hg. Environmental Science & Technology, 44: 4191-4197.

Yang, H. et al., 2010a. Historical reconstruction of mercury pollution across the Tibetan Plateau using lake sediments. Environmental Science & Technology, 44: 2918-2942.

Yang, H., Engstrom, D., Rose, N., 2010b. Recent changes in atmospheric mercury deposition recorded in the sediments of remote equatorial lakes in the Rwenzori Mountains, Uganda. Environmental Science & Technology, 44: 6570-6575.

Yin, R., Feng, X., Shi, W., 2010. Application of the stable-isotope system to the study of sources and fate of Hg in the environment: A review. Applied Geochemistry, 25.

Yin, R. et al., 2012a. Mercury isotope variations between bioavailable mercury fractions and total mercury in mercury contaminated soil in Wanshan Mercury Mine, SW China. Chemical Geology.

Yin, R. et al., 2012b. Mercury speciation and mercury isotope fractionation during ore roasting process and their implication to source identification of downstream sediment in the Wanshan mercury mining area, SW China. Chemical Geology.

Yudovich, Y.E., Ketris, M.P., 2005. Mercury in coal: a review Part 2. Coal use and environmental problems. International Journal of Coal Geology, 62.

Zeller, C., 2011. TVA Kingston recovery project Roane County, TN, TVA-Kingston Fly Ash Release Environmental Research Symposium, Harriman, Tennessee.

Zheng, W., Hintelmann, H., 2010. Nuclear field shift effect in isotope fractionation of mercury during abiotic reduction in the absence of light. The journal of physical chemistry. A, 114(12): 4238-4245.

CHAPTER 3

Mercury isotope ratios as tools for tracking geochemical transformations in the East Fork Poplar Creek, Tennessee

ABSTRACT

Mercury (Hg) stable isotope analyses of water, sediment and fish samples were used to identify and quantify natural chemical transformations of Hg in the East Fork Poplar Creek (EFPC), located near Oak Ridge, Tennessee. The EFPC is contaminated with Hg used decades ago in an electrochemical process at a thermonuclear weapons complex. Results indicate that Hg currently leaching out of the complex is not isotopically fractionated (δ^{202}Hg = 0.15±0.10‰); strongly contaminated sediments ([Hg] = 2380 ppm) presumed to have been deposited during active Hg use at the complex are also not strongly fractioned. There is no evidence that the electrochemical process caused isotopic fractionation in the Hg that was and currently is released from the Y-12 plant. Thus, this Hg does not have an unusual isotopic signature that could be used to trace its migration. We suggest the Hg contamination from chlor-alkali plants employing Hg in similar electrochemical processes probably also lacks strong isotopic fractionation. Recent stream sediments from EFPC show a small range of isotopic fractionation (0.33‰). In contrast, stream sediments from nominally uncontaminated reference sites located 8 to 20 km from the Y-12 plant contained Hg strongly enriched in lighter isotopes (δ^{202}Hg = −6.90±0.43‰, 2SD). Using these results as an estimate of local background Hg, some of the Hg isotope variation in EFPC sediments can be explained by mixing between background and contaminated Hg. Some sediment values

cannot be explained by simple mixing models, implying small amounts of isotopic fractionation have been caused by chemical transformation of Hg in the system. Small but systematic isotopic shifts observed in fish indicate a small amount of mass-independent isotopic fractionation (Δ^{199}Hg = −0.03 to 0.08‰, Δ^{201}Hg = −0.07 to 0.04‰) consistent with minor (up to 10%) Hg loss from the water resulting from photochemical reduction of Hg. Overall, the data set suggests that only minor amounts of Hg isotope fractionation process have occurred in the sediments, waters, and biological systems sampled.

INTRODUCTION

Hg contamination. Mercury is a widespread global contaminant (U.S. Environmental Protection Agency, 1997; U.S. Environmental Protection Agency, 2006). Modern anthropogenic inputs of Hg to the environment are dominated by coal combustion and precious metal mining (U.S. Environmental Protection Agency, 1997; Streets et al., 2009). However, various industrial processes require large amounts of Hg, which pose a large potential for contamination (Maxson, 2004; U.S. Environmental Protection Agency, 2008; World Chlorine Council, 2012). According to the EPA, the United States has over 4700 water bodies affected by Hg (U.S. Environmental Protection Agency, 2014).Production of chlorine products and NaOH via the "chlor-alkali" process has been a large contributor of Hg to the environment (Miller, 1989; Jasinski, 1995; Streets et al., 2009; Streets et al., 2011; OSPAR Commission, 2013). Over time, many Hg cell chlor-alkali plants have been decommissioned; however, Hg contamination caused by these plants is prevalent in many countries (Miller, 1989; OSPAR Commission, 2013; U.S. Environmental Protection Agency, 2014). In 2011, the chlor-alkali industry in Western Europe lost 26.4% of its Hg through products, waste water and air (OSPAR Commission, 2013). Hg was also released due to its use in the production of thermonuclear weapons until the 1960s (Bruce et al., 1999; Brooks and

Southworth, 2011). According to a report filed by ChemRisk® (1999), up to 2.4 million pounds of Hg were lost or unaccounted for in the Y-12 complex in Oak Ridge, Tennessee, due to weapons production processes (Bruce et al., 1999).

Brooks and Southworth (2011) provide a detailed history of Hg contamination at the Y-12 nuclear complex. Briefly, the complex, located at Oak Ridge, Tennessee, USA, was involved in thermonuclear weapons production processes during the 1950s and '60s. One method of enrichment of ^{6}Li used an electrochemical process somewhat similar to the "chlor-alkali" process, in which a sheet of Hg was used as the cathode. Over the lifespan of the Y-12 complex, up to 350 tons of Hg were released directly into the watershed draining the complex—the East Fork of Poplar Creek (EFPC). Releases to the soils happened over 8 large spill events, where not all the Hg was recovered from the soil. Releases to the water occurred during nitric acid washing of the Hg during the late 1950s before its use.

Inorganic Hg exists in the environment as Hg(0) and Hg(II). Hg(0) is relatively nonreactive, insoluble, and volatile, with atmospheric residence times of up to a year (U.S. Environmental Protection Agency, 1997). Hg(II) is soluble and highly reactive, and forms strong complexes with many dissolved ligands and solid surfaces. Hg(II) is also commonly microbially transformed to methylmercury (MeHg); a highly toxic form of Hg that bioaccumulates in aquatic environments (U.S. Environmental Protection Agency, 1997; Hsu-Kim et al., 2013). This bioaccumulation can affect the reproductive success and thyroidal hormone levels of fish and birds (Wada et al., 2009; Mulder et al., 2012; Wiener, 2013), and the cognitive and physical abilities of fledglings and rats (Heinz and Hoffman, 2003; Piedrafita et al., 2008; Kenow et al., 2010; Felipo, 2012). Negative cognitive and physiological effects on people have also been observed (Gallagher and Meliker,

2012; Shigeru et al., 2014), and have prompted many fish advisories (U.S. Environmental Protection Agency, 2011).

Hg isotope geochemistry. Hg has 7 stable isotopes (196, 198, 199, 200, 201, 202, and 204). The relative abundances of these isotopes are expressed using ratios against ^{198}Hg and are reported in δ-notation as defined by:

$$\delta^{xxx}Hg = \left(\frac{R^{xxx}_{sample}}{R^{xxx}_{standard}} - 1\right) * 1000‰ \quad (1)$$

Where R^{xxx}_{sample} and $R^{xxx}_{standard}$ are the ^{xxx}Hg/^{198}Hg ratios of the sample and an interlaboratory standard (NIST SRM 3133), respectively.

Multiple processes can alter the relative abundances of these isotopes. During chemical transformations of Hg, the lighter isotopes may react more readily than the heavier isotopes. Alternatively, equilibrium between two Hg-bearing phases tends to partition light and heavy isotopes unequally (Wiederhold et al., 2010; Jiskra et al., 2012). These effects are called mass dependent fractionation (MDF). Reactions that are known to cause MDF are: Equilibration between aqueous and adsorbed species (Wiederhold et al., 2010; Jiskra et al., 2012); methylation (Rodríguez-González et al., 2009); microbial reduction (Kritee et al., 2007; Kritee et al., 2008); abiotic reduction (Bergquist and Blum, 2007); and evaporation (Zheng et al., 2007; Estrade et al., 2009; Ghosh et al., 2013). MDF is determined by measuring δ^{202}Hg.

Recently, Hg has been shown to exhibit isotopic fractionation that deviates from the theoretical relationships predicted for MDF. This phenomenon is called mass independent fractionation (MIF) (Bergquist and Blum, 2007; Zheng et al., 2007; Estrade et al., 2009; Gratz et al., 2010; Perrot et al., 2010; Zheng and Hintelmann, 2010; Chen et al., 2012; Perrot et al., 2012; Ghosh et al., 2013). There are currently three processes known to generate MIF: The first and largest is called the magnetic isotope effect (MIE), which affects only the odd isotopes of Hg as a result of their nuclear

spins. When certain photochemical reactions occur, interactions between electron spins and nuclear spins affect the reaction rates of the odd mass number isotopes (Bergquist and Blum, 2007). This causes the odd isotopes' abundances to depart from those predicted for purely mass-dependent fractionation.

MIF is expressed as the deviation of a measured δ value of an isotope ratio ($^{199}Hg/^{198}Hg$, $^{200}Hg/^{198}Hg$,or $^{201}Hg/^{198}Hg$) from the δ value expected from MDF alone. By convention, $\delta^{202}Hg$ is used as the indicator of MDF, leading to the following expressions for MIF (Blum and Bergquist, 2007):

$$\Delta^{199}Hg = 1000 * \left(\left[\ln\left(\left(\delta^{199}Hg/1000\right)+1\right)\right] - 0.252\left[\ln\left(\left(\delta^{202}Hg/1000\right)+1\right)\right]\right) \quad (2)$$

$$\Delta^{200}Hg = 1000 * \left(\left[\ln\left(\left(\delta^{200}Hg/1000\right)+1\right)\right] - 0.502\left[\ln\left(\left(\delta^{202}Hg/1000\right)+1\right)\right]\right) \quad (3)$$

$$\Delta^{201}Hg = 1000 * \left(\left[\ln\left(\left(\delta^{201}Hg/1000\right)+1\right)\right] - 0.752\left[\ln\left(\left(\delta^{202}Hg/1000\right)+1\right)\right]\right) \quad (4)$$

Δ^{199}Hg and Δ^{201}Hg values of several per mil have been generated in experiments with photochemical Hg(II) reduction or photochemical demethylation (Bergquist and Blum, 2007), and in natural systems where photochemical effects are thought to be important (Bergquist and Blum, 2007; Perrot et al., 2010; Perrot et al., 2012; Tsui et al., 2012).

Much weaker MIF arises from the phenomenon known as the Nuclear Field Shift or the Nuclear Volume Effect (NVE). Interaction of certain electron orbitals with the nucleus depends on the size of the nucleus, and thus, the various Hg isotopes differ slightly in their chemical properties and NVE-driven isotopic fractionation occurs. Because nuclear size correlates closely with nuclear mass, NVE causes effects that are very similar to MDF. However, small deviations from MDF occur because nuclear volume is not a perfectly linear function of mass, with the odd isotopes anomalously small (Schauble, 2007). Thus, processes that cause mass dependent isotopic

fractionation are usually accompanied by small shifts in Δ^{199}Hg and Δ^{201}Hg. Such effects have been detected in evaporation off of metallic Hg (Zheng et al., 2007; Estrade et al., 2009; Ghosh et al., 2013), rainfall (Gratz et al., 2010; Chen et al., 2012), and dark abiotic reduction of Hg(II) (Zheng and Hintelmann, 2010).

Δ^{200}Hg values usually conform to mass-dependent fractionation, and thus are often used as a check on analytical quality. However, small deviations have been observed in a few rainfall samples (Gratz et al., 2010; Chen et al., 2012). Finally, compact fluorescent lighting devices have been shown to generate large shifts in Δ^{199}Hg, Δ^{200}Hg, and Δ^{201}Hg, thought to be caused by "self-shielding" of Hg from the intense ultraviolet radiation inside (Mead et al., 2013).

Objectives. To date, very few Hg isotope studies have concentrated on Hg transformations in streams and floodplains impacted by industrial contamination. Such environments often contain abundant organic matter, juxtaposition of oxidizing and reducing environments, and abundant microbial activity. Accordingly, Hg is likely to undergo chemical transformations that affect its environmental impact. For example, reduction of dissolved Hg(II) produces Hg(0) that could escape the system via volatilization. This reaction should be detectable isotopically, as an increase in δ^{202}Hg in the remaining Hg(II) (Kritee et al., 2007; Kritee et al., 2008). This study aims to examine isotopic variability in the Hg currently found in the watershed contaminated by activities at the Y-12 complex, with the broader goal of developing this new isotopic tool for use in many similar sites.

In this study, we present Hg isotope data from a brief survey of sediment, fish and water in the EFPC and attempt to use the data to address the following questions:

Do industrial electrochemical processes like the chlor-alkali process release isotopically distinctive Hg that can be traced in the environment?

Do strong isotopic contrasts exists among the various potential sources of Hg in the system (e.g. Hg deposited in floodplain sediment decades ago versus Hg currently emitted from the Y-12 complex)?

Can chemical transformations of Hg that affect its transport and impact on an ecosystem be revealed by Hg isotopic data? In particular, has Hg in the system, and especially in biota, been strongly affected by dark Hg(II) reduction, photochemical Hg(II) reduction, or photochemical demethylation?

The EFPC is a good location for this initial study due to the fact that the creek originates in the Y-12 complex, with a clear Hg source at relatively high concentration with relatively little potential for cross contamination from other unknown sources. Also this location has an intensive sampling campaign in progress, and an archive of samples taken over time by Oak Ridge National Laboratory.

MATERIALS AND METHODS

Field setting. The EFPC originates within the Y-12 complex (Figure 3.1). Its headwaters have been buried and converted into the storm drainage network of the complex. The rest of the upper reaches of the creek are channelized. Its flow path takes it out of the Oak Ridge Reservation (ORR) through the town of Oak Ridge, Tennessee, after which it flows southwest and reenters the ORR and flows into Poplar Creek. The underground drainage system was constituted of process and cooling water, groundwater from sumps and cracks, and runoff from storm events. The point at which the water exits the storm drainage network into the open, channelized ditch, is referred to

as Outfall 200 (OF200). The Hg flowing out of OF200 is industrial Hg dissolved by the chlorinated municipal waters provided by the city of Oak Ridge (Brooks and Southworth, 2011).

Remedial efforts in the EFPC began in 1989 (Brooks and Southworth, 2011). The remedial efforts included renovation of most storm drains within the Y-12 complex, dechlorination of the remaining inputs to the EFPC surface waters (only after being discharged at OF200), stabilization of stream banks, bypassing a lake, and treating all Hg-contaminated natural spring flow. In 1996, the EFPC base flow was restored to 0.31 $m^3 s^{-1}$; up from 0.09–0.14 $m^3 s^{-1}$. This caused enhanced bank erosion, which caused an increase in Hg flux. A project to stabilize the stream banks was completed in 2000. In late 2005, an activated charcoal treatment system was installed at an Hg-contaminated natural spring, 800 m downstream of OF200, to capture one Hg input (Brooks and Southworth, 2011).

The EFPC floodplain sediments contain organic materials and coal combustion residuals sourced from power plants on the premises during the complex's active years. A layer of very high Hg concentrations has been identified in the EFPC floodplain and is referred to as the Black Layer. The layer can be up to 61cm thick and have concentrations up to 3000 mg/kg Hg (Harris et al., 1996; Southworth et al., 2000). Mercury in the sediments is associated with dark particles. Analysis of the sediments and water show that Hg is present as Hg(II), metallic Hg (Hg(0)), and as metacinnabar (Barnett et al., 1995; Gerlach et al., 1995; Harris et al., 1996). Other contaminants present in the water and shallow groundwater along the EFPC include PCBs in fish, tetrachloroethene, and radionuclides (Williams and Hanley, 1993).

Three reference sites have been chosen to serve as nominally uncontaminated reference sites for Hg studies in the EFPC. These sites have not been directly affected by Hg released from the Y-12 complex and thus provide information about the local background Hg. The Bear Creek watershed

is separated from the EFPC watershed by a drainage divide between the east and west side of the Bear Creek Valley (Bailey and Lee, 1991). It flows from the western edge of the Y-12 complex into the EFPC downstream of East Fork Kilometer 6 (EFK 6, 6.0 kilometers upstream of the creek's confluence with Poplar Creek). White Oak Creek flows southwest through Oak Ridge National Laboratory into the Clinch River. Hinds Creek is the only reference creek that is not within the ORR. It is 20 km northeast of Oak Ridge, Tennessee, and flows west into the Clinch River at Clinton, Tennessee. Hinds creek, while not being contaminated by activities at the ORR was up until 2006 on the EPA's list of contaminated creeks due to farming effluent (Marshall, 2007).

Sampling and analytical methods. Sediment samples consisted of fine material less than 500μm in size. Samples were collected on the same day from within the stream at East Fork Poplar Creek Kilometer 23.4 (EFK 23.4, kilometers upstream of the creek's confluence with Poplar Creek), EFK 22.3, EFK 18.6, EFK 17.8, EFK 6.3, and EFK 5 from 1996–2012 by either scraping the fine sediment off larger pebbles or by using a 500μm sieve to separate fine sediments from larger pebbles. Sediment samples were freeze-dried. Samples ranging in mass up to 100mg were digested overnight using 4mL hot (95°C) aqua regia (3:1 HCl:HNO_3).

Water samples were collected in 2012 into 1L acid-cleaned HDPE bottles. Seven water samples were taken along the stream, starting at OF200 (EFK 26), 0.6 km downstream at EFK 25.4, EFK 23.4, EFK 22.3, EFK 18.6, EFK 17.8, EFK 13.8, and EFK 5. The water was filtered through a 0.2μm filter in order to remove fine suspended particles potentially carrying adsorbed Hg. The samples were acidified and oxidized using 10mL HCl and 1mL 0.2M BrCl, respectively, in order to maintain the Hg in solution. The BrCl was made following EPA method 1631 (U.S. Environmental Protection Agency, 2002).

The fish samples were filets of redbreast sunfish (*Lepornis auritus*). Sunfish are sedentary fish and were used as indicators of Hg exposure until 2004, when their population dropped too low to collect representative samples at certain locations along the EFPC (Mathews et al., 2012). Fish samples were collected in 2004 using a backpack-mounted electro-zapping apparatus. Filets were kept frozen until use. Samples were digested overnight using a 7:3 HNO_3:H_2SO_4 mixture at 95°C.

Samples with concentrations less than 2 mg kg^{-1} in the water or digests were preconcentrated using anion exchange procedures modified from Malinovsky et al. (2008). Briefly, AG1-X8 resin (0.4ml bed volume) was washed with 5% (m/v) thiourea, and conditioned with 2M HCl. After sample solutions were passed through the column, it was rinsed with 5mL 0.1M HNO_3, and Hg was eluted using 4ml 5% thiourea solution. Fresh thiourea solution was made prior to each ion exchange session. The final Hg concentrations of sample solutions used for mass spectrometry were 1–3 ng g^{-1}.

Mass spectrometry followed the "double spike" methods of Mead and Johnson (2010). Samples were spiked before preparation with a calibrated ^{196}Hg + ^{204}Hg solution and allowed to chemically equilibrate overnight. Isotopic compositions were measured on a Nu Plasma multi-collector inductively coupled plasma mass spectrometer (MC-ICP-MS) at the University of Illinois at Urbana-Champaign by cold vapor generation, using $SnCl_2$ as a reductant. For samples containing thiourea, the $SnCl_2$ solution was prepared in a 5% (m/v) NaOH solution in order to enable the $SnCl_2$ to reduce the thiourea-complexed Hg(II). The instrument's mass bias was determined using the measured $^{204}Hg/^{196}Hg$ ratio as described in Mead and Johnson (2010). Isobaric interferences were monitored by measuring $^{194}Pt^+$, $^{203}Tl^+$, $^{206}Pb^+$, and $^{196}HgH^+$. Results were corrected for HgH^+ interferences on masses 199, 200, 201, and 202. Pt, Tl, and Pb interferences were always found to be negligible.

The long-term reproducibility of the isotopic method was evaluated for samples from the EFPC and the reference sites by preparing and analyzing samples multiple times on different days. There were a total of 32 replicate analyses of 17 EFPC samples with a δ^{202}Hg root mean square difference of 0.04‰ (calculated following Hyslop and White (2009)); therefore, we estimate our 95% confidence interval to be ±0.08‰. The Δ^{199}Hg and Δ^{201}Hg 95% confidence intervals for EFPC samples are ±0.06‰ and ±0.07‰, respectively. The 95% confidence intervals for the sediment samples from the reference sites are ±0.20‰ for δ^{202}Hg, ±0.03 for Δ^{199}Hg, and ±0.03 for Δ^{201}Hg (11 replicate samples).

RESULTS

Water samples. The total dissolved Hg concentration in the 2012 EFPC water decreased from 0.65 μg L^{-1} at outfall 200 to 0.028 μg L^{-1} at EFK 6 (21 kilometers downstream). The samples show a small amount of variation in δ^{202}Hg with values close to 0‰ and slightly negative with one exception: The OF200 water sample has a slightly positive δ^{202}Hg value (Figure 3.2, Table 3.1). The next sample, 0.5km downstream of OF200, had a value 0.6‰ lower, but then the remaining water samples followed a weak positive δ^{202}Hg trend (−0.46‰ to −0.19‰) with increasing distance downstream from location EFK 25.4 to EFK 6 (Figure 3.2).

The water samples have an increasing Δ^{201}Hg with decreasing concentrations downstream of Outfall 200 (Figure 3.3, Table 3.1). The increase in the value is consistent with contamination of ^{201}Hg in the water samples. Tracer experiments using ^{201}Hg-enriched Hg^{2+} were conducted at Oak Ridge and are discussed below. The Δ^{199}Hg in the water does not show any indication of contamination, and was always less than 0.07‰ (Table 3.1), which indicates no significant MIF is present in the water.

Sediment. The sediment samples from the reference sites have low concentrations (<1.5 ppm) and extremely negative δ^{202}Hg values (−6.9‰) (Figure 3.4, Table 3.1). The samples were measured multiple times in order to verify their negative value. The values measured are some of the most negative values reported in natural samples. Natural samples, including coals, ash, cinnabar, sediments, and precipitation do not get more negative than −5‰ (Ridley and Stetson, 2006; Biswas et al., 2008; Smith et al., 2008; Foucher et al., 2009; Lefticariu et al., 2011; Sherman et al., 2012; Sun et al., 2013; Donovan et al., 2014). These samples are ~30 times more concentrated and significantly more negative in δ^{202}Hg than nominally uncontaminated sediments from a river in the region (0.035 ± 0.009 mg kg^{-1}, δ^{202}Hg = −1.17 ± 0.13‰) (Bartov et al., 2013).

The EFPC sediments generally contain less Hg and are more negative in δ^{202}Hg with increasing distance downstream of OF200. The recent (2010 and 2012) EFPC sediments have more positive δ^{202}Hg values than the water from the same location. The sediments appear to track some chemical changes in the Hg isotopes over time. For the EFPC sediments, the 1996 samples become ~0.8‰ more negative from EFK 23.4 to EFK 6. The 2007 EFK samples follow the same trend as the 1996 samples but to a lesser extent, only ~0.2‰ difference. The 2010 EFK 6 samples and all the 2012 EFK samples downstream of EFK 23.4 average δ^{202}Hg = −0.10 ± 0.27‰ (2SD). The EFK 22.3 sediment sample plots as the most negative sample out of the EFPC at δ^{202}Hg = −1.14‰, similar to values of nominally uncontaminated regional background measured by Bartov et al. (2013).

The sediments immediately out of the drainage pipe at OF200 have δ^{202}Hg values from 1996 and 2010 averaging −0.12 ± 0.24‰ (2SD). However, the 2012 OF200 sample plots with a δ^{202}Hg value of 0.88‰ ± 0.11‰ (2SD) (Figure 3.4, Table 3.1). That particular sample contained much more fine black sediment than the other samples that were mostly brown and platy. The contaminated

sediment layer known as the "Black Layer", which has the potential of being the major source of Hg into the system, plots at values of δ^{202}Hg = −0.15 ± 0.11‰, 2380 ppm (Table 3.1).

The sediments from the EFPC and reference sites did not show large Δ^{199}Hg and Δ^{201}Hg values for any location or time (figure5, Table 3.1). The EFPC samples all have slightly negative Δ^{199}Hg and Δ^{201}Hg; all the sediments originating in the reference creeks had slightly positive Δ^{199}Hg and Δ^{201}Hg values.

Fish samples. The fish samples all have slightly negative δ^{202}Hg values; they range from −0.56‰ to −0.11‰ with a slight positive trend with distance downstream. The upstream samples have an average value of −0.48 ± 0.10‰ (n = 4), whereas the downstream samples have an average of −0.28 ± 0.17‰ (n = 4) (Table 3.1). The δ^{202}Hg values of the fish samples were similar to those of the waters from the same locations.

The fish exhibit a small amount of MIF. They range from −0.10‰ to 0.11‰ for Δ^{199}Hg and −0.10‰ to 0.08‰ for Δ^{201}Hg. The fish exhibit a positive MIF trend with distance downstream. The samples range from Δ^{201}Hg = −0.10‰ upstream to 0.08‰ downstream and Δ^{199}Hg = −0.10‰ upstream to 0.11‰ downstream. Figure 3.5 shows the fish samples lie on a positive Δ^{199}Hg vs Δ^{201}Hg trend with a slope of 1.06.

DISCUSSION

^{201}Hg contamination in water samples. Facilities at Oak Ridge National Laboratory used to handle the water samples of this study also hosted Hg methylation experiments that involved ^{201}Hg as a tracer (Moberly et al., 2012). Relatively large amounts of ^{201}Hg were used and very large ^{201}Hg/^{198}Hg ratios were common in the experiments. The water samples of the present study had low amounts of cross contamination from the methylation experiments. The Δ^{201}Hg values of the water show unreasonable, positive values (Figure 3.3, Table 3.1) and we conclude that this type of

contamination must have occurred. The linearity of Figure 3.3 shows that the data conforms to a trend that is consistent with mixing between a very enriched ^{201}Hg source and the value coming out of OF200. Therefore, we disregard the Δ^{201}Hg of the water samples and with it lose our ability to identify any photochemical transformations that occurred in the water.

Reference sites and the regional background. The sediments from the reference sites have highly negative δ^{202}Hg values (Figure 3.4). These values are more negative than any others published to date for natural samples. They also have slightly greater δ^{202}Hg uncertainty than other sediment samples from this study. This may have been caused by 1) greater heterogeneity, or 2) greater sensitivity of these low concentration samples to contamination during preparation and analysis. However, laboratory blanks prepared with the samples always contained less than 5% of the minimum mass of Hg in a sample, and the maximum error would be 0.35‰. The sediments have some degree of heterogeneity in them, which account for the larger uncertainty in their measurements. The slightly greater uncertainty on δ^{202}Hg has no effect on our interpretations of the reference sites.

The observed highly negative δ^{202}Hg values in these samples suggest the existence of some unusual process(es) affecting the Hg in these sediments. The fact that the three reference sites are 8km, 9km, and 20km distant from the Y-12, and separated from each other by between 1km and 29km implies that this is not an isolated occurrence. We suggest that small creeks in the area have similar geochemical properties that cause significant fractionation of Hg. The exact nature of the Hg isotope-fractionating process is not clear. However, recent studies suggest strong Hg mass dependent fractionation associated with plants (Demers et al., 2013; Wiederhold et al., 2013; Yin et al., 2013). These studies have analyzed lichens, poplar, aspen, and rice leaves and found δ^{202}Hg to get as light as −3.38‰. The studies concluded that the uptake step of atmospheric Hg into the

leaves fractionated the lighter isotopes into the leaves, while transfer of Hg from the roots to the leaves did not induce a large fractionation. It is possible that more extreme fractionation in plants could occur, but more study is needed.

Sediments and coal ash from the Emory and Clinch Rivers, 22km to 29km southwest of the Y-12 complex, also show negative δ^{202}Hg values (Bartov et al., 2013), but they are less extreme values. Coal ash samples ranged from −2.21 to −1.40‰, while nominally uncontaminated sediments ranged from −1.30 to −0.94‰. It appears that all regional background Hg, including historical Hg deposition from coal ash, are isotopically negative and distinct from the Y-12 released Hg.

Isotopic characteristics of the Hg contamination. We assume the δ^{202}Hg values of the Hg supplies used for the electrochemical process were similar to those of known ore deposits. Hg ore and hydrothermal rocks show some variability, but have an average δ^{202}Hg value that is slightly negative but close to zero (Foucher et al., 2009; Yin et al., 2010; Wiederhold et al., 2013). Since most of the worldwide supply of Hg was used by the Y-12 plant at the time the Hg-intensive process was in use (Brooks and Southworth, 2011), it is likely that the Hg was aggregated from various sources and its δ^{202}Hg was close to zero.

The water sample from Outfall 200 in 2012 plots close to δ^{202}Hg = 0‰ (Figure 3.2). The recent sediments from the EFPC and the "black layer" also plot close to δ^{202}Hg = 0‰. The data show no evidence that any Hg released from the Y-12 plant was significantly fractionated relative to the initial Hg source. That is perhaps surprising, considering one would expect to see fractionation associated with the electrochemical process the Hg was used for and/or the nitric acid washing steps it was subjected to. However, it is likely that the amount of isotopically fractionated Hg lost

due to the electrochemical processing was small relative to the bulk amount of Hg spilled. The data suggest this was the case.

Sediments from Outfall 200 could potentially be affected by different sources within the Y-12 complex. The sediments from OF200 from 1996 and 2010 have identical δ^{202}Hg and concentration within the uncertainty of measurements. The sediment sample from 2012, has a higher concentration and δ^{202}Hg = 0.88‰ (Figure 3.4), a significant change from 14 years of apparent stability. This was probably caused by inclusion in the sediment of fine particles from the storm drain system. The Y-12 complex had a Hg recovery furnace also connected to the storm drain that exits at OF200 (Brooks and Southworth, 2011). These particles are probably remnants from the Hg recovery system. The combustion system was connected to the drainage system of the plant, and so, small amounts of left-over ash and sediments can periodically get swept through the system and deposit at the mouth of the drainage pipe. Calcine sediments can have relatively high concentrations of Hg and positive δ^{202}Hg (Gehrke et al., 2011; Wiederhold et al., 2013), which is consistent with what we observe at the OF200 sediment sample.

The floodplain sediments are indistinguishable from the contaminant Hg. The "black layer" sediments are thought to be present in the floodplain and contain high concentrations of Hg (~2380 mg kg^{-1}) that was spilled in the 1950s and '60s. Accordingly, this layer is a potential huge source of stored sedimentary Hg that can be remobilized into the EFPC. Unfortunately, it is not isotopically distinct from more recent inputs to the system, which are represented by the values found for the storm-drain pipe from 1996–2010. The black layer most likely contains Hg spilled as part of the 8 large spills that occurred during the life of the plant, where not all of the metallic Hg was recovered from the sediments. Importantly, the lack of any apparent isotopic shift over many years of residence in the sediments is indicative that the large inventory of buried Hg is

chemically stable and is not subjected to active redox cycling. Accordingly, the Hg spilled in the 1950's that could be remobilized from the sediments is isotopically indistinguishable Hg that is leaching from the drainage system. This is somewhat unfortunate, as Hg remobilized from floodplain sediment cannot be traced isotopically. However, it does suggest that Hg sources from the Y-12 plant, regardless of its exact history, has a single isotopic signature so it can be traced regionally.

Hg reactions and stability in EFPC sediments. The in-creek EFPC sediment samples show evidence for decreasing Hg chemical transformations over time (Figure 3.4, Figure 3.6). We expect that the sediments from within the EFPC are going to be a mixture of the background Hg present in the region and contaminant Hg from Outfall 200 or the "black layer" (Donovan et al., 2014). However, the 1996 and 2007 sediments—samples taken during the active remediation of the creek—show a pattern in the creek that is not possible to explain by any mixing of any of the sources, either OF200 or the black layer (Figure 3.6). Several sediment samples are up to 0.51‰ lighter than the mixing curve would predict. The fact that mixing could not explain these data, suggests that some natural chemical transformation of Hg in the EFPC was still taking place during the remediation efforts. Lake Reality was known to have been biogeochemically productive and a Hg source to the downstream EFPC (Brooks and Southworth, 2011). The 2007 samples from the same two locations (EFK 23.4 and EFK 6.3) becoming more positive is probably caused by the spilled Hg from the black layer overprinting any indication of natural transformation in the sediments as the remediation efforts change the biogeochemical conditions in the EFPC.

The EFPC sediment samples appear to trend toward more positive δ^{202}Hg values over time, with the sediment samples from 2010 onward being indistinguishable from the spilled Hg in the "black layer". This implies that as the remediation efforts changed the biogeochemical conditions in the

creek, less natural chemical transformations was occurring. Whereas earlier samples showed shifts in the negative direction that are best described by biogeochemical transformations, remediation appears to have diminished those effects, causing the measured values in the sediments to shift from light values up to the contaminant Hg values measured coming out of OF200 and the "black layer".

With the exception of one sample (EFK 22.3) the sediments' δ^{202}Hg values don't differ much from the waters' values (0.01–0.35‰); this implies that chemical transformations moving Hg between the sediments and the water are minor. Sorption effects between the sediments and the water would impart an observable fractionation of the Hg isotopes to either positive or negative depending on the adsorbent material (Wiederhold et al., 2010; Jiskra et al., 2012). The Δ^{199}Hg of the water is 0.09‰ greater than the Δ^{199}Hg of the sediment ($p<0.0001$). That could be due to a very small amount of a photochemical reduction signal in the odd isotopes of the water.

The EFK 22.3 sample has a more negative δ^{202}Hg value than the samples upstream and downstream from it (Figure 3.4). The sediments also deviate from the water collected at the same location. This particular sampling location is on the confluence of a small tributary into the EFPC. It is important to note that it is indistinguishable from the 2007 EFK 23.4 sample, a location immediately upstream and in the main branch of the creek. It is possible that the discrepancy in the measured values of the sediments from this location is evidence for old, more fractionated Hg being stored in different locations in the system such as this tributary into the EFPC.

Hg reactions in EFPC waters. The EFPC sediments do not show evidence for Hg cycling. The water samples collected show a weak increase in δ^{202}Hg with increasing distance downstream of OF200; however, this shift is not necessarily due to any chemical transformations happening in the creek. It is very likely that this trend is caused by addition of different sources of Hg. The lower

δ^{202}Hg values at EFK 25.4 are likely related to various Hg treatment activities upstream (dechlorination, input of fresh water, and the active- charcoal system). The shift back to ~0‰ values downstream is potentially caused by other inputs, such as Hg released from sediments. Accordingly, it is not possible to extract any chemical transformation signatures from the δ^{202}Hg data.

Whereas the water samples provide information about the one day on which samples were taken, the EFPC fish have the potential to store information about chemical transformations in the system over a longer period of time due to their ability to integrate Hg over time. It has been shown that little Hg isotopic fractionation occurs in fish (Kwon et al., 2012; Kwon et al., 2013) during trophic transfer of food. Bergquist and Blum (2007) measured multiple fish samples from different locations and showed that it is possible to detect, in fish tissue, large amounts of MIF that corresponds to photochemical reactions occurring abiotically. The advantage of sampling fish tissues is that they give a sense of the average conditions in the creek, as opposed to water sampled at one moment in time. For example, if the water was sampled during a sunny day, the isotopes could show more extreme fractionation related to photochemical reactions that is not representative of the average state of the system.

Kwon et al. (2012) and Kwon et al. (2013) showed that the isotopic compositions of fish readjust to a change in the isotopic value the fish consume over a time period between 80–183 days. Therefore, it is safe to assume that the fish faithfully track the average conditions present in the ecosystem and are not greatly biased toward the immediate conditions at the time of sampling. The MIF values in the EFPC fish show a positive trend together with the δ^{202}Hg with increasing distance downstream (Figure 3.7), which implies that they are recording some small amount of chemical transformations of the Hg in the EFPC waters. The slope of the Δ^{199}Hg vs Δ^{201}Hg plot is

1.06 ± 0.20, similar to the slope observed for Hg(II) photoreduction by Bergquist and Blum (2007) (Figure 3.5). Using the equations from Bergquist and Blum (2007), we calculate a maximum of 10% photoreduction of the Hg in the water.

Conclusions. The Hg isotope results from Hg in waters currently coming out of the storm drain of the Y-12 complex and sediment found close to that location indicate that the electrochemical process and any other processes used in the Y-12 plant complex did not fractionate the Hg isotopes. Tentatively, we suggest that Hg released from similar electrochemical operations used in cell chlor-alkali plants that exist around the world (Maxson, 2004; U.S. Environmental Protection Agency, 2008; World Chlorine Council, 2012) will also be isotopically unfractionated relative to industrial Hg supplies. It is very likely that any fractionation induced by the electrochemical process had little impact on the very large amount of Hg present in the bath, and therefore, would be undetectable even if electrochemical cells using Hg do induce a fractionation.

The Hg in the EFPC appears to undergo minor photochemical reduction in the creek water, with up to 10% of loss of Hg due to photochemical reduction of dissolved Hg(II). The water and fish samples are consistent with each other in this regard. The water samples represent Hg isotopic fractionation in the environment during the day of sampling, while fish represent a time averaged fractionation. The fact that the water and fish provide consistent indications of chemical reactions, strengthens our confidence that fish can be used as integrators of Hg processes in the water column as opposed to the potential day-to-day noise of sampling just the water.

The δ^{202}Hg values of creek sediments reflect mixing of Y-12 Hg with the regional background, and also suggest that small amounts of biogeochemical transformations of Hg occurred, but waned over time due to the implementation of the multiple remedial actions. The extremely negative δ^{202}Hg values of the nominally uncontaminated reference sites suggest strong biogeochemical

cycling of the relatively small amounts of Hg at those sites. Sediments from the EFPC have δ^{202}Hg values ranging from the values inferred for the original contaminant to values about 1‰ lower. Mixing models suggest that only small amounts of this shift toward lower values is caused by mixing of Y-12 Hg with the regional background Hg. Older sediments show greater shifts, and recent sediments show very small shifts, suggesting that the biogeochemical conditions of the EFPC were changed by the Hg remediation efforts of the complex. This lack of strong redox cycling observed in recent stream sediments suggest the Hg found in the creek poses lesser risk, as it is less likely to be converted to the more dangerous methylated forms.

This study demonstrates the importance of analyzing Hg isotopes in multiple sample types from multiple time periods in order to understand Hg cycling through an environmental system. The water samples allowed us to characterize the Hg currently associated with the sources and processes of the Y-12 plant. However, the importance of multiple samples, and knowledge of the history of the site played an important role in understanding complicating factors for interpretation of isotopic trends observed.

FIGURES AND TABLES

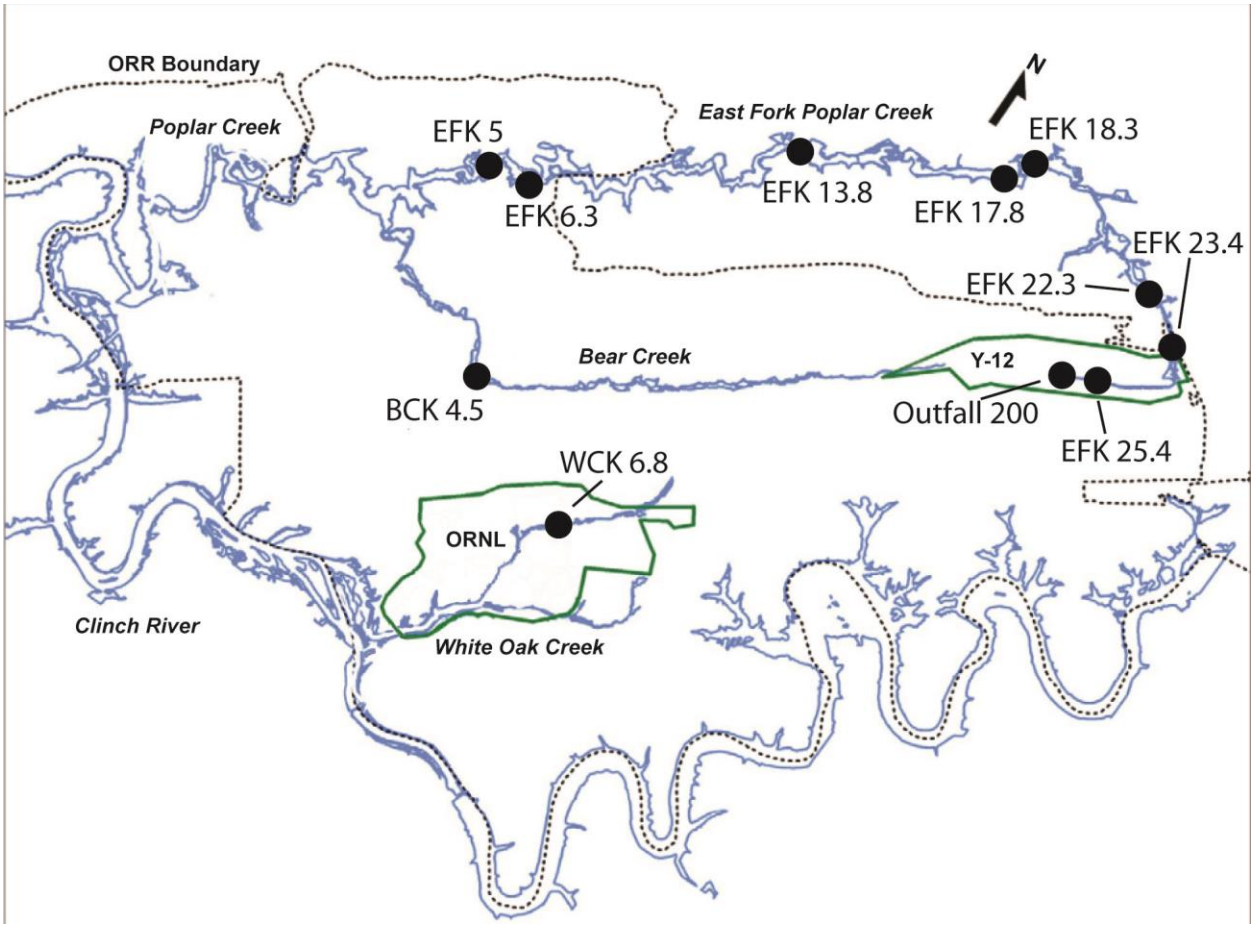

Figure 3.1. Map of the Oak Ridge Reservation. Hinds Creek is ~20km northeast of the ORR. Image adapted from Mathews et al. (2012).

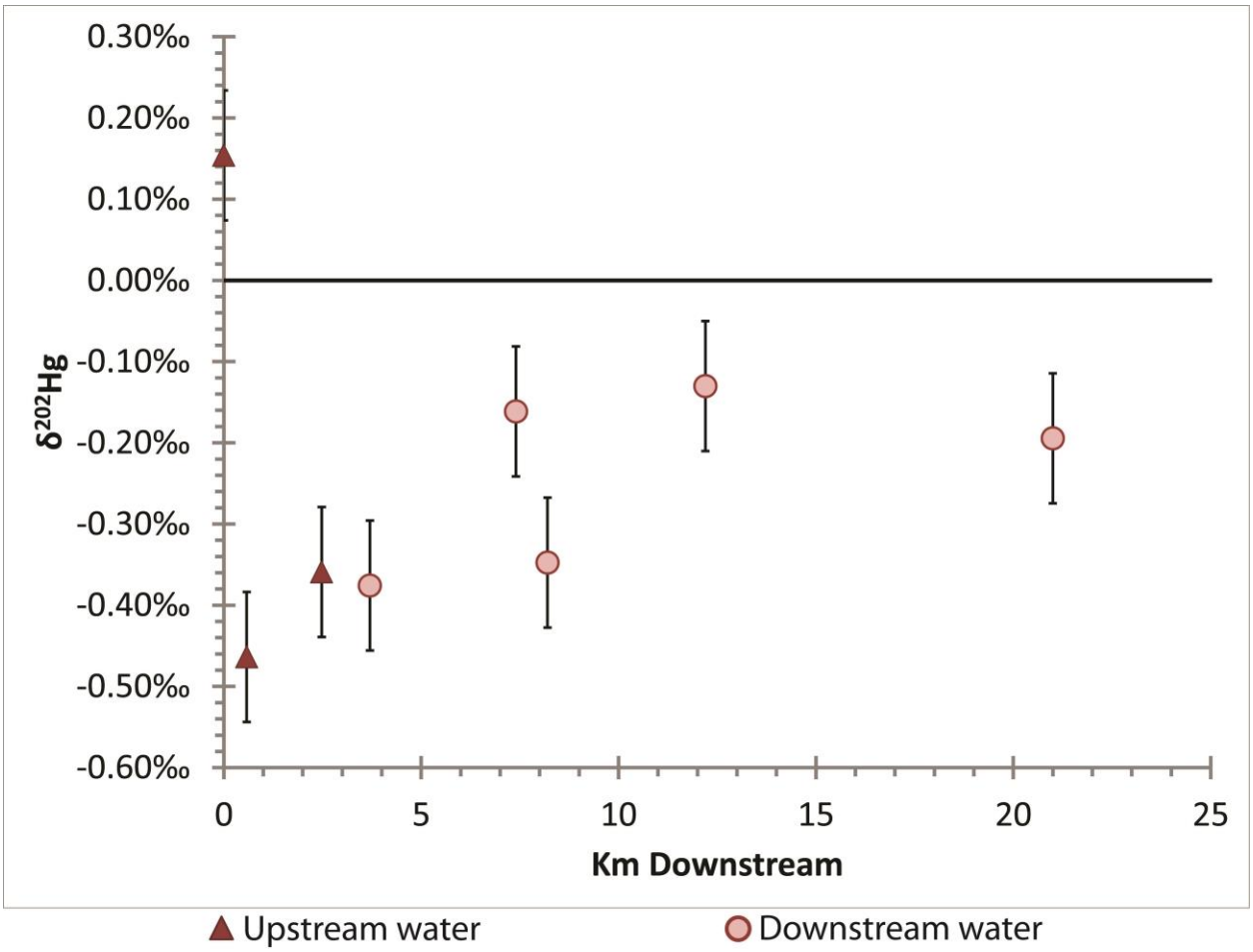

Figure 3.2. δ^{202}Hg of water samples vs. distance downstream of the EFPC.

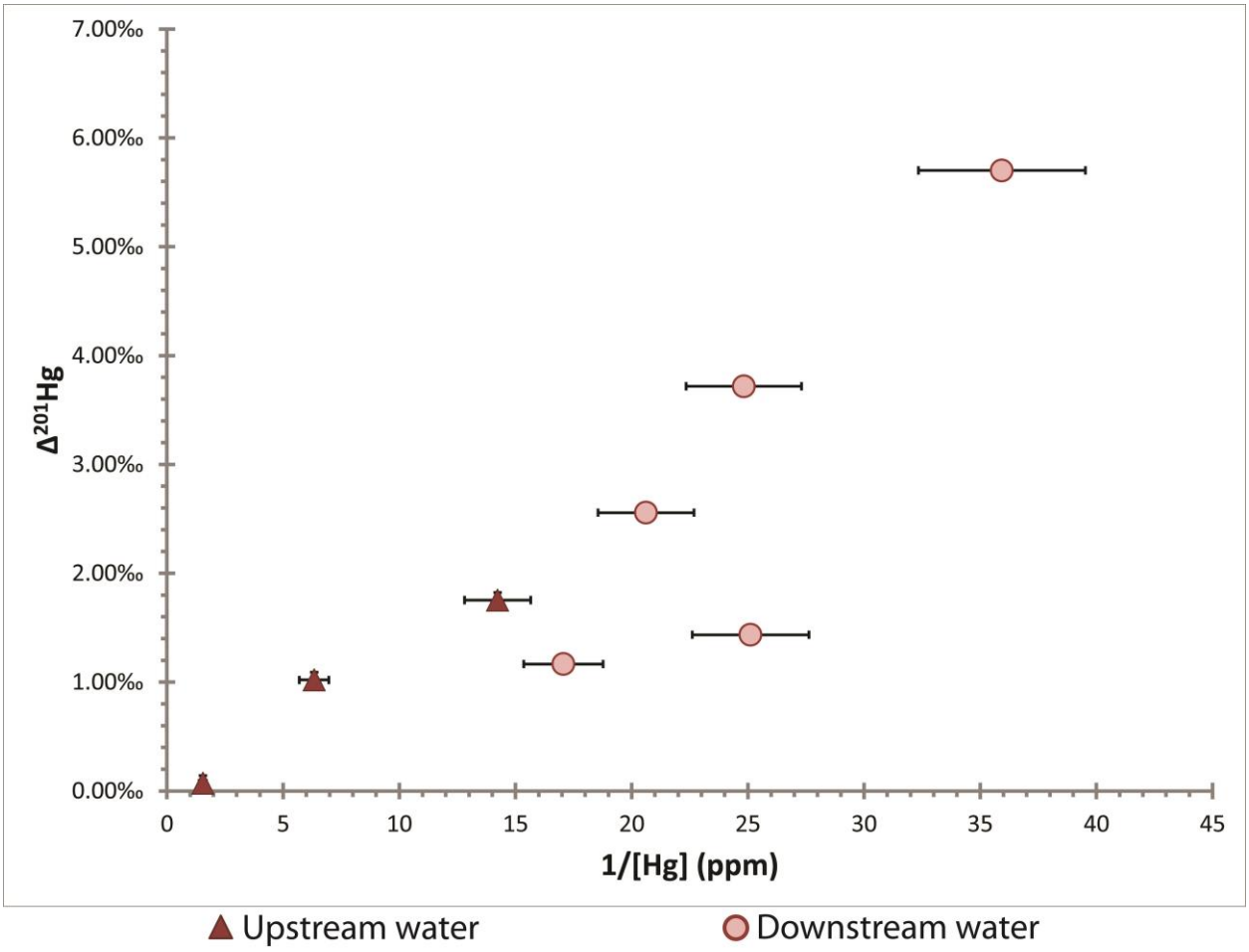

Figure 3.3. Δ^{201}Hg versus 1/[Hg] in water samples.

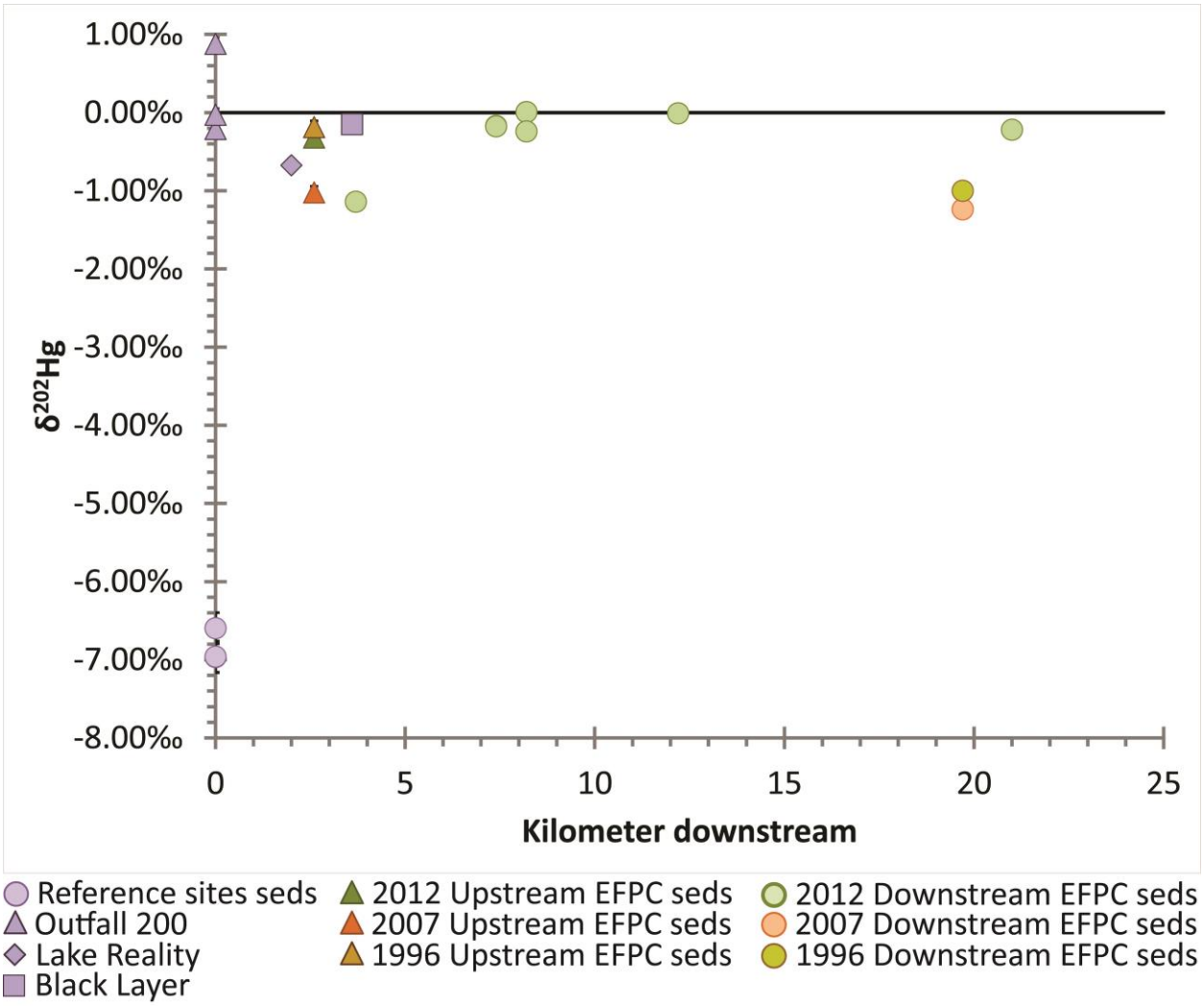

Figure 3.4. δ^{202}Hg in sediment vs. distance downstream from OF200. The Black Layer is floodplain sediment sampled at EFK 22.4, not sediment from within the EFPC. The reference sites' sediments are plotted at 0km arbitrarily.

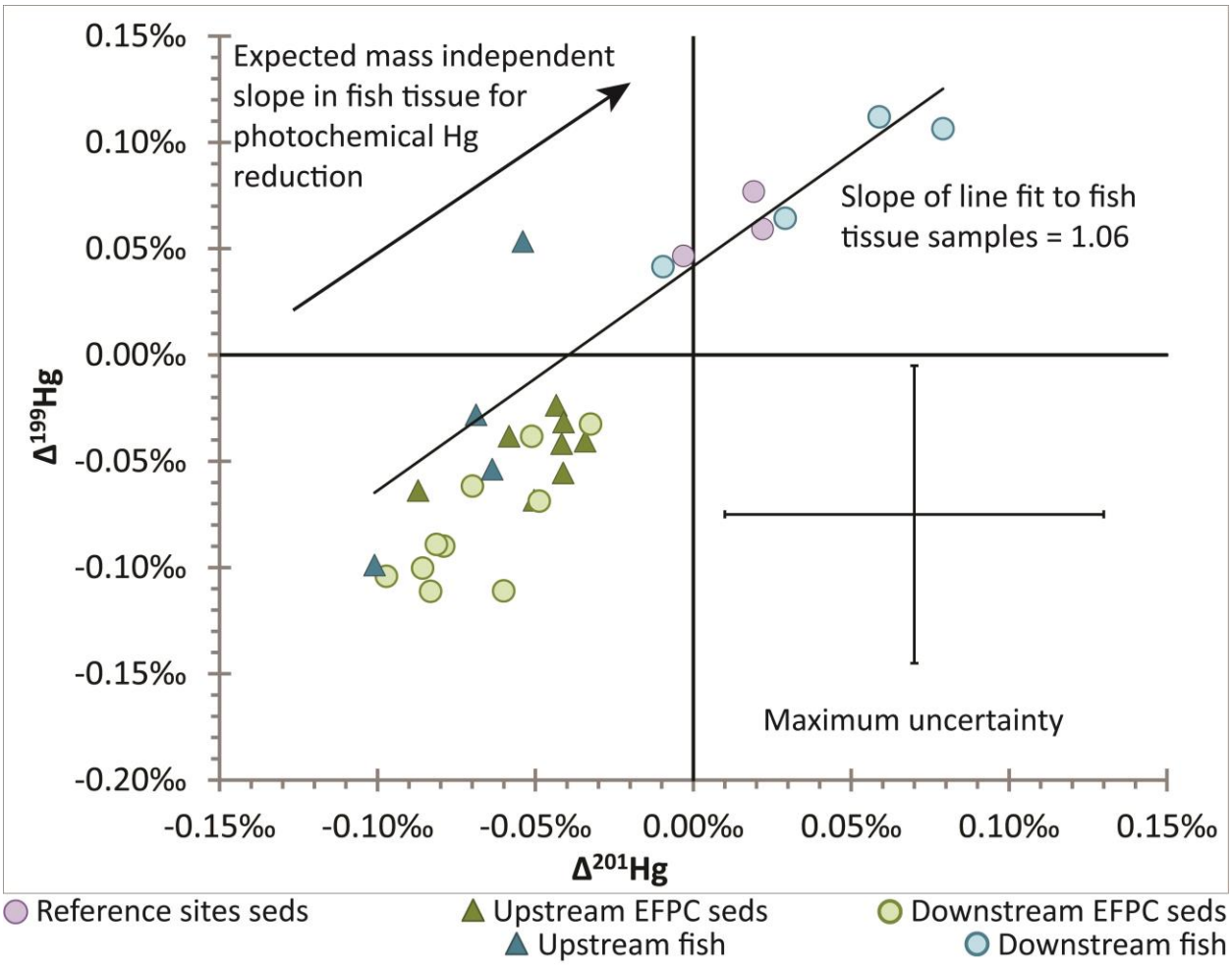

Figure 3.5. Δ^{199}Hg vs. Δ^{201}Hg. All the EFPC sediments are condensed into the green triangles and circles. The slope of the fish samples is 1.06, consistent with Hg photoreduction.

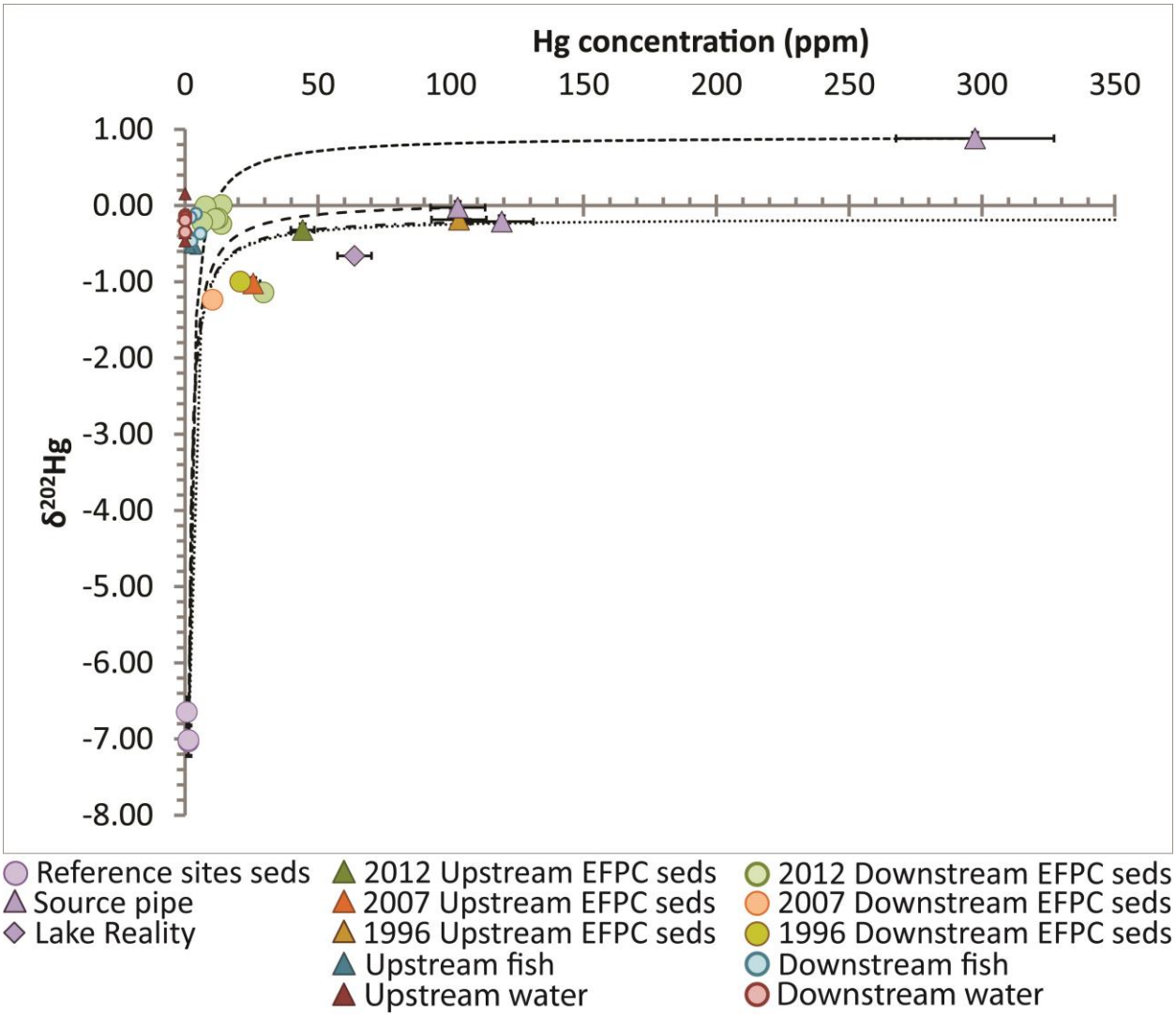

Figure 3.6. δ^{202}Hg vs. Hg concentration. The Black Layer plots off the figure with δ^{202}Hg = −0.15‰ and [Hg] = 2380 ppm. The dotted line represents a mixing curve between the Black Layer and the reference sites. The dashed lines represent mixing curves between the source pipe and the reference sites.

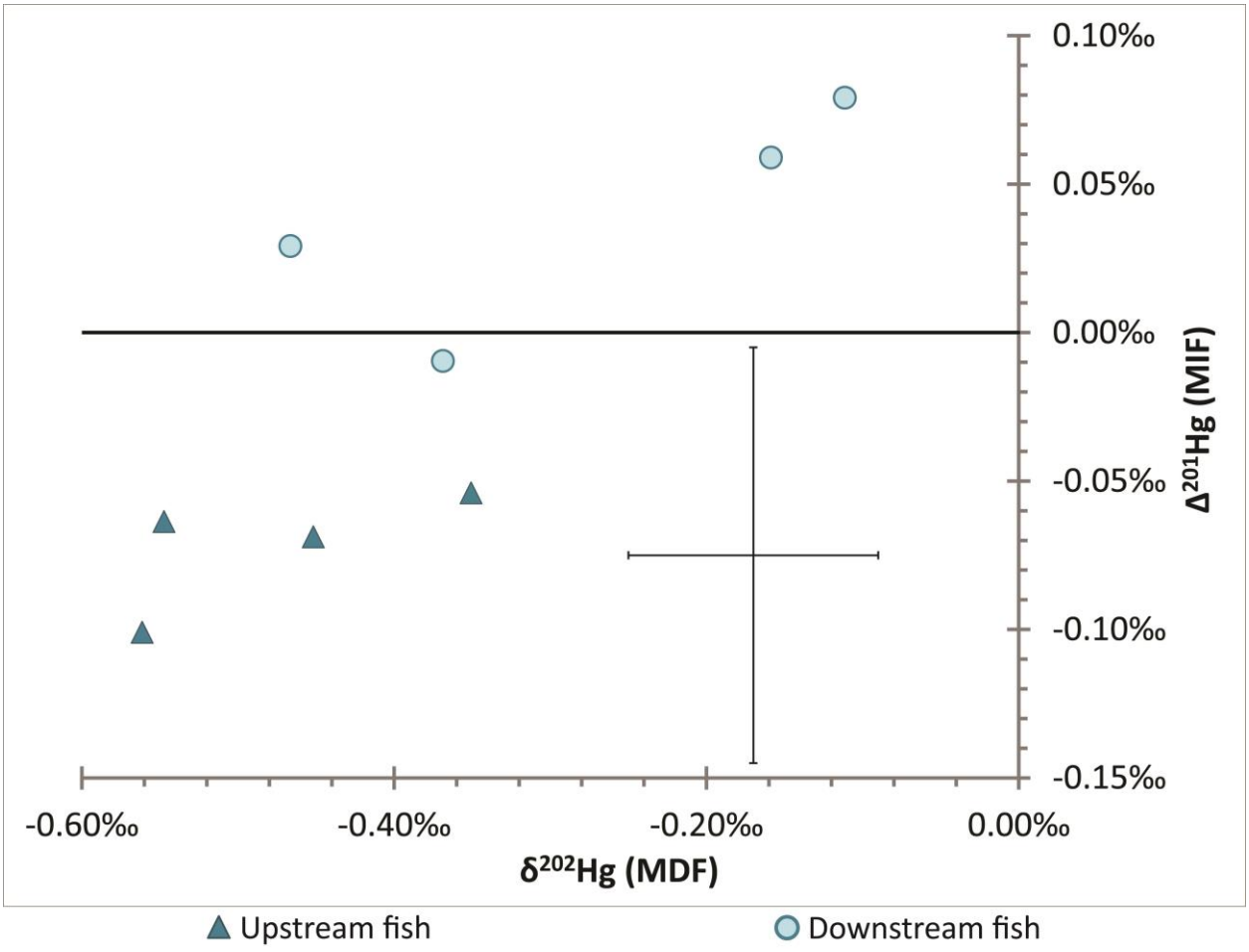

Figure 3.7. Δ^{201}Hg vs. δ^{202}Hg in fish tissue. There is a positive trend from the upstream fish to the downstream fish samples, implying the fish are recording natural chemical transformations of the Hg in the EFPC water.

Table 3.1. Analytical results

Sample	Year sampled	Concentration[a]	δ^{202}Hg	Δ^{199}Hg	Δ^{201}Hg
Floodplain Sediment					
Black Layer	1996	2380	-0.20‰	-0.05‰	-0.07‰
Replicate analysis	1996	2380	-0.10‰	-0.04‰	0.01‰
Replicate analysis	1996	2380	-0.14‰	-0.04‰	-0.04‰
Replicate analysis	1996	2380	-0.16‰	-0.03‰	-0.04‰
EFPC Stream Sediment, 1996–1998					
OF 200	1996	119	-0.30‰	0.00‰	-0.03‰
Replicate analysis	1996	119	-0.15‰	-0.05‰	-0.04‰
Replicate analysis	1996	119	-0.18‰	-0.02‰	-0.05‰
EFK 23.4	1996	103	-0.22‰	-0.05‰	-0.07‰
Replicate analysis	1996	103	-0.18‰	-0.04‰	0.00‰
Replicate analysis	1996	103	-0.15‰	-0.03‰	-0.05‰
EFK 6.3	1996	20.7	-1.07‰	-0.06‰	-0.06‰
Replicate analysis	1996	20.7	-0.95‰	-0.03‰	-0.02‰
Replicate analysis	1996	20.7	-0.98‰	-0.01‰	-0.02‰
Lake Reality	1998	63.7	-0.71‰	-0.05‰	-0.04‰
Replicate analysis	1998	63.7	-0.65‰	-0.01‰	-0.04‰
Replicate analysis	1998	63.7	-0.66‰	-0.03‰	-0.04‰
EFPC Stream Sediment, 2007					
EFK 23.4	2007	25.6	-1.02‰	-0.03‰	-0.04‰
Duplicate analysis	2007	25.6	-1.03‰	-0.04‰	-0.07‰
EFK 6.3	2007	10.32	-1.25‰	-0.04‰	-0.05‰
Duplicate analysis	2007	10.32	-1.22‰	-0.03‰	-0.06‰
EFPC Stream Sediment, 2010					
OF 200	2010	103	0.03‰	-0.04‰	-0.05‰
Replicate analysis	2010	103	-0.08‰	-0.05‰	-0.03‰
Replicate analysis	2010	103	-0.02‰	-0.07‰	-0.05‰
EFK 6.3	2010	9.47	0.13‰	-0.13‰	-0.09‰
Replicate analysis	2010	9.47	0.09‰	-0.11‰	-0.07‰
Replicate analysis	2010	9.47	0.09‰	-0.09‰	-0.09‰
EFPC Stream Sediment, 2012					
OF 200	2012	297	0.88‰	-0.06‰	-0.09‰
EFK 23.4	2012	44.3	-0.32‰	-0.07‰	-0.05‰
EFK 22.3	2012	29.5	-1.14‰	-0.07‰	-0.05‰
EFK 18.6	2012	12.2	-0.17‰	-0.09‰	-0.08‰
EFK 18.6[b]	2012	11.8	-0.18‰	-0.11‰	-0.06‰
EFK 17.8	2011	13.8	0.01‰	-0.10‰	-0.10‰
EFK 17.8[b]	2012	13.6	-0.24‰	-0.06‰	-0.07‰

Table 3.1. (Cont.)

Sample	Year sampled	Concentration[a]	δ^{202}Hg	Δ^{199}Hg	Δ^{201}Hg
EFK 13.8	2012	7.64	-0.01‰	-0.09‰	-0.08‰
EFK 5	2012	6.41	-0.22‰	-0.10‰	-0.09‰
Reference Sites (Background)					
WCK 6.8	1995	1.25	-7.07‰	0.09‰	0.02‰
Replicate analysis	1995	1.25	-6.90‰	0.02‰	0.00‰
Replicate analysis	1995	1.25	-7.13‰	0.08‰	0.03‰
Replicate analysis	1995	1.25	-6.76‰	0.04‰	0.04‰
BCK 4.5	2006	1.25	-6.99‰	0.07‰	0.01‰
Replicate analysis	2006	1.25	-6.94‰	0.08‰	0.02‰
Replicate analysis	2006	1.25	-7.11‰	0.10‰	0.04‰
Replicate analysis	2006	1.25	-6.80‰	0.06‰	0.00‰
Hinds_Cr.	2007	0.619	-6.81‰	0.04‰	0.02‰
Replicate analysis	2007	0.619	-6.48‰	0.05‰	-0.03‰
Replicate analysis	2007	0.619	-6.50‰	0.04‰	0.01‰
Fish, 2004					
Upstream Fish 1 (EFK 23.4)	2004	4.08	-0.52‰	-0.10‰	-0.07‰
Duplicate analysis	2004	4.08	-0.61‰	-0.10‰	-0.13‰
Upstream Fish 2 (EFK 23.4)	2004	1.77	-0.57‰	-0.08‰	-0.09‰
Duplicate analysis	2004	1.77	-0.52‰	-0.03‰	-0.04‰
Upstream Fish 3 (EFK 23.4)	2004	1.62	-0.37‰	0.02‰	-0.08‰
Duplicate analysis	2004	1.62	-0.33‰	0.08‰	-0.03‰
Upstream Fish 4 (EFK 23.4)	2004	2.31	-0.45‰	-0.01‰	-0.08‰
Duplicate analysis	2004	2.31	-0.46‰	-0.04‰	-0.06‰
Downstream Fish 1 (EFK 6)	2004	4.04	-0.07‰	0.11‰	0.07‰
Duplicate analysis	2004	4.04	-0.15‰	0.11‰	0.09‰
Downstream Fish 2 (EFK 6)	2004	2.05	-0.16‰	0.08‰	0.02‰
Duplicate analysis	2004	2.05	-0.16‰	0.14‰	0.10‰
Downstream Fish 3 (EFK 6)	2004	5.79	-0.36‰	0.02‰	-0.03‰
Duplicate analysis	2004	5.79	-0.37‰	0.06‰	0.01‰
Downstream Fish 4 (EFK 6)	2004	2.42	-0.50‰	0.06‰	0.05‰
Duplicate analysis	2004	2.42	-0.43‰	0.07‰	0.00‰
Water, 2012					
OF200	2012	0.647	0.15‰	-0.07‰	0.07‰
EFK 25.4[c]	2012	0.158	-0.46‰	0.01‰	1.02‰
EFK 23.4[c]	2012	0.0703	-0.36‰	0.05‰	1.75‰
EFK 22.3[c]	2012	0.0586	-0.38‰	0.05‰	1.17‰
EFK 18.6[c]	2012	0.0485	-0.16‰	-0.01‰	2.56‰
EFK 17.8[c]	2012	0.0398	-0.35‰	0.03‰	1.43‰

Table 3.1. (Cont.)

Sample	Year sampled	Concentration[a]	δ^{202}Hg	Δ^{199}Hg	Δ^{201}Hg
EFK 13.8[c]	2012	0.0403	-0.13‰	0.04‰	3.72‰
EFK 5[c]	2012	0.0278	-0.19‰	0.00‰	5.70‰

[a] Concentrations are in mg kg^{-1} for sediments and fish samples, and μg L^{-1} for water samples

[b] Separate sample sampled on the same day

[c] Sample disregarded due to ^{201}Hg contamination

REFERENCES

Bailey, Z.C., Lee, R.W., 1991. Hydrogeology and Geochemistry in Bear Creek and Union Valleys, near Oak Ridge, Tennessee. 90-4008, U.S. Geological Survey, Nashville, Tennessee.

Barnett, M. et al., 1995. Characterization of mercury species in contaminated floodplain soils. Water, Air, & Soil Pollution, 80(1): 1105-1108.

Bartov, G. et al., 2013. Environmental Impacts of the Tennessee Valley Authority Kingston Coal Ash Spill. 1. Source Apportionment Using Mercury Stable Isotopes. Environmental Science & Technology, 47(4): 2092-2099.

Bergquist, B., Blum, J., 2007. Mass-dependent and -independent fractionation of Hg isotopes by photoreduction in aquatic systems. Science (New York, N.Y.), 318: 417-437.

Biswas, A., Blum, J., Bergquist, B., Keeler, G., Xie, Z., 2008. Natural mercury isotope variation in coal deposits and organic soils. Environmental Science & Technology, 42: 8303-8312.

Blum, J., Bergquist, B., 2007. Reporting of variations in the natural isotopic composition of mercury. Analytical and Bioanalytical Chemistry, 388: 353-362.

Brooks, S., Southworth, G., 2011. History of mercury use and environmental contamination at the Oak Ridge Y-12 Plant. Environmental pollution (Barking, Essex : 1987), 159: 219-247.

Bruce, G.M., Flack, S.M., Mongan, T.R., Widner, T.E., 1999. Mercury Releases from Lithium Enrichement at the Oak Ridge Y-12 Plant -- A Reconstruction of Historical Releases and Off-Site Doses and Health Risks, ChemRisk.

Chen, J., Hintelmann, H., Feng, X., Dimock, B., 2012. Unusual fractionation of both odd and even mercury isotopes in precipitation from Peterborough, ON, Canada. Geochimica et Cosmochimica Acta, 90.

Demers, J.D., Blum, J.D., Zak, D.R., 2013. Mercury isotopes in a forested ecosystem: Implications for air-surface exchange dynamics and the global mercury cycle. Global Biogeochemical Cycles, 27.

Donovan, P.M. et al., 2014. Identification of multiple mercury sources to stream sediments near Oak Ridge, TN, USA. Environmental Science & Technology, 48: 3666-3674.

Estrade, N., Carignan, J., Sonke, J.E., Donard, O.F.X., 2009. Mercury isotope fractionation during liquid–vapor evaporation experiments. Geochimica et Cosmochimica Acta, 73.

Felipo, V., 2012. Methylmercury during development impairs the glutamate-NO-cGMP pathway and learning. Toxicology Letters, 211.

Foucher, D., Ogrinc, Hintelmann, H., 2009. Tracing Mercury Contamination from the Idrija Mining Region (Slovenia) to the Gulf of Trieste Using Hg Isotope Ratio Measurements. Environmental Science & Technology, 43.

Gallagher, C., Meliker, J., 2012. Mercury and thyroid autoantibodies in U.S. women, NHANES 2007-2008. Environment international, 40: 39-43.

Gehrke, G.E., Blum, J.D., Marvin-DiPasquale, M., 2011. Sources of mercury to San Francisco Bay surface sediment as revealed by mercury stable isotopes. Geochimica et Cosmochimica Acta, 75.

Gerlach, C.L. et al., 1995. Characterization of Mercury Contamination at the East Fork Poplar Creek Site, Oak Ridge, Tennessee: A Case Study. EPA/600/R-95/110, Cincinnati, OH Springfield, VA.

Ghosh, S., Schauble, E.A., Couloume, G.L., Blum, J.D., Bergquist, B.A., 2013. Estimation of nuclear volume dependent fractionation of mercury isotopes in equilibrium liquid–vapor evaporation experiments. Chemical Geology, 336.

Gratz, L., Keeler, G., Blum, J., Sherman, L., 2010. Isotopic composition and fractionation of mercury in Great Lakes precipitation and ambient air. Environmental science & technology, 44(20): 7764-7770.

Harris, L. et al., 1996. Imaging and microanalyses of mercury in flood plain soils of east fork poplar creek. Water, Air, & Soil Pollution, 86(1): 51-69.

Heinz, G., Hoffman, D., 2003. Embryotoxic thresholds of mercury: estimates from individual mallard eggs. Archives of environmental contamination and toxicology, 44(2): 257-264.

Hsu-Kim, H., Kucharzyk, K., Zhang, T., Deshusses, M., 2013. Mechanisms regulating mercury bioavailability for methylating microorganisms in the aquatic environment: a critical review. Environmental science & technology, 47(6): 2441-2456.

Hyslop, N.P., White, W.H., 2009. Estimating Precision Using Duplicate Measurements. Journal of the Air & Waste Management Association, 59.

Jasinski, S.M., 1995. The Materials Flow of Mercury in the United States. Resources, Conservation and Recycling, 15: 145-179.

Jiskra, M., Wiederhold, J., Bourdon, B., Kretzschmar, R., 2012. Solution Speciation Controls Mercury Isotope Fractionation of Hg(II) Sorption to Goethite. Environmental science & technology, 46: 6654-6716.

Kenow, K., Hines, R., Meyer, M., Suarez, S., Gray, B., 2010. Effects of methylmercury exposure on the behavior of captive-reared common loon (*Gavia immer*) chicks. Ecotoxicology (London, England), 19(5): 933-944.

Kritee, K., Blum, J., Barkay, T., 2008. Mercury stable isotope fractionation during reduction of Hg(II) by different microbial pathways. Environmental Science & Technology, 42: 9171-9178.

Kritee, K., Blum, J., Johnson, M., Bergquist, B., Barkay, T., 2007. Mercury stable isotope fractionation during reduction of Hg(II) to Hg(0) by mercury resistant microorganisms. Environmental Science & Technology, 41: 1889-1984.

Kwon, S. et al., 2012. Absence of Fractionation of Mercury Isotopes during Trophic Transfer of Methylmercury to Freshwater Fish in Captivity. Environmental science & technology, 46(14): 7527-7534.

Kwon, S., Blum, J., Chirby, M., Chesney, E., 2013. Application of mercury isotopes for tracing trophic transfer and internal distribution of mercury in marine fish feeding experiments. Environmental toxicology and chemistry / SETAC.

Lefticariu, L., Blum, J., Gleason, J., 2011. Mercury Isotopic Evidence for Multiple Mercury Sources in Coal from the Illinois Basin. Environmental Science & Technology, 45: 1724–1729.

Malinovsky, D., Sturgeon, R., Yang, L., 2008. Anion-exchange chromatographic separation of Hg for isotope ratio measurements by multicollector ICPMS. Analytical Chemistry, 80: 2548-2603.

Marshall, S., 2007. Livestock Management Restores Waterbody, U.S. Evnironmental Protection Agency Office of Water, Washington, DC.

Mathews, T. et al., 2012. Decreasing aqueous mercury concentrations to meet the water quality criterion in fish: Examining the water-fish relationship in two point-source contaminated streams. The Science of the total environment, 443C: 836-843.

Maxson, P., 2004. Mercury Flows In Europe and the World: The Impact of Decommissioned Chlor-Alkali Plants, European Commission Directorate General for Environment, Brussels, Belgium.

Mead, C., Johnson, T., 2010. Hg stable isotope analysis by the double-spike method. Analytical and Bioanalytical Chemistry, 397: 1529-1567.

Mead, C., Lyons, J., Johnson, T., Anbar, A., 2013. Unique Hg stable isotope signatures of compact fluorescent lamp-sourced Hg. Environmental Science & Technology, 47(6): 2542-2547.

Miller, D.R., 1989. Mercury in Canadian Rivers. In: Bourdeau, P., Haines, J.A., Klein, W., Murti, C.R.K. (Eds.), Ecotoxicology and Climate. John Wiley & Sons Ltd, pp. 373-381.

Moberly, J. et al., 2012. Role of morphological growth state and gene expression in Desulfovibrio africanus strain Walvis Bay mercury methylation. Environmental science & technology, 46(9): 4926-4932.

Mulder, P. et al., 2012. Mercury in Molar Excess of Selenium Interferes with Thyroid Hormone Function in Free-Ranging Freshwater Fish. Environmental science & technology.

OSPAR Commission, 2013. Mercury Losses from the Chlor-Alkali Industry in 2011. 600/2013.

Perrot, V. et al., 2010. Tracing sources and bioaccumulation of mercury in fish of Lake Baikal--Angara River using Hg isotopic composition. Environmental Science & Technology, 44: 8030-8037.

Perrot, V. et al., 2012. Higher mass-independent isotope fractionation of methylmercury in the pelagic food web of lake baikal (Russia). Environmental science & technology, 46(11): 5902-5911.

Piedrafita, B., Erceg, S., Cauli, O., Felipo, V., 2008. Developmental exposure to polychlorinated biphenyls or methylmercury, but not to its combination, impairs the glutamate-nitric oxide-cyclic GMP pathway and learning in 3-month-old rats. Neuroscience, 154(4): 1408-1416.

Ridley, W.I., Stetson, S.J., 2006. A review of isotopic composition as an indicator of the natural and anthropogenic behavior of mercury. Applied Geochemistry, 21.

Rodríguez-González, P. et al., 2009. Species-specific stable isotope fractionation of mercury during Hg(II) methylation by an anaerobic bacteria (*Desulfobulbus propionicus*) under dark conditions. Environmental Science & Technology, 43: 9183-9191.

Schauble, E., 2007. Role of nuclear volume in driving equilibrium stable isotope fractionation of mercury, thallium, and other very heavy elements. Geochimica et Cosmochimica Acta, 71: 2170-2189.

Sherman, L., Blum, J., Keeler, G., Demers, J., Dvonch, J., 2012. Investigation of local mercury deposition from a coal-fired power plant using mercury isotopes. Environmental science & technology, 46: 382-472.

Shigeru, T. et al., 2014. Signs and symptoms of methylmercury contamination in a First Nations community in Northwestern Ontario, Canada. Science of The Total Environment, 468-469.

Smith, C.N., Kesler, S.E., Blum, J.D., Rytuba, J.J., 2008. Isotope geochemistry of mercury in source rocks, mineral deposits and spring deposits of the California Coast Ranges, USA. Earth and Planetary Science Letters, 269.

Southworth, G.R., Turner, R.R., Peterson, M.J., Bogle, M.A., Ryon, M.G., 2000. Response of mercury contamination in fish to decreased aqueous concentrations and loading of inorganic mercury in a small stream. Environmental monitoring and assessment, 63(3): 481-494.

Streets, D. et al., 2011. All-time releases of mercury to the atmosphere from human activities. Environmental science & technology, 45(24): 10485-10491.

Streets, D., Zhang, Q., Wu, Y., 2009. Projections of global mercury emissions in 2050. Environmental science & technology, 43(8): 2983-2988.

Sun, R. et al., 2013. Mercury stable isotope fractionation in six utility boilers of two large coal-fired power plants. Chemical Geology, 336.

Tsui, M. et al., 2012. Sources and transfers of methylmercury in adjacent river and forest food webs. Environmental science & technology, 46(20): 10957-10964.

U.S. Environmental Protection Agency, 1997. Mercury study report to Congress 2. EPA-452/R-97-003, Office of Air Quality and Planning and Standards, Office of Research and Development, U.S. Environmental Protection Agency, Washington, DC.

U.S. Environmental Protection Agency, 2002. Method 1631, Revision E: Mercury in water by oxidation, purge and trap, and cold vapor atomic fluorescence spectrometry. EPA-821-R-02-019.

U.S. Environmental Protection Agency, 2006. EPA's roadmap for mercury. EPA-HQ-OPPT-2005-0013, U.S. Environmental Protection Agency, Washington, DC.

U.S. Environmental Protection Agency, 2008. Fact Sheet: Proposed Amendments to Air Toxics Standard: Mercury Emissions from Mercury Cell Chlor-Alkali Plants.

U.S. Environmental Protection Agency, 2011. 2010 Biennial National Listing of Fish Advisories. EPA-820-F-11-014.

U.S. Environmental Protection Agency, 2014. National Summary of Impaired Waters and TMDL Information.

Wada, H., Cristol, D., McNabb, F., Hopkins, W., 2009. Suppressed adrenocortical responses and thyroid hormone levels in birds near a mercury-contaminated river. Environmental science & technology, 43(15): 6031-6038.

Wiederhold, J. et al., 2013. Mercury Isotope Signatures as Tracers for Hg Cycling at the New Idria Hg Mine. Environmental science & technology.

Wiederhold, J.G. et al., 2010. Equilibrium mercury isotope fractionation between dissolved Hg (II) species and thiol-bound Hg. Environmental Science & Technology, 44: 4191-4197.

Wiener, J., 2013. Mercury exposed: advances in environmental analysis and ecotoxicology of a highly toxic metal. Environmental toxicology and chemistry / SETAC, 32(10): 2175-2178.

Williams, R.L., Hanley, J.E., 1993. Public Health Consultation: Y-12 Weapons Plant Chemical Releases into East Fork Poplar Creek Oak Ridge, Tennessee, Division of Health Assessment and Consultation, Agency for Toxic Substances and Disease Registry.

World Chlorine Council, 2012. Global Mercury Cell Production Data (in thousands of metric tons of chlorine capacity). United Nations Environment Programme.

Yin, R., Feng, X., Meng, B., 2013. Stable Mercury Isotope Variation in Rice Plants (*Oryza sativa* L.) from the Wanshan Hg Mining District, SW China. Environmental science & technology.

Yin, R., Feng, X., Shi, W., 2010. Application of the stable-isotope system to the study of sources and fate of Hg in the environment: A review. Applied Geochemistry, 25.

Zheng, W., Foucher, D., Hintelmann, H., 2007. Mercury isotope fractionation during volatilization of Hg (0) from solution into the gas phase. Journal of Analytical Atomic Spectrometry, 22(9): 1097-1104.

Zheng, W., Hintelmann, H., 2010. Nuclear field shift effect in isotope fractionation of mercury during abiotic reduction in the absence of light. The journal of physical chemistry. A, 114(12): 4238-4245.

CHAPTER 4

Mercury isotope exchange between dissolved Hg(0) and Hg(II)

ABSTRACT

Mercury (Hg) stable isotopes have developed into powerful tools of tracing Hg sources and chemical transformations in the environment. Dissolved Hg(0) and Hg(II) often coexist in the environment; if they exchange isotopes at substantial rates, Hg isotope ratios could be greatly affected without chemical transformations taking place. This would have far-reaching consequences for our ability to interpret isotopic data collected in the field. We conducted experiments aimed at determining the rate at which isotopes are exchanged and isotopic equilibrium between dissolved Hg(II) and Hg(0) in a simple matrix (5mM $NaHCO_3$ and 1mM NaCl) under anoxic conditions. The dissolved Hg(0) pool was generated by a metallic Hg bead in a silicone tube, equilibrated with the water for 5 days. Hg(II) was injected and mixed with a smaller, unintended Hg(II) pool already present. The combined Hg(II) pool and the Hg(0) were initially far from isotopic equilibrium, but shifted close to expected isotopic equilibrium values within minutes. The Hg isotopes appear to have reached isotopic equilibrium in less than 48 hours. The δ^{202}Hg difference between the Hg(II) pool and the dissolved Hg(0) pool were measured at 2.32‰ and 2.53‰ for the two experiments, respectively. The rapid exchange observed is likely related to the formation of Hg(I) dimers (Hg_2^{2+}), which greatly enhance the exchange of two electrons between Hg(II) and Hg(0) atoms, resulting in isotopic exchange. More complex matrices containing stronger ligands such as thiols should be investigated in order to better predict isotopic exchange rates in natural waters.

INTRODUCTION

Mercury (Hg) is a globally circulating contaminant (U.S. Environmental Protection Agency, 1997; U.S. Environmental Protection Agency, 2006). It is a redox-active element, with two main oxidation states in nature. Hg(0) is volatile, sparingly soluble, less toxic and less reactive relative to Hg(II), which is highly soluble, reactive, and has the ability to transform into methylmercury, a very toxic form of Hg (Hsu-Kim et al., 2013). Accordingly, mercury's redox chemistry plays a major role in its bioavailability and environmental impacts. Hg has been found ubiquitously in many environmental settings, from snow in the arctic to the amazon (Harada et al., 2001; Blum, 2011). Hg contamination is an important environmental issue due to its toxicity to humans and animals (Dietz et al., 2012; Syversen and Kaur, 2012). Recently, isotope ratios have been shown to be powerful tools in detecting and tracing Hg as it moves through the environment (Foucher et al., 2009; Feng et al., 2010; Perrot et al., 2010; Estrade et al., 2011; Gehrke et al., 2011b; Liu et al., 2011; Day et al., 2012; Sherman et al., 2012; Bartov et al., 2013; Wiederhold et al., 2013; Yin et al., 2013b; Donovan et al., 2014; Li et al., 2014; Tsui et al., 2014).

Hg readily goes through redox changes once it enters the environment, which means that both Hg(II) and Hg(0) are very likely to be in contact with each other. Hg(0) released into the environment can easily get oxidized by dissolved O_2 in water (de Magalhães and Tubino, 1995; Amyot et al., 1997). O'Concubhair et al. (2012) have observed that Hg(0) can also get oxidized in polar ice without the need for photochemistry. Hg(0) can also be oxidized in anoxic conditions, conditions that are not usually associated with oxidizing potential. Thiol compounds (Zheng et al., 2013), anaerobic bacteria (Hu et al., 2013) and dissolved organic matter (Zheng et al., 2012) can oxidize Hg(0) under anoxic conditions. Zheng et al. (2012) have also observed that dissolved organic matter has the ability to also reduce Hg(II) under the same anoxic conditions, which means

that Hg(II) and Hg(0) have the potential to coexist in anoxic waters regardless of whether it enters the environment as Hg(II) or Hg(0). Hg(II) has been observed to be reduced abiotically (Bergquist and Blum, 2007; Zheng and Hintelmann, 2009; Zheng and Hintelmann, 2010a; Zheng and Hintelmann, 2010b; Pasakarnis et al., 2013) and microbially (Kritee et al., 2007; Kritee et al., 2008). These redox changes of Hg may result in Hg(0) and Hg(II) coexisting with one another in the environment.

Hg isotope geochemistry. Recently, Hg isotope ratio measurements have been shown to be powerful tools, useful for tracing Hg as it moves through the environment and for detecting certain biogeochemical processes that affect its environmental behavior. Hg has 7 stable isotopes, ranging in mass from 196 to 204. Variations in the relative abundances of these isotopes are expressed as variations in the $^{199}Hg/^{198}Hg$, $^{200}Hg/^{198}Hg$, $^{201}Hg/^{198}Hg$, and $^{202}Hg/^{198}Hg$ ratios. The other two isotopes (196 and 204) are generally not used due to their low natural abundances. The measured variations are reported as per mil (‰, parts per thousand) deviations from NIST 3133, an accepted inter-laboratory standard, using δ-notation, defined as:

$$\delta^{202}Hg = \left(\frac{^{202}/_{198}Hg_{sample}}{^{202}/_{198}Hg_{standard}} - 1\right) * 1000‰ \quad (1)$$

Hg isotope ratio deviations can be caused by a few different types of isotopic fractionation. The first of these is referred to as mass dependent fractionation (MDF). During chemical reactions of Hg, the lighter isotopes tend to react at a slightly faster rate than the heavier isotopes, causing the product to be enriched in the lighter isotopes. Reactions that have been observed to exhibit MDF include reduction of Hg(II) to Hg(0) (microbial (Kritee et al., 2007; Kritee et al., 2008) and abiotic (Bergquist and Blum, 2007)), evaporation (Estrade et al., 2009; Ghosh et al., 2013), methylation (Rodríguez-González et al., 2009; Jiménez-Moreno et al., 2013), and equilibration between

aqueous and adsorbed species (Wiederhold et al., 2010; Jiskra et al., 2012). The $^{202}Hg/^{198}Hg$ ratio, expressed as $\delta^{202}Hg$, is used to quantify MDF.

Hg has also been shown to exhibit mass independent fractionation (MIF) (Bergquist and Blum, 2007; Estrade et al., 2009; Mead et al., 2013). MIF occurs when chemical processes fractionate Hg isotopes in a manner not related to their difference in mass. MIF is expressed as the deviation of an isotope ratio (i.e. $^{199}Hg/^{198}Hg$, $^{200}Hg/^{198}Hg$, or $^{201}Hg/^{198}Hg$) from the value expected assuming MDF alone, as indicated by the measured $\delta^{202}Hg$. MIF is expressed using "capital delta'-notation defined as:

$$\Delta^{199}Hg = 1000 * \left(\left[\ln\left(\left(\delta^{199}Hg/1000\right)+1\right)\right] - 0.252\left[\ln\left(\left(\delta^{202}Hg/1000\right)+1\right)\right]\right) \quad (2)$$

$$\Delta^{200}Hg = 1000 * \left(\left[\ln\left(\left(\delta^{200}Hg/1000\right)+1\right)\right] - 0.502\left[\ln\left(\left(\delta^{202}Hg/1000\right)+1\right)\right]\right) \quad (3)$$

$$\Delta^{201}Hg = 1000 * \left(\left[\ln\left(\left(\delta^{201}Hg/1000\right)+1\right)\right] - 0.752\left[\ln\left(\left(\delta^{202}Hg/1000\right)+1\right)\right]\right) \quad (4)$$

Currently, three processes are known to generate MIF: The first, and largest, is the magnetic isotope effect (MIE), which affects only the odd isotopes of Hg (^{199}Hg and ^{201}Hg) which have nuclear spins. During photochemical transformations, in which radical pairs are formed, the nuclei of the odd isotopes are able to exchange their spin with unpaired electrons and this affects the reaction rates of the odd isotopes. Bergquist and Blum (2007) observed MIE in photochemical reduction of Hg(II) and methyl-Hg.

The second phenomenon, known as the nuclear field shift or nuclear volume effect (NVE), affects all Hg isotopes. The interaction of certain electron orbitals with the nucleus depends on the size of the nucleus. Therefore, the different Hg isotopes differ slightly in their chemical properties due to differences in nuclear size, resulting in NVE and thus isotopic fractionation. For Hg, the 6s electrons are the orbitals affected by Hg(0)-Hg(II) redox reactions, and it happens that the sense of fractionation, with Hg(0) being depleted in the heavier isotopes, is the same as for MDF.

Furthermore, the effects of nuclear size are close to a linear function of mass, and thus, the effect of NVE are very similar to MDF (Schauble, 2007). However, the ^{199}Hg and ^{201}Hg nuclear sizes depart slightly from this linear relationship, and are anomalously small, resulting in small deviations of ^{199}Hg/^{202}Hg and ^{201}Hg/^{202}Hg from values consistent with MDF (i.e. non-zero values of Δ^{199}Hg and Δ^{201}Hg).

The ^{200}Hg/^{198}Hg ratio is generally used as a check for analytical quality, as it usually conforms to MDF. However, small deviations from MDF have been observed for this ratio in rainfall (Gratz et al., 2010; Chen et al., 2012). Large MIF effects in all Hg isotopes, including ^{200}Hg, have been observed in compact fluorescent lighting. These MIF effects are believed to be caused by "self-shielding" of Hg from the intense ultraviolet radiation produced inside (Mead et al., 2013).

Applications of Hg stable isotopes. Recently, Hg isotope fractionation has been developed as a very powerful tool that enables us to follow Hg systematics in the environment. There have been many studies looking at the isotopic compositions of environmental sources of Hg such as coals, cinnabar, fumaroles, mine tailings and calcine sediments, and chondrites (Evans et al., 2001; Lauretta et al., 2001; Hintelmann and Lu, 2003; Smith et al., 2005; Biswas et al., 2008; Smith et al., 2008; Sonke et al., 2008; Gehrke et al., 2011b; Lefticariu et al., 2011; Yin et al., 2014). In order to understand how Hg isotopes respond to chemical processes as Hg moves through the environment, experiments with redox reactions and other chemical transformations (such as sorption and methylation) were conducted. Experiments have shown that Hg fractionates both mass dependently and independently during reduction (both abiotic and microbially mediated (Bergquist and Blum, 2007; Kritee et al., 2007; Kritee et al., 2008; Zheng and Hintelmann, 2009; Zheng and Hintelmann, 2010b)). Abiotic and microbially mediated Hg demethylation have also been shown to induce MDF and MIF (Bergquist and Blum, 2007; Kritee et al., 2009). Methylation

experiments conducted using microbes and methylcobalamin have reported detectable isotopic fractionation during Hg methylation (Rodríguez-González et al., 2009; Jiménez-Moreno et al., 2013). Finally, recent experiments have shown that trophic transfer of Hg does not induce an isotopic fractionation (Kwon et al., 2012; Kwon et al., 2013); this is an important isotope effect of Hg when it moves through the environment.

Scientists have applied the knowledge gained through experimental work to track Hg and its chemical transformations in the environment. Apportioning of contaminant Hg from mines and industrial spills is now possible (Foucher et al., 2009; Liu et al., 2011; Sherman et al., 2012; Bartov et al., 2013; Donovan et al., 2014). It is also possible to use Hg isotopes in order to identify different sources affecting animals and people (Laffont et al., 2009; Perrot et al., 2010; Gehrke et al., 2011a; Laffont et al., 2011; Day et al., 2012; Perrot et al., 2012; Tsui et al., 2012; Sherman et al., 2013; Kwon et al., 2014; Li et al., 2014). Interestingly, plants have been found to fractionate Hg as they take it up from the environment (Ghosh et al., 2008; Demers et al., 2013; Yin et al., 2013). Mercury isotope fractionation has also been used in order to track Hg cycling through the environment (Yin et al., 2012; Foucher et al., 2013; Wiederhold et al., 2013), while other studies have also reported anomalous isotopic fractionation values in precipitation and ambient air, which are believed to be associated with the "self-shielding" effect being observed in the environment (Gratz et al., 2010; Chen et al., 2012).

Non-kinetic isotope fractionation effects. In order to apply Hg isotopes as tools for tracking Hg sources and chemical transformations through the environment, we must understand all relevant processes that might induce an isotopic fractionation. Kinetic processes that change the redox state of Hg have been the focus of most work attempting to reveal how Hg isotope ratios are affected by chemical processes. However, there are equilibrium processes, such as adsorption, that

don't involve a change in the Hg redox state. Wiederhold et al. (2010) and Jiskra et al. (2012) observed a mass dependent fractionation associated with aqueous Hg adsorbing onto a thiol-resin (0.53–0.62‰) and Goethite (0.34‰). Aside from adsorption, isotopic exchange between coexisting Hg(II) and Hg(0) also has the potential to shift the isotopic values observed in the environment. When dissolved Hg(II) and Hg(0) coexist, they have the potential to exchange isotopes in the following reaction:

$$^{198}Hg(II) + {}^{202}Hg(0) = {}^{202}Hg(II) + {}^{198}Hg(0) \quad (5)$$

The net result of this reaction is isotopic exchange between the two redox states without net redox reaction in the system. If this reaction proceeds at a substantial rate, the ^{202}Hg/^{199}Hg ratios of the two Hg pools will shift until equilibrium is attained.

No studies of the isotopic exchange of Hg(0) and Hg(II) have been conducted to date. However, isotopic exchange has been observed with other elements such as sulfur (Sakai and Dickson, 1978; Ohmoto and Lasaga, 1982) oxygen (Chiba and Sakai, 1985; Fritz et al., 1989), iron (Anbar et al., 2000; Roe et al., 2003; Welch et al., 2003), chromium, and uranium (Wang, 2013). It has been observed that Fe(II) and Fe(III) exhibit very rapid isotopic exchange that rapidly establishes isotopic equilibrium (e.g. in less than a minute (Welch et al., 2003)). The rapid isotopic exchange is not surprising given the fact that a single electron transfer accomplishes isotopic exchange between Fe(II) and Fe(III), without any change of Fe-O coordination. More recently, isotopic exchange rates for uranium (2 electrons transferred, U(IV)–U(VI)) and chromium (3 electrons, Cr(III)–Cr(IV)) have been found to be much slower than that of Fe (Wang, 2013). Presumably this is because isotopic exchange in these cases requires coordination changes and transfer of multiple electrons. However, exchange may be fast enough in some cases to significantly alter the isotopic compositions of coexisting Cr(III) and Cr(VI), or U(VI) and U(IV) (Wang, 2013).

In the case of Hg, isotopic exchange (equation 5) could likewise have important effects on Hg isotope ratios in certain geochemical systems. For example, artisanal gold mining in the Amazon jungle has resulted in large amounts of metallic Hg(0) contaminating the river basin (Harada et al., 2001; Laffont et al., 2009). As dissolved Hg(0) is oxidized to Hg(II), both species are in contact with each other. If, isotopic exchange between them occurs at a sufficient rate, it would overprint isotopic fractionation caused by kinetic processes. Measured values would thus record only the isotopic equilibrium and not previous kinetic processes. The rate of isotopic exchange must be determined before the importance of such effects can be assessed.

In this study, we present data from experiments designed to determine if isotopic exchange between dissolved Hg(II) and Hg(0) species is fast enough to significantly affect isotope ratios of these species, and determine the equilibrium fractionation factor if indeed equilibrium can be attained. In order to examine exchange in the absence of net redox reactions, experiments consisted of Hg(0) and Hg(II) coexisting in aqueous solution in dark, anoxic conditions, with a simple $NaHCO_3$ and NaCl matrix.

METHODS

Experimental design. The experiments were conducted in a buffer solution containing 5mM $NaHCO_3$ and 1mM NaCl, dissolved in 18.2MΩ cm^{-1} water. The experiments were designed to be saturated with Hg(0) in the solution and have an excess of Hg(0). For each experimental bottle, a Hg(0) source was created by placing a ~0.1 mg drop of metallic Hg (Sigma-Aldrich®, electronic grade, 99.9999%) in a short segment of acid-cleaned silicone rubber tubing and plugging the tubing ends with silicone-filled pipette tips. With this configuration, Hg(0) can diffuse through the tubing and into the solution, but metallic Hg(0) is retained. Three acid-cleaned 125mL serum bottles were filled with 100mL of the buffer solution, and a Hg(0)-containing silicone tube was

added to each. Two other serum bottles were made up as identical control experiments, except they did not contain Hg(0); one had an empty, sealed silicone tube, and the other only had the experimental solution in it. All bottles were purged of O_2 by bubbling with ultra-pure N_2 gas for at least an hour and were left with a positive N_2 pressure. The bottles were wrapped in aluminum foil to avoid photochemical reactions and allowed to equilibrate for at least 5 days. This allowed ample time for the buffer solution's dissolved Hg(0) concentration and isotopic values to reach equilibrium with the metallic Hg(0).

The Hg(II) stock solution was made with the goal of obtaining an isotopically light solution that would be far from isotopic equilibrium with the dissolved Hg(0) in the experiments. A small drop of the stock metallic Hg(0) was placed in a stoppered serum bottle, and a stream of O_2-free N_2 was passed through the headspace. Hg(0) vapor, evaporated from the metallic Hg(0), was swept into a 100mL 0.2M BrCl trap solution until its concentration reached about 10 mg/L. The BrCl solution was made following the EPA Method 1631 (U.S. Environmental Protection Agency, 2002). Once the desired Hg concentration was reached, the BrCl trap was deoxygenated by bubbling O_2-free N_2 gas into open air for two hours, then sealed. The headspace was then flushed with O_2-free N_2 for another 40 minutes to obtain an O_2-free stock solution. At the start of the experiment, 1.5mL of the Hg(II) stock solution was injected into 4 of the 5 bottles (Experiments A and B, and two Hg(II)-only controls), leaving one Hg(0)-containing bottle as a control experiment with no Hg(II) injected. The Hg(0)-only control had a 1.5mL N_2 injection in order to have the same volume change as the other 4 bottles. The final Hg(II) concentration target in each bottle was 150ppb.

Experiments were sampled 3 times in the first 20 minutes after injection, and then at 2, 24, and 48 hours after injection. All sampling syringes were deoxygenated by pulling 6 syringe volumes of O_2-free N_2 gas from an active N_2 flow. At each sampling time, a 1mL aliquot was removed from

the reactor and injected into an open, acid-cleaned glass tube for Hg(0)-stripping. Hg(0) was swept from the sample solution by bubbling for 5 minutes with a stream of O_2-free N_2 that was passed into 20mL of 10% (v/v) BrCl trapping solution. The Hg(II) remained in the sample solution, which was mixed with a 7.5mL 1% BrCl solution to ensure stability during storage. For the Hg(0)-absent experiments, containing only Hg(II), 1mL aliquots were removed and injected directly into 10mL 1% BrCl solutions without the purging step. Samples were analyzed for isotope ratios directly without a matrix removal step because matrix components present do not interfere in any way with the isotopic analysis.

Mass spectrometry. Mass spectrometry followed the methods of Mead and Johnson (2010). Samples were diluted, then spiked with a calibrated $^{204}Hg/^{196}Hg$ double spike. Isotopic compositions ($^{199}Hg/^{198}Hg$, $^{200}Hg/^{198}Hg$, $^{201}Hg/^{198}Hg$, $^{202}Hg/^{198}Hg$) were measured on a Nu Plasma multi-collector inductively coupled plasma mass spectrometer (MC-ICP-MS) at the University of Illinois Urbana-Champaign. Hg was introduced into the instrument using cold vapor generation. During analysis, sample concentrations were between 1 and 3 ppb and the ^{202}Hg intensity was typically 1.2V for a 1 ppb solution. During data collection, each sample was measured 50 times with a 5 second integration time per measurement. On-peak zeroes were measured for 2.5 minutes before sample analysis begins. The instrument's mass bias was determined from the measured $^{204}Hg/^{196}Hg$ ratio using an iterative deconvolution routine described in Mead and Johnson (2010). Isobaric interferences were monitored by measuring $^{194}Pt^+$, $^{203}Tl^+$, $^{206}Pb^+$, and $^{196}HgH^+$. Results were corrected for HgH^+ interferences on masses 199, 200, 201, and 202. Pt, Tl, and Pb interferences were always found to be negligible.

The long-term reproducibility of the isotopic method was determined by preparing and analyzing 6 replicate samples out of the 55 samples analyzed in total. The root mean square $\delta^{202}Hg$ difference

for these replicates, calculated following Hyslop and White (2009), was found to be 0.06‰; therefore, we estimate our 95% confidence interval to be ±0.13‰. The 95% confidence intervals for Δ^{199}Hg and Δ^{201}Hg are calculated as 0.04‰ and 0.02‰, respectively. Concentrations were determined via isotope dilution using the double spike to sample ratio. The 95% confidence interval for concentrations is 2%.

RESULTS

Injected Hg(II). The two Hg(II)-only controls averaged 145.0 ± 4.1 μg L^{-1} (1SD) throughout the experiment, very close to the expected 150 μg L^{-1}, with very minor changes over time. That indicates that the injection of Hg(II) stock solution was precise and accurate. The consistency of the concentrations over time indicates there is no gain of Hg(II) contamination nor major loss due to reduction or adsorption. Also, δ^{202}Hg values were constant within the analytical uncertainty (average −1.81 ± 0.06‰ (1SD); Table 4.1, Figure 4.2), further supporting the idea that there are no unintended processes affecting the Hg(II).

Hg(0) concentrations. Experiment C, the Hg(0)-only control, had a dissolved Hg(0) concentration around 40 μg L^{-1}, close to the expected theoretical equilibrium value in the presence of Hg metal. However, after the injection of 1.5 mL N_2 gas (done to match the pressure increase of the actual experiments, A and B), the dissolved Hg(0) concentration increased by 39% in the first half hour before returning to its initial value. The Hg(0) concentrations of experiments A and B also varied in the first half hour after injection; however, their concentrations decreased before recovering to their initial values (Table 4.1).

Bottles A, B, and C do not converge to the same Hg(0) concentration after 48 hours. That indicates either a lack of equilibrium with the metallic Hg, or that the equilibrium was different, depending on the exact conditions in each of the bottles.

Unintended Hg(II) prior to Hg(II) injections. Unintended dissolved Hg(II) was present in experiments A, B, and C prior to Hg(II) injection, when the solutions should have contained only Hg(0). The samples taken after injection had higher Hg(II) concentrations than expected, indicating that unintended Hg(II) carried over from before the Hg(II) injections. Roughly 27% of the Hg(II) injected in bottle A and 41% of the injected Hg(II) in bottle B was composed of this Hg(II) contamination. The amounts of contamination, calculated by subtracting the known mass of injected Hg(II) from the measured Hg(II) after injection, are 52.9 μg L^{-1} and 102.1 μg L^{-1} for bottles A and B, respectively. The contaminant Hg(II) can also be calculated from pre-injection measurements, by subtracting the Hg(0) fraction from the measured total Hg. These calculations give values that are both ~24 μg L^{-1} lower (29.9 μg L^{-1} and 79.7 μg L^{-1}, respectively) (Table 4.1).

Total dissolved Hg and Hg(0) isotopic values were measured for samples taken prior to the injection of Hg(II) at the start the experiments. We estimate the isotopic composition of the contaminant Hg(II using the isotopic mass balance equation:

$$\delta_{Mixture} m_{Mixture} = \delta_A m_A + \delta_B m_B \quad (6)$$

Where δ and m are the δ-value and mass of components, and the subscripts refer to the mixture (total Hg) and components A and B. The contaminant Hg(II) δ^{202}Hg values were found to be −0.55‰, 0.07‰, and −0.05‰ for bottles A, B, and C (Hg(0)-only control), respectively. These calculations indicate that the contaminant Hg(II) was isotopically heavy relative to both Hg(0) and injected Hg(II) pools. Using the calculated δ-values and concentrations of the contaminant, the known concentration and measured δ^{202}Hg of the injected Hg(II), and equation 6, we calculated

the starting δ^{202}Hg values of the dissolved Hg(II), immediately after Hg(II) injections, to be −1.46‰ and −1.03‰, respectively (Table 4.1, Figure 4.3).

Isotopic evolution. Isotopic shifts occurred quickly in the first few minutes after Hg(II) injection (Figures 4.2, 4.3, and 4.4); the Hg(0) δ^{202}Hg values of experiments A and B dropped from pre-injection values of −1.90‰ and −1.85‰, respectively, to −3.17‰ and −3.10‰, respectively. After this initial rapid shift; a slower increase followed, with the δ^{202}Hg becoming progressively greater over the 48 hours of sampling, ending at −2.73‰ and −2.76‰, respectively. The δ^{202}Hg value of the Hg(0) in bottle C, the Hg(0)-only control, dropped to −2.73‰ after the blank N_2 injection, then slowly increased to −1.96‰ after 48 hours (Table 4.1, Figure 4.2).

The δ^{202}Hg values of the Hg(II) fractions of experiments A and B also shifted rapidly in the first few minutes, increasing to −0.49‰ and −0.23‰, respectively, from the calculated starting values of −1.46‰ and −1.03‰, respectively. After the first few minutes, a slower increase occurred, with the Hg(II) δ^{202}Hg values increasing roughly in parallel with the Hg(0) values.

The δ^{202}Hg difference between the Hg(II) and Hg(0) pools rapidly increased from 0.51‰ and 0.81‰, respectively, to 1.93‰ and 2.28‰, respectively, within a few minutes after the injection of Hg(II) into experiments A and B (Figure 4.3). After that, difference increased more slowly over time, for both bottles. However, bottle B always had a larger isotopic difference than bottle A (Table 4.2, Figure 4.4). The final δ^{202}Hg differences between the Hg(II) and Hg(0) pools in experiments A and B were calculated to be 2.32‰ and 2.53‰, respectively.

DISCUSSION

Hg(0) concentrations changes in the Hg(0)-only control. The Hg(0) concentrations and isotopic values of the Hg(0)-only control were expected to remain constant after the start of the experiments, but changes were observed. Shortly after the injection of 1.5mL of N_2 designed to

match the pressure increase in experiments A and B as they started, the Hg(0) concentrations increased and the δ^{202}Hg values decreased before starting to recover after 1.2 hours (Figures 4.2, 4.3). These effects must be caused by the increased pressure induced by the N_2 injection, because no other changes occurred. The initial injection of N_2 gas was not followed by a removal of the same volume, and therefore increased pressure in the bottle. We expect pressure changes to affect the metallic Hg-dissolved Hg(0) and dissolved Hg(0)-headspace Hg(0) equilibria. The possibility of O_2 incursion into the bottle is highly unlikely since the N_2 gas used is ultra-high purity and is passed through a copper scrubber. While O_2 could affect the isotopic values by causing oxidation, that would cause the Hg(0) concentrations to decrease rather than increase, as observed. The increase in pressure due to the N_2 injection likely changed the gaseous Hg(0)-dissolved Hg(0) equilibrium and caused the Hg(0) in the headspace to get re-dissolved which increased the concentrations and dropped its isotopic values.

Hg(II) contamination. The significant unintended Hg(II) pools present prior to the Hg(II) injection (Table 4.1) in experiments A and B were likely caused by oxidation of Hg(0). It is possible that during the Hg(0) equilibration time with the liquid, O_2 trapped in the silicone tube diffused into the water and oxidized the Hg(0) into Hg(II). The silicone caulk also appears to breakdown slightly in the water, and air pockets could have burst into the water, releasing O_2. However, the presence of two sources of Hg(II) has little impact on the interpretation of the data. The starting δ^{202}Hg values of the Hg(II) immediately after injection, before significant isotopic exchange occurred, while not measured directly, are well constrained by mass balance. In order to check the sensitivity of the calculated values to our assumptions, we performed the calculations using both approaches to estimating Hg(II) concentrations present before injection (see results). The maximum difference between the two calculated values is 0.06‰.

In both experiments, A and B, the measured Hg(II) after injection exceeds the sum of the injected Hg(II) and the Hg(II) inferred from the pre-injection data by 24 μg L^{-1}. This suggests that there might have been oxidation of Hg(0) immediately after injection of Hg(II). Since the Hg(II) stock used was made by bubbling Hg(0) vapor into a 0.2M BrCl trap, it is possible that a trace of BrCl remained in the injected solution, which would have rapidly oxidized some Hg(0) in the experiments. If we assume a scenario in which rapid oxidation took place after injection, we can recalculate the expected Hg(II) δ^{202}Hg value we would expect. However, the Hg(II) generated by oxidation, if any, was small and has little effect on data interpretation. If we assume the oxidized Hg(II) was 0.15‰ (2‰ heavier than the Hg(0); a worst case scenario), and use equation 6, the calculated initial Hg(II)-values only shift by +0.08‰ and +0.01‰ for bottles A and B, respectively.

The initial large drop in the Hg(0) isotopic values (Table 4.1, Figure 4.3), could be caused in part by this potential rapid oxidation. Since there are no published data on the isotopic fractionation factor associated with oxidation of Hg(0), we begin with a worst-case fractionation factor of +2‰. Using a Rayleigh model, we calculate that 35% of the Hg(0) initially present in the bottles would need to oxidize to cause all of the observed shift. However, the concentration drop from the pre-injection Hg(0) measurements and the first sample post-injection only 12% for bottle A, and 14% for bottle B. The concentrations in bottle C increased by 9% shortly after the N_2 injection; if we allow the concentrations of bottles A and B to increase by 9 % as well, we get a concentration drop of 19% and 21%, respectively, which is still too small of a concentration drop if oxidation is causing the observed isotopic shift. In summary, the worst-case Hg(0) oxidation scenario cannot fully account for the large decrease observed in the δ^{202}Hg values of the Hg(0) in experiments A

and B. More moderate scenarios produce greater mismatch to the data, and we conclude that isotopic exchange must have occurred.

Adsorption. There is no evidence for adsorption of Hg(II) or Hg(0) onto solid surfaces in the experimental bottles, so we rule this process out as a cause of the observed isotopic shifts. The aqueous concentrations of Hg(II) remain constant throughout the experiment, and the Hg(0) concentrations recover to their pre-injection values shortly after the Hg(II) injection (Figure 4.1). Secondly, both Hg(II)-only control experiments did not change concentration-wise or isotopically over time., which is what we would expect if sorption was taking place (Wiederhold et al., 2010; Jiskra et al., 2012).

Hg(0) and Hg(II) isotopic exchange. The processes considered above (oxidation and sorption) cannot account for the rapid isotopic shifts in both Hg(0) and Hg(II) in the first few minutes; isotopic exchange is the only remaining process that could cause the observed isotopic shifts. After injection of the Hg(II), the offset between the dissolved Hg(0) and Hg(II) pools increased from 0.44‰ and 0.82‰, respectively, to 1.93‰ and 2.28‰, respectively. The offset was attained by a small positive shift in the Hg(II) pool and a large negative shift in the Hg(0) fraction. That is expected for isotopic exchange between the two pools, as the concentrations of Hg(II) were about three times larger than the Hg(0) concentrations. As isotopic equilibrium was approached, the rate of change slowed and equilibrium was apparently reached over the next few hours, with the final isotopic offset within the range of calculated values for equilibrium between Hg(0) and various Hg(II) species given by Schauble (2007) (Table 4.2, Figures 4.3, 4.4). Unfortunately, it is not possible to use any one calculated isotopic value for the equilibrium offset because the speciation of the Hg(II) in the experiments is not a single dissolved Hg(II) species. We expect the speciation in the BrCl trap was $HgCl_4$; however, once injected into the experiments, it respeciated to a

combination of $HgCl_2$, $HgCl_3$, and $HgCl_4$. Schauble (2007) calculated the equilibrium offset of $HgCl_2$ and $HgCl_4$ from Hg(0) and found that different Hg(II) complexes have different equilibrium offsets from Hg(0); therefore, we expect the final equilibrium offset between the dissolved Hg(II) and Hg(0) in our experiments to be within the range of 2.19–2.78‰.

The difference between the offsets in experiments A and B (Table 4.2, Figure 4.4) is puzzling, as the experiments were very nearly identical. However, differences in Hg(II) speciation may have existed because of unintended ligands present due to silicone caulk breakdown observed in the bottles. Silicone caulk is composed of multiple silicone polymers containing organic compounds (Waterford Plant, 2007; DAP Products Inc., 2013). These polymers hydrolyze and release acetate, which has the ability to form complexes with Hg easily (Farrah and Pickering, 1978; Sigel and Sigel, 1997; Franta, 2012; Organization for Economic Cooperation and Development, 2012). Calculations by Schauble (2007) show that different Hg(II) complexes have different isotopic offsets from Hg(0) at equilibrium. It is likely the silicone caulk released different amounts of acetate in the different bottles, leading to a difference in Hg(II)-acetate complex formation between the bottles. Although we cannot be sure this difference was great enough to cause the observed discrepancy between the experiments, it provides a plausible scenario.

The Hg(0)-only control had a smaller final offset between the $\delta^{202}Hg$ values of Hg(II) and Hg(0) compared to experiments A and B. The BrCl trap was made using 6M HCl and high concentrations of Cl^- and Br^-. While the dilution of the BrCl matrix is large, the BrCl matrix was still able to acidify experiments A and B and ensure the speciation of the Hg(II) in the bottles be dominated by Cl^-. Hg(0)-only control bottle C was only injected with 1.5mL N_2. The 5mM $NaHCO_3$ present in bottle C kept the pH high enough to make $Hg(OH)_2$ complexes the dominant Hg(II) species. While we do not have calculations for the expected equilibrium fractionation for any of the Hg(II)

species in the bottle C, it is likely that the difference in Hg(II) speciation was the cause for the lower equilibrium offset detected.

Calculating the mass balance of the experiments allows us to check and verify that the isotopic shift we observe is correct. Using equation 6 we calculated the total Hg isotopic composition present in the bottles after injection by using the mass of Hg(II) injected and measured total Hg concentrations prior to injection. There is very good agreement between the mass balance calculations and observations, indicating that what we observed is due to the isotopic exchange. It is important to note that the $Hg(0)_g$ fraction of the experiments is unknown, and it is assumed, as mentioned above, that the Hg(0) bead did not isotopically interact with the dissolved Hg(0) fraction for the first 0.3 hours of the experiments.

The slow increase of the $\delta^{202}Hg$ values of both Hg(0) and Hg(II) that occurs after 1.8 hours is consistent with known processes. Because of the shifts that occurred in the first minutes of the experiments, the dissolved Hg(0) and the metallic Hg(0) were forced out of equilibrium. The metallic Hg bead has a much larger mass than the dissolved Hg(0), and therefore, we expect the $\delta^{202}Hg$ of the dissolved Hg(0) to evolve towards isotopic equilibrium with the metallic Hg, i.e., towards the pre-injection value. This equilibration occurs via diffusion through the silicone tubing, and accordingly, we expect it to be rather slow, which we observe. If the Hg(II) and Hg(0) are near isotopic equilibrium, we would expect both pools to shift in parallel to each other as we observe.

Mass independent fractionation. The nuclear volume effect is apparent in the isotopic fractionation observed in the experiments. Figure 4.5 shows the measured $\delta^{199}Hg$, $\delta^{200}Hg$, and $\delta^{201}Hg$ values plotted versus the measured $\delta^{202}Hg$ in the experimental samples. All the data fall off the fractionation lines calculated based on mass dependent fractionation. The slopes of the data are consistent with slopes calculated for a combination of the nuclear volume effect and mass

dependent fractionation, based on the most recent published measurements of nuclear radii (Schauble, 2007; Angeli and Marinova, 2013).

Isotopic exchange mechanisms. The rapid isotopic exchange we observed can be rationalized based on known aspects of Hg chemistry. Hg(0)-Hg(II) isotopic exchange requires transfer of two electrons, similar to isotopic exchange between U(IV) and U(VI). It is expected that exchange rates are slower when more electrons must be transferred between atoms. Cr, which requires transfer of three electrons in order to reach isotopic equilibrium, exhibits very slow isotopic exchange, with concentrated solutions requiring years to attain isotopic equilibrium at room temperature (Wang, 2013). At the other extreme, Fe reaches isotopic equilibrium within minutes due to the fact that its redox couple is only a 1 electron difference (Fe(II) and Fe(III)) and no change of coordination takes place. U(IV)-U(VI) exchange involves transfer of two electrons, and requires the intermediate U(V) species to interact with another U atom before the exchange is complete. Wang (2013), used very high concentrations of U (0.032 mol L^{-1}) in order to be able to reach isotopic equilibrium in 15 days.

We expect Hg exchange to occur through a similar processes, with electrons transferred one at a time, and a Hg(I) species as an intermediate product:

$$^{198}Hg(II) + {}^{202}Hg(0) = {}^{198}Hg(I) + {}^{202}Hg(I) \quad (7)$$

$$^{198}Hg(I) + {}^{202}Hg(I) = {}^{198}Hg(0) + {}^{202}Hg(II) \quad (8)$$

Accordingly, we originally expected exchange to occur over days or weeks. The concentrations in our experiments were 0.25 μmol L^{-1} for the dissolved Hg(0) and 1.25 μmol L^{-1} for the injected Hg(II), significantly lower concentrations than those of the U experiments. The lower concentrations should decrease the probability of Hg(0)-Hg(II) interactions, and thus we

hypothesized an exchange rate much slower than the rate observed by Wang (2013) for U(IV)-U(VI) exchange.

However, our results indicate that Hg approaches isotopic equilibrium surprisingly fast—within 48 hours. This suggests strong interaction between Hg(0) and Hg(II) that enhances electron exchange, the mechanism by which Hg isotopic exchange occurs. Such interaction is known to occur, in that coexisting Hg(0) and Hg(II) readily form a Hg(I) dimer (Hg_2^{2+}) (Armstrong and Halpern, 1956; Armstrong and Halpern, 1957; Moser and Voigt, 1957; Greenwood and Earnshaw, 1997; Catalano et al., 2002). The presence of this dimer, even if only in small abundance, will allow enhanced electron transfer. Thus, isotopic exchange would occur according to the following reactions showing the formation and decomposition of the dimer:

$$^{198}Hg(II) + {}^{202}Hg(0) = {}^{198}Hg^{202}Hg(I) \quad (9)$$

$$^{198}Hg^{202}Hg(I) = {}^{198}Hg(0) + {}^{202}Hg(II) \quad (10)$$

Reactions 9 and 10 are more likely to occur, as opposed to reactions 7 and 8, since monoatomic aqueous Hg(I) species are relatively unstable in solutions (Armstrong and Halpern, 1956; Moser and Voigt, 1957). Greenwood and Earnshaw (1997) summarize multiple lines of evidence supporting the existence of Hg(I) dimer, rather than monoatomic Hg(I). The Hg(I) dimer allows Hg to exchange the two isotopes quickly and reach isotopic equilibrium very rapidly.

Future implications. We have shown experimentally that Hg(0) and Hg(II) exchange isotopes very quickly in a simple NaCl matrix. Isotopic exchange is especially important as Hg isotopes are to be used to track Hg chemical transformations in the environment, where both Hg(0) and Hg(II) will be in contact with each other. The speed at which Hg approached isotopic equilibrium is surprisingly fast, approaching equilibrium in less than 48 hours. There are multiple chemical transformations that induce kinetic fractionation of Hg such as abiotic and microbial reduction

(Bergquist and Blum, 2007; Kritee et al., 2007; Kritee et al., 2008; Zheng and Hintelmann, 2009; Zheng and Hintelmann, 2010a; Zheng and Hintelmann, 2010b), demethylation (Bergquist and Blum, 2007; Kritee et al., 2009), and methylation (Rodríguez-González et al., 2009; Jiménez-Moreno et al., 2013); however, all of these processes would be overwritten by rapid attainment of isotopic equilibrium. Therefore, the Hg(0)-Hg(II) exchange kinetics need to be considered and studied further in order to assess whether field samples aimed at tracking kinetic effects are potentially overprinted by equilibrium fractionation.

More research should be conducted in order to elucidate the effect of stronger complexing ligands and lower concentrations on Hg isotope exchange. The experiments conducted had a very simple matrix, whereas natural environments have much more complicated matrices with stronger ligands than chloride. Experiments containing more complicated matrices and ligands, such as thiol groups, are needed in order to quantify mercury's ability to reach isotopic equilibrium in more natural settings. We expect that ligands such as thiols will slow down the isotopic exchange by decreasing the formation of the Hg(I) dimer. It is quite possible that as opposed to the present study, which suggests quick isotopic exchange between Hg(0) and Hg(II), natural systems will have very slow isotopic exchange due to complexation with carboxyl and thiol ligands, which is known to greatly decrease the activity of Hg(II) (Miller et al., 2009; Skyllberg and Drott, 2010; Gu et al., 2011).

CONCLUSIONS

Isotopic exchange between dissolved Hg(0) and Hg(II) in a simple NaCl matrix is fast. The offset between the total dissolved Hg(II) (unintended Hg(II) and injected Hg(II)) and Hg(0) evolved from 0.44‰ and 0.82‰, respectively, to 1.93‰ and 2.28‰, respectively, in the first few minutes after injection. While some of the offset was due to mixing of the two Hg(II) pools, it was not enough

to create the observed offset. After the initial jump, the Hg(II) isotopes evolved parallel to the Hg(0) isotopes as the metallic Hg and dissolved Hg(0) slowly re-equilibrated. Equilibrium was approached within 48 hours, much faster than originally expected; the creation of Hg(I) dimer is likely the reason Hg(0) and Hg(II) were able to transfer electrons so efficiently.

The equilibrium fractionation between dissolved Hg(0) and Hg(II) was found to be −2.32‰ and −2.53‰ for experiments A and B, respectively. The equilibrium fractionation is consistent with isotopic offset calculations between different Hg(II) species and Hg(0) conducted by Schauble (2007). The difference in equilibrium offsets between the two experimental bottles is likely due to the release of ligands from the silicone caulk used in the experiments. The lower isotopic offset measured in the Hg(0)-only control is likely due to the complicated Hg(II) speciation present in that bottle relative to experiments A and B.

Compared to our experiments, natural systems have lower concentrations of Hg(0) and Hg(II) and have much stronger ligands such as thiols, both of which are expected to slow down isotopic exchange by decreasing the Hg(I) dimer formation. More studies need to be conducted in order to understand Hg isotope exchange and equilibrium fractionation under more relevant conditions.

FIGURES AND TABLES

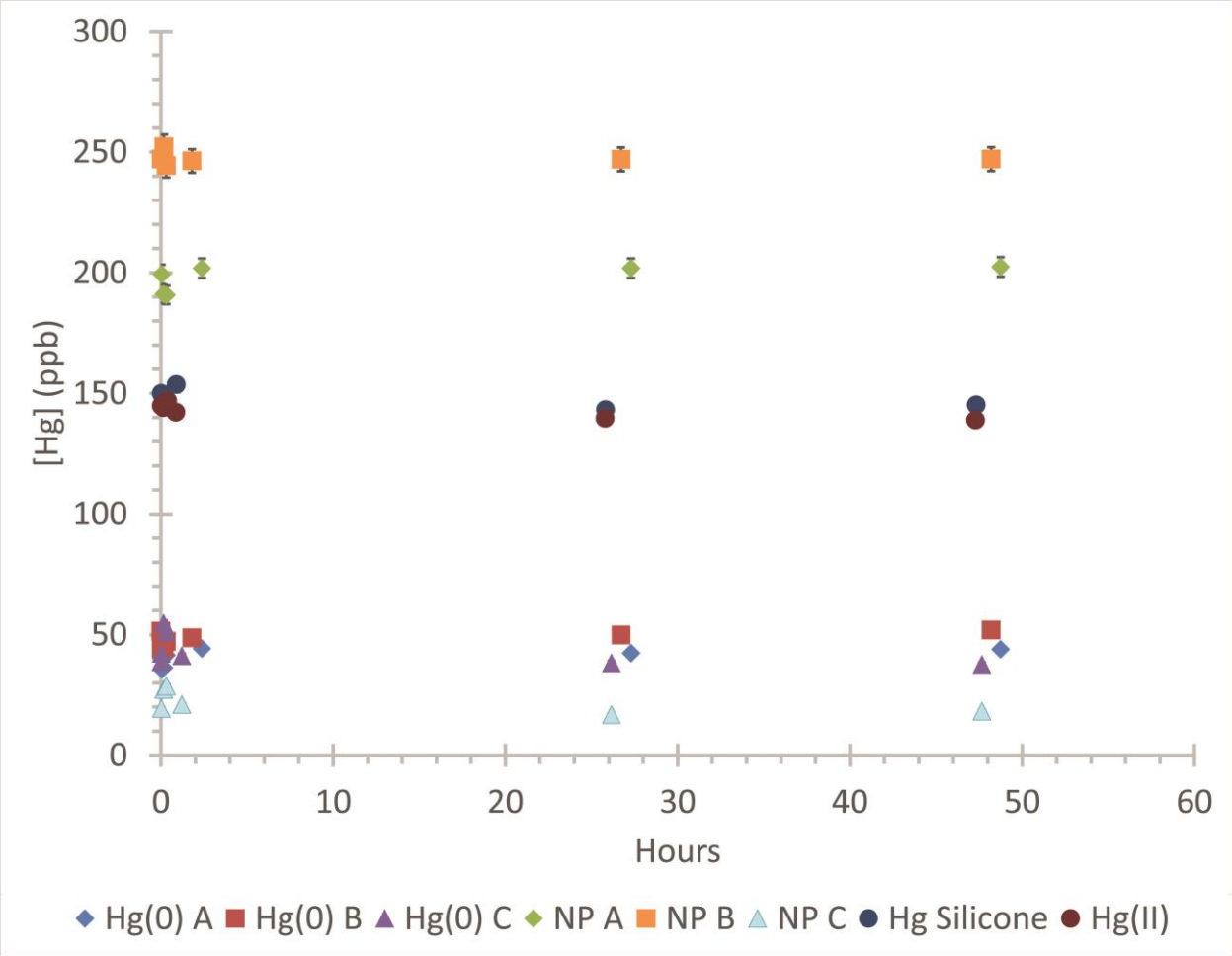

Figure 4.1. Concentration of Hg versus time after Hg(II) injection (hours) in experiments A, B and Hg(II)-only controls, and after injection of an equal volume of N_2 gas in the Hg(0)-only control. Significant changes in Hg(0) concentration occurred during the first few minutes in all experiments. Significant changes in Hg(II) were not observed. Expanded view of the first 3 hours is in Appendix B.

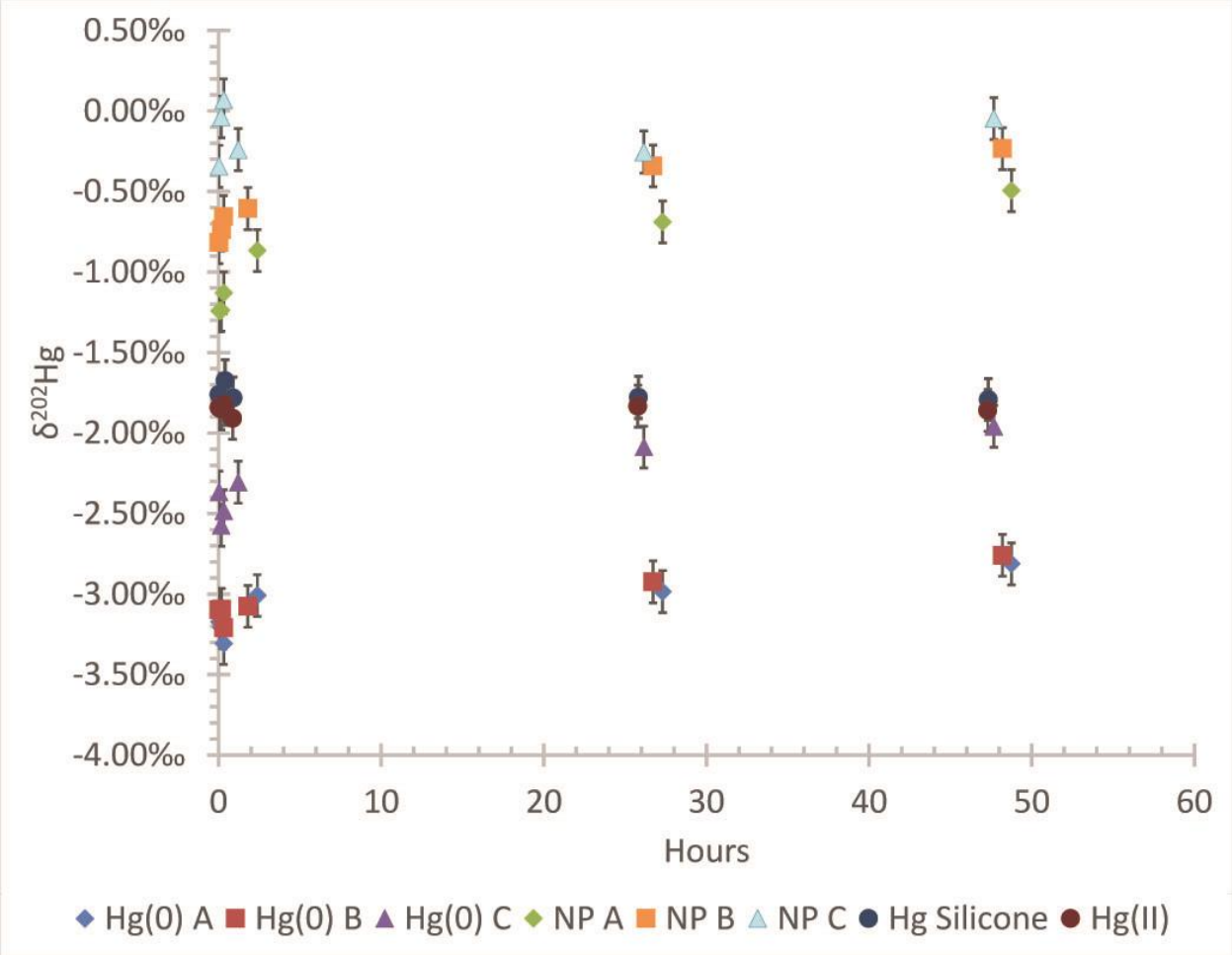

Figure 4.2. δ^{202}Hg versus time after injection (hours). Expanded view of the first 3 hours is in Appendix B.

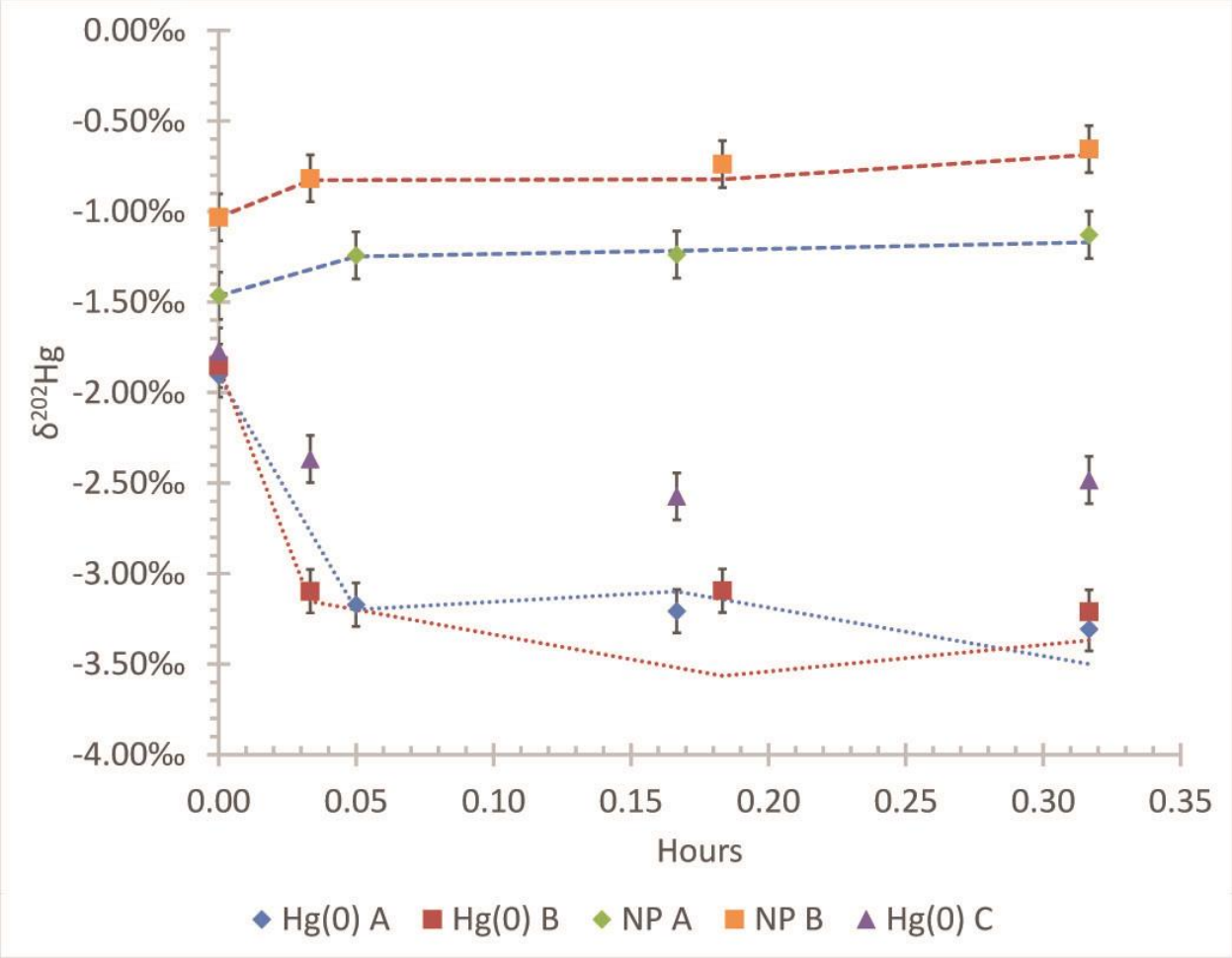

Figure 4.3. δ^{202}Hg versus time post injection (hours). Graph shows the first 20 minutes of the experiment before the Hg(0) source starts to affect the dissolved Hg(0). The dashed lines are the mass balance calculated δ^{202}Hg values for the Hg(0) pool (short dashed lines) and Hg(II) pool (long dashed lines).

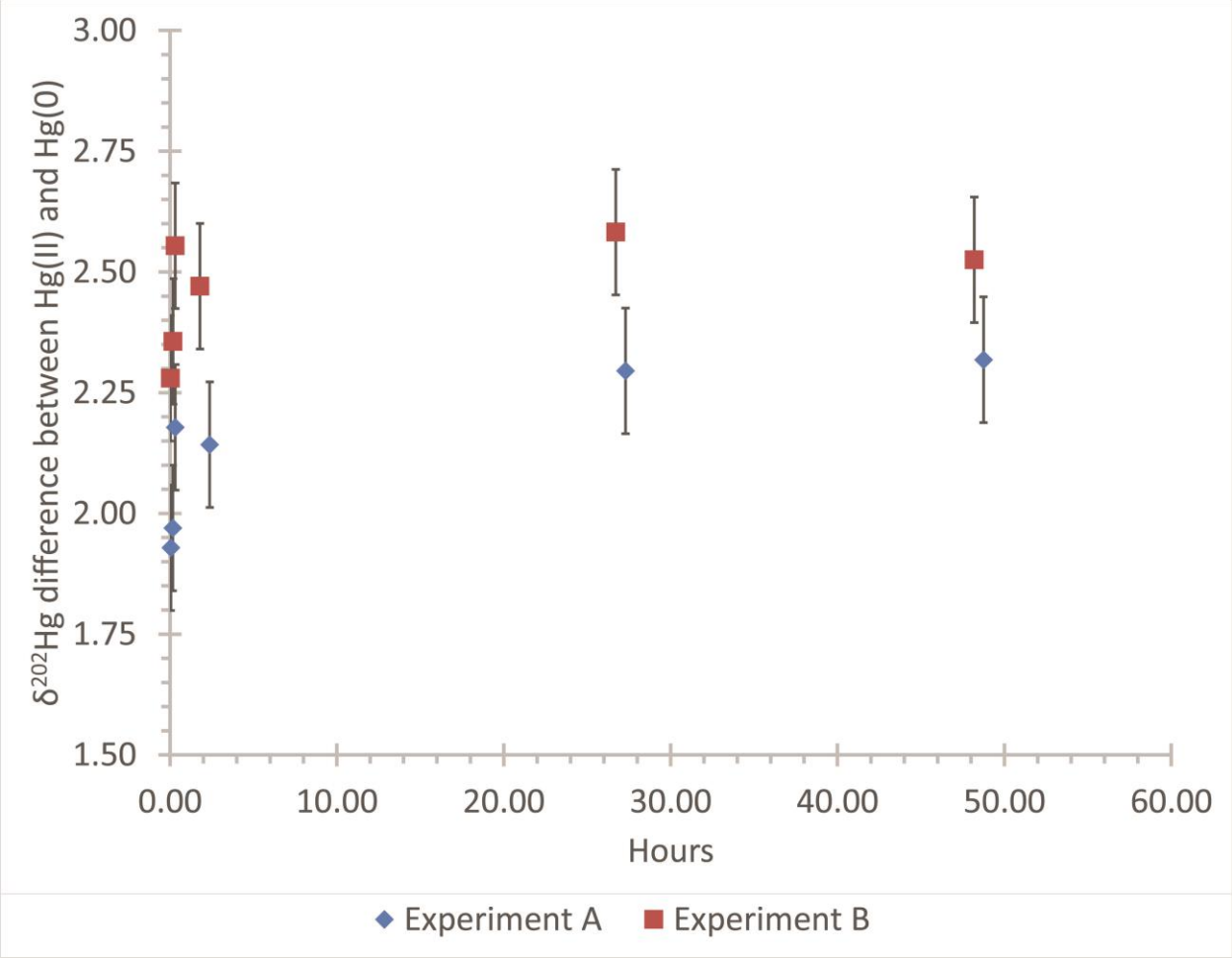

Figure 4.4. Difference between the Hg(II) fraction and the Hg(0) in experiments A (diamonds) and B (squares) versus time post injection (hours). The Difference appears to increase very rapidly and then stabilize around 28 hours. Expanded view of the first 3 hours is in Appendix B.

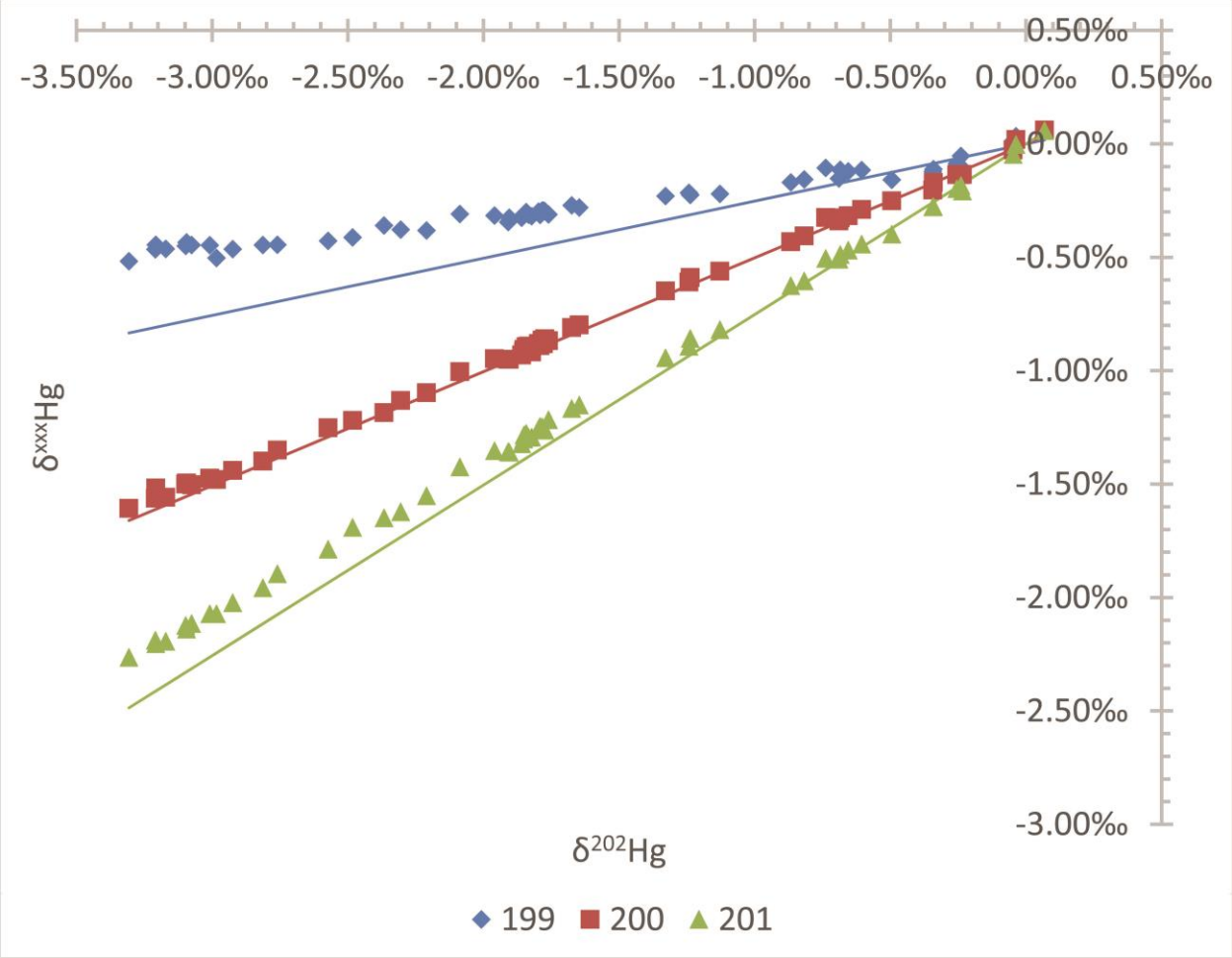

Figure 4.5. $\delta^{xxx}Hg$ versus $\delta^{202}Hg$. Dashed lines are calculated MDF lines based on theoretical values.

Table 4.1. Analytical results

Sample	Time (hr)	Concentration[a] (ppb)	$\delta^{202}Hg$[b]	$\Delta^{199}Hg$[c]	$\Delta^{201}Hg$[d]
		Secondary standard and Hg(II) stock solution			
Almaden	---	1000	-0.48‰	-0.03‰	-0.04‰
Hg(II) stock	---	9674.5	-1.77‰	0.15‰	0.07‰
		Experiment A			
Total Hg A	Pre-injection	70.4	-1.33‰	0.10‰	0.06‰
Hg(0) A 0	Pre-injection	40.5	-1.90‰	0.16‰	0.07‰
Hg(0) A 1	0.05	35.6	-3.17‰	0.34‰	0.19‰
Hg(0) A 2	0.17	36.3	-3.21‰	0.36‰	0.21‰
Hg(0) A 3	0.32	41.6	-3.31‰	0.32‰	0.22‰
Hg(0) A 4	2.38	44.2	-3.01‰	0.31‰	0.19‰
Hg(0) A 5	27.30	42.4	-2.98‰	0.25‰	0.17‰
Hg(0) A 6[e]	48.75	43.9	-2.81‰	0.26‰	0.16‰
NP Hg A 0[f]	Pre-injection	29.9	-0.55‰	-0.10‰	-0.38‰
NP Hg A 1	0.05	199.4	-1.24‰	0.10‰	0.04‰
NP Hg A 2	0.17	191.2	-1.24‰	0.09‰	0.07‰
NP Hg A 3	0.32	190.8	-1.13‰	0.06‰	0.03‰
NP Hg A 4[e]	2.38	201.9	-0.87‰	0.05‰	0.03‰
NP Hg A 5	27.30	201.8	-0.69‰	0.02‰	0.01‰
NP Hg A 6	48.75	202.4	-0.49‰	-0.03‰	-0.03‰
		Experiment B			
Total Hg B	Pre-injection	131.3	-0.68‰	0.06‰	0.03‰
Hg(0) B 0	Pre-injection	51.5	-1.85‰	0.16‰	0.09‰
Hg(0) B 1	0.03	44.5	-3.10‰	0.33‰	0.21‰
Hg(0) B 2	0.18	44.9	-3.09‰	0.35‰	0.19‰
Hg(0) B 3	0.32	47.1	-3.21‰	0.35‰	0.23‰
Hg(0) B 4	1.80	48.7	-3.08‰	0.33‰	0.20‰
Hg(0) B 5[e]	26.72	49.8	-2.92‰	0.27‰	0.18‰
Hg(0) B 6	48.20	51.9	-2.76‰	0.25‰	0.18‰
NP Hg B 0[f]	Pre-injection	79.7	0.07‰	0.01‰	0.04‰
NP Hg B 1[e]	0.03	247.1	-0.82‰	0.05‰	0.01‰
NP Hg B 2	0.18	252.2	-0.74‰	0.08‰	0.05‰
NP Hg B 3	0.32	244.3	-0.66‰	0.04‰	0.02‰
NP Hg B 4	1.80	246.3	-0.61‰	0.04‰	0.01‰
NP Hg B 5	26.72	247.0	-0.34‰	-0.03‰	-0.02‰
NP Hg B 6	48.20	247.1	-0.23‰	-0.05‰	-0.03‰

Table 4.1. (Cont.)

Sample	Time (hr)	Concentration[a] (ppb)	$\delta^{202}Hg$[b]	$\Delta^{199}Hg$[c]	$\Delta^{201}Hg$[d]
		Hg(0)-only Control			
Total Hg C	Pre-injection	53.1	-1.65‰	0.13‰	0.09‰
Hg(0) C 0[e]	Pre-injection	38.8	-2.21‰	0.18‰	0.11‰
Hg(0) C 1	0.03	42.3	-2.37‰	0.24‰	0.13‰
Hg(0) C 2	0.17	54.7	-2.57‰	0.22‰	0.15‰
Hg(0) C 3	0.32	51.0	-2.48‰	0.21‰	0.18‰
Hg(0) C 4	1.22	41.3	-2.31‰	0.20‰	0.11‰
Hg(0) C 5	26.15	38.3	-2.09‰	0.22‰	0.15‰
Hg(0) C 6	47.67	37.7	-1.96‰	0.18‰	0.12‰
NP Hg C 0[f]	Pre-injection	13.7	-0.05‰	-0.02‰	-0.02‰
NP Hg C 1	0.03	19.4	-0.34‰	-0.04‰	-0.02‰
NP Hg C 2	0.17	27.3	-0.04‰	0.04‰	0.02‰
NP Hg C 3	0.32	28.7	0.07‰	0.04‰	0.01‰
NP Hg C 4	1.22	21.1	-0.24‰	0.01‰	0.00‰
NP Hg C 5	26.15	16.9	-0.26‰	-0.02‰	-0.01‰
NP Hg C 6	47.67	18.3	-0.05‰	0.03‰	-0.01‰
		Hg(II)-only Controls			
Hg Silicone 1	0.03	150.0	-1.76‰	0.13‰	0.11‰
Hg Silicone 2[e]	0.17	144.6	-1.80‰	0.15‰	0.09‰
Hg Silicone 3	0.40	146.9	-1.67‰	0.15‰	0.09‰
Hg Silicone 4	0.90	153.6	-1.78‰	0.16‰	0.09‰
Hg Silicone 5	25.82	143.3	-1.78‰	0.15‰	0.08‰
Hg Silicone 6	47.33	145.2	-1.79‰	0.14‰	0.10‰
Hg(II) 1	0.03	144.9	-1.84‰	0.16‰	0.11‰
Hg(II) 2	0.15	144.0	-1.85‰	0.15‰	0.11‰
Hg(II) 3[e]	0.37	146.8	-1.82‰	0.14‰	0.08‰
Hg(II) 4	0.87	142.2	-1.91‰	0.14‰	0.08‰
Hg(II) 5	25.78	139.7	-1.83‰	0.15‰	0.09‰
Hg(II) 6	47.30	138.9	-1.86‰	0.14‰	0.08‰

[a] ±2% uncertainty

[b] ± 0.13‰ uncertainty

[c] ± 0.04‰ uncertainty

[d] ±0.02‰ uncertainty

[e] Average of duplicate samples

[f] Calculated by mass balance

Table 4.2. Calculated δ^{202}Hg difference between the Hg(II) pool and the Hg(0) pool.

Sample	Time (hr)	ΔHg(II):Hg(0)
	Experiment A	
NP Hg A 1	0.05	1.93‰
NP Hg A 2	0.17	1.97‰
NP Hg A 3	0.32	2.18‰
NP Hg A 4	2.38	2.14‰
NP Hg A 5	27.30	2.30‰
NP Hg A 6	48.75	2.32‰
	Experiment B	
NP Hg B 1	0.03	2.28‰
NP Hg B 2	0.18	2.36‰
NP Hg B 3	0.32	2.55‰
NP Hg B 4	1.80	2.47‰
NP Hg B 5	26.72	2.58‰
NP Hg B 6	48.20	2.53‰

REFERENCES

Amyot, M., Gill, G.A., Morel, F.M.M., 1997. Production and Loss of Dissolved Gaseous Mercury in Coastal Seawater. Environmental Science & Technology, 31.

Anbar, A.D., Roe, J.E., Barling, J., Nealson, K.H., 2000. Nonbiological fractionation of iron isotopes. Science, 288.

Angeli, I., Marinova, K.P., 2013. Table of experimental nuclear ground state charge radii: An update. Atomic Data and Nuclear Data Tables, 99.

Armstrong, A.M., Halpern, J., 1956. The Reaction between Mercury (I) and Thallium (III) in Aqueous Solution: Evidence for the Dismutation of Hg2++. The Journal of Physical Chemistry, 60.

Armstrong, A.M., Halpern, J., 1957. Kinetics of the oxidation of mercury (I) by thallium (III) in aqueous solution. Canadian Journal of Chemistry, 35.

Bartov, G. et al., 2013. Environmental Impacts of the Tennessee Valley Authority Kingston Coal Ash Spill. 1. Source Apportionment Using Mercury Stable Isotopes. Environmental Science & Technology, 47(4): 2092-2099.

Bergquist, B., Blum, J., 2007. Mass-dependent and -independent fractionation of Hg isotopes by photoreduction in aquatic systems. Science (New York, N.Y.), 318: 417-437.

Biswas, A., Blum, J., Bergquist, B., Keeler, G., Xie, Z., 2008. Natural mercury isotope variation in coal deposits and organic soils. Environmental Science & Technology, 42: 8303-8312.

Blum, J., 2011. Applications of stable mercury isotopes to biogeochemistry. In: Baskaran, M. (Ed.), Handbook of Environmental Isotope Geochemistry.

Catalano, V.J., Malwitz, M.A., Noll, B.C., 2002. Pd (0) and Pt (0) metallocryptands encapsulating a spinning mercurous dimer. Inorganic chemistry, 41: 6553-6559.

Chen, J., Hintelmann, H., Feng, X., Dimock, B., 2012. Unusual fractionation of both odd and even mercury isotopes in precipitation from Peterborough, ON, Canada. Geochimica et Cosmochimica Acta, 90.

Chiba, H., Sakai, H., 1985. Oxygen isotope exchange rate between dissolved sulfate and water at hydrothermal temperatures. Geochimica et Cosmochimica Acta, 49: 993-1000.

DAP Products Inc., 2013. Xiameter Acetoxy Cure Silicone Sealant; MSDS No. 00008641001, Baltimore, MD.

Day, R. et al., 2012. Mercury stable isotopes in seabird eggs reflect a gradient from terrestrial geogenic to oceanic mercury reservoirs. Environmental Science & Technology, 46: 5327-5362.

de Magalhães, M., Tubino, M., 1995. A possible path for mercury in biological systems: the oxidation of metallic mercury by molecular oxygen in aqueous solutions. The Science of the total environment, 170(3): 229-239.

Demers, J.D., Blum, J.D., Zak, D.R., 2013. Mercury isotopes in a forested ecosystem: Implications for air-surface exchange dynamics and the global mercury cycle. Global Biogeochemical Cycles, 27.

Dietz, R. et al., 2012. What are the toxicological effects of mercury in Arctic biota? The Science of the total environment, 443C: 775-790.

Donovan, P.M. et al., 2014. Identification of multiple mercury sources to stream sediments near Oak Ridge, TN, USA. Environmental Science & Technology, 48: 3666-3674.

Estrade, N., Carignan, J., Donard, O., 2011. Tracing and Quantifying Anthropogenic Mercury Sources in Soils of Northern France Using Isotopic Signatures. Environmental science & technology, 45: 1235–1242.

Estrade, N., Carignan, J., Sonke, J.E., Donard, O.F.X., 2009. Mercury isotope fractionation during liquid–vapor evaporation experiments. Geochimica et Cosmochimica Acta, 73.

Evans, R.D., Holger, H., Peter, J.D., 2001. Measurement of high precision isotope ratios for mercury from coals using transient signals. Journal of Analytical Atomic Spectrometry, 16.

Farrah, H., Pickering, W.P., 1978. The sorption of mercury species by clay minerals. Water, Air, & Soil Pollution, 9: 23-31.

Feng, X. et al., 2010. Tracing mercury contamination sources in sediments using mercury isotope compositions. Environmental Science & Technology, 44: 3363-3371.

Foucher, D., Hintelmann, H., Al, T.A., MacQuarrie, K.T., 2013. Mercury isotope fractionation in waters and sediments of the Murray Brook mine watershed (New Brunswick, Canada): Tracing mercury contamination and transformation. Chemical Geology, 336(0): 87-95.

Foucher, D., Ogrinc, Hintelmann, H., 2009. Tracing Mercury Contamination from the Idrija Mining Region (Slovenia) to the Gulf of Trieste Using Hg Isotope Ratio Measurements. Environmental Science & Technology, 43.

Franta, I., 2012. Elastomers and Rubber Compounding Materials. Elsevier Science.

Fritz, P., Basharmal, G.M., Drimmie, R.J., Ibsen, J., Qureshi, R.M., 1989. Oxygen isotope exchange between sulphate and water during bacterial reduction of sulphate. Chemical Geology: Isotope Geoscience section, 79(2): 99105.

Gehrke, G., Blum, J., Slotton, D., Greenfield, B., 2011a. Mercury isotopes link mercury in San Francisco Bay forage fish to surface sediments. Environmental science & technology, 45(4): 1264-1270.

Gehrke, G.E., Blum, J.D., Marvin-DiPasquale, M., 2011b. Sources of mercury to San Francisco Bay surface sediment as revealed by mercury stable isotopes. Geochimica et Cosmochimica Acta, 75.

Ghosh, S., Schauble, E.A., Couloume, G.L., Blum, J.D., Bergquist, B.A., 2013. Estimation of nuclear volume dependent fractionation of mercury isotopes in equilibrium liquid–vapor evaporation experiments. Chemical Geology, 336.

Ghosh, S., Xu, Y., Humayun, M., Odom, L., 2008. Mass-independent fractionation of mercury isotopes in the environment. Geochemistry Geophysics Geosystems, 9.

Gratz, L., Keeler, G., Blum, J., Sherman, L., 2010. Isotopic composition and fractionation of mercury in Great Lakes precipitation and ambient air. Environmental science & technology, 44(20): 7764-7770.

Greenwood, N.N., Earnshaw, A., 1997. Chemistry of the Elements. Elsevier, Oxford.

Gu, B. et al., 2011. Mercury reduction and complexation by natural organic matter in anoxic environments. Proceedings of the National Academy of Sciences of the United States of America, 108: 1479-1562.

Harada, M. et al., 2001. Mercury pollution in the Tapajos River basin, Amazon: mercury level of head hair and health effects. Environment International, 27: 285-375.

Hintelmann, H., Lu, S., 2003. High precision isotope ratio measurements of mercury isotopes in cinnabar ores using multi-collector inductively coupled plasma mass spectrometry. The Analyst, 128.

Hsu-Kim, H., Kucharzyk, K., Zhang, T., Deshusses, M., 2013. Mechanisms regulating mercury bioavailability for methylating microorganisms in the aquatic environment: a critical review. Environmental science & technology, 47(6): 2441-2456.

Hu, H. et al., 2013. Oxidation and methylation of dissolved elemental mercury by anaerobic bacteria. Nature Geoscience.

Hyslop, N.P., White, W.H., 2009. Estimating Precision Using Duplicate Measurements. Journal of the Air & Waste Management Association, 59.

Jiménez-Moreno, M., Perrot, V., Vladimir, N.E., Monperrus, M., Amouroux, D., 2013. Chemical kinetic isotope fractionation of mercury during abiotic methylation of Hg(II) by methylcobalamin in aqueous chloride media. Chemical Geology, 336: 26-36.

Jiskra, M., Wiederhold, J., Bourdon, B., Kretzschmar, R., 2012. Solution Speciation Controls Mercury Isotope Fractionation of Hg(II) Sorption to Goethite. Environmental science & technology, 46: 6654-6716.

Kritee, K., Barkay, T., Blum, J.D., 2009. Mass dependent stable isotope fractionation of mercury during *mer* mediated microbial degradation of monomethylmercury. Geochimica et Cosmochimica Acta.

Kritee, K., Blum, J., Barkay, T., 2008. Mercury stable isotope fractionation during reduction of Hg(II) by different microbial pathways. Environmental Science & Technology, 42: 9171-9178.

Kritee, K., Blum, J., Johnson, M., Bergquist, B., Barkay, T., 2007. Mercury stable isotope fractionation during reduction of Hg(II) to Hg(0) by mercury resistant microorganisms. Environmental Science & Technology, 41: 1889-1984.

Kwon, S. et al., 2012. Absence of Fractionation of Mercury Isotopes during Trophic Transfer of Methylmercury to Freshwater Fish in Captivity. Environmental science & technology, 46(14): 7527-7534.

Kwon, S., Blum, J., Chirby, M., Chesney, E., 2013. Application of mercury isotopes for tracing trophic transfer and internal distribution of mercury in marine fish feeding experiments. Environmental toxicology and chemistry / SETAC.

Kwon, S.Y., Blum, J.D., Chen, C.Y., Meattey, D.E., 2014. Mercury isotope study of sources and exposure pathways of methylmercury in estuarine food webs in the northeastern USA. Environmental Science & Technology, 48: 10089-10097.

Laffont, L. et al., 2009. Anomalous mercury isotopic compositions of fish and human hair in the Bolivian Amazon. Environmental science & technology, 43(23): 8985-8990.

Laffont, L. et al., 2011. Hg speciation and stable isotope signatures in human hair as a tracer for dietary and occupational exposure to mercury. Environmental science & technology, 45: 9910-9916.

Lauretta, D.S., Klaue, B., Blum, J.D., Buseck, P.R., 2001. Mercury abundances and isotopic compositions in the Murchison (CM) and Allende (CV) carbonaceous chondrites. Geochimica et Cosmochimica Acta, 65(16): 2807-2818.

Lefticariu, L., Blum, J., Gleason, J., 2011. Mercury Isotopic Evidence for Multiple Mercury Sources in Coal from the Illinois Basin. Environmental Science & Technology, 45: 1724–1729.

Li, M. et al., 2014. Assessing sources of human methylmercury exposure using stable mercury isotopes. Environmental Science & Technology, 48: 8800-8806.

Liu, J., Feng, X., Yin, R., Zhu, W., Li, Z., 2011. Mercury distributions and mercury isotope signatures in sediments of Dongjiang, the Pearl River Delta, China. Chemical Geology, 287.

Mead, C., Johnson, T., 2010. Hg stable isotope analysis by the double-spike method. Analytical and Bioanalytical Chemistry, 397: 1529-1567.

Mead, C., Lyons, J., Johnson, T., Anbar, A., 2013. Unique Hg stable isotope signatures of compact fluorescent lamp-sourced Hg. Environmental Science & Technology, 47(6): 2542-2547.

Miller, C., Southworth, G., Brooks, S., Liang, L., Gu, B., 2009. Kinetic controls on the complexation between mercury and dissolved organic matter in a contaminated environment. Environmental science & technology, 43(22): 8548-8553.

Moser, H.C., Voigt, A.F., 1957. Dismutation of the mercurous dimer in dilute solutions. Journal of the American Chemical Society, 79(8): 1837-1839.

O'Concubhair, R., O'Sullivan, D., Sodeau, J., 2012. Dark oxidation of dissolved gaseous mercury in polar ice mimics. Environmental science & technology, 46(9): 4829-4836.

Ohmoto, H., Lasaga, A.C., 1982. Kinetics of reactions between aqueous sulfates and sulfides in hydrothermal systems. Geochimica et Cosmochimica Acta, 46: 1727-1745.

Organization for Economic Cooperation and Development, 2012. SIDS initial assessment profiles agreed in the course of the OECD HPV chemicals programme from 1993-2011 Part 5, Inter-organization Programme for the Sound Managmenet of Chemicals, Paris.

Pasakarnis, T. et al., 2013. Influence of Chloride and Fe(II) Content on the Reduction of Hg(II) by Magnetite. Environmental science & technology.

Perrot, V. et al., 2010. Tracing sources and bioaccumulation of mercury in fish of Lake Baikal--Angara River using Hg isotopic composition. Environmental Science & Technology, 44: 8030-8037.

Perrot, V. et al., 2012. Higher mass-independent isotope fractionation of methylmercury in the pelagic food web of lake baikal (Russia). Environmental science & technology, 46(11): 5902-5911.

Rodríguez-González, P. et al., 2009. Species-specific stable isotope fractionation of mercury during Hg(II) methylation by an anaerobic bacteria (*Desulfobulbus propionicus*) under dark conditions. Environmental Science & Technology, 43: 9183-9191.

Roe, J.E., Anbar, A.D., Barling, J., 2003. Nonbiological fractionation of Fe isotopes: evidence of an equilibrium isotope effect. Chemical Geology, 195: 69-85.

Sakai, H., Dickson, F.W., 1978. Experimental determination of the rate and equilibrium fractionation factors of sulfur isotope exchange between sulfate and sulfide in slightly acid solutions at 300°C and 1000 bars. Earth and Planetary Science Letters, 39.

Schauble, E., 2007. Role of nuclear volume in driving equilibrium stable isotope fractionation of mercury, thallium, and other very heavy elements. Geochimica et Cosmochimica Acta, 71: 2170-2189.

Sherman, L., Blum, J., Keeler, G., Demers, J., Dvonch, J., 2012. Investigation of local mercury deposition from a coal-fired power plant using mercury isotopes. Environmental science & technology, 46: 382-472.

Sherman, L.S., Blum, J.D., Franzblau, A., Basu, N., 2013. New insight into biomarkers of human mercury exposure using naturally occurring mercury stable isotopes. Environmental science & technology, 47(7): 3403-3409.

Sigel, A., Sigel, H., 1997. Metal Ions in Biological Systems: Volume 34: Mercury and its Effects on Environment and Biology. CRC Press, New York.

Skyllberg, U., Drott, A., 2010. Competition between disordered iron sulfide and natural organic matter associated thiols for mercury(II)-an EXAFS study. Environmental science & technology, 44(4): 1254-1259.

Smith, C.N., Kesler, S.E., Blum, J.D., Rytuba, J.J., 2008. Isotope geochemistry of mercury in source rocks, mineral deposits and spring deposits of the California Coast Ranges, USA. Earth and Planetary Science Letters, 269.

Smith, C.N., Kesler, S.E., Klaue, B., Blum, J.D., 2005. Mercury isotope fractionation in fossil hydrothermal systems. Geology, 33.

Sonke, J.E., Zambardi, T., Toutain, J.P., 2008. Indirect gold trap–MC-ICP-MS coupling for Hg stable isotope analysis using a syringe injection interface. Journal of Analytical Atomic Spectrometry, 23: 569-573.

Syversen, T., Kaur, P., 2012. The toxicology of mercury and its compounds. Journal of trace elements in medicine and biology : organ of the Society for Minerals and Trace Elements (GMS), 26(4): 215-226.

Tsui, M. et al., 2012. Sources and transfers of methylmercury in adjacent river and forest food webs. Environmental science & technology, 46(20): 10957-10964.

Tsui, M.T.-K. et al., 2014. Variation in Terrestrial and Aquatic Sources of Methylmercury in Stream Predators as Revealed by Stable Mercury Isotopes. Environmental Science & Technology, 48: 10128-10135.

U.S. Environmental Protection Agency, 1997. Mercury study report to Congress 2. EPA-452/R-97-003, Office of Air Quality and Planning and Standards, Office of Research and Development, U.S. Environmental Protection Agency, Washington, DC.

U.S. Environmental Protection Agency, 2002. Method 1631, Revision E: Mercury in water by oxidation, purge and trap, and cold vapor atomic fluorescence spectrometry. EPA-821-R-02-019.

U.S. Environmental Protection Agency, 2006. EPA's roadmap for mercury. EPA-HQ-OPPT-2005-0013, U.S. Environmental Protection Agency, Washington, DC.

Wang, X., 2013. Chromium and uranium isotopic exchange kinetics and isotope fractionation during oxidation of tetravalent uranium by dissolved oxygen. Doctoral Thesis, University of Illinois Urbana-Champaign.

Waterford Plant, 2007. Silicone sealant; MSDS No. SCS1201, Waterford, NY.

Welch, S.A., Beard, B.L., Johnson, C.M., Braterman, P.S., 2003. Kinetic and equilibrium Fe isotope fractionation between aqueous Fe (II) and Fe (III). Geochimica et Cosmochimica Acta, 67(22): 4231-4250.

Wiederhold, J. et al., 2013. Mercury Isotope Signatures as Tracers for Hg Cycling at the New Idria Hg Mine. Environmental science & technology.

Wiederhold, J.G. et al., 2010. Equilibrium mercury isotope fractionation between dissolved Hg (II) species and thiol-bound Hg. Environmental Science & Technology, 44: 4191-4197.

Yin, R., Feng, X., Chen, J., 2014. Mercury Stable Isotope Compositions in Coals from Major Coal Producing Fields in China and Their Geochemical and Environmental Implications. Environmental Science & Technology, 48: 5565-5574.

Yin, R., Feng, X., Meng, B., 2013a. Stable Mercury Isotope Variation in Rice Plants (*Oryza sativa* L.) from the Wanshan Hg Mining District, SW China. Environmental science & technology.

Yin, R. et al., 2012. Mercury speciation and mercury isotope fractionation during ore roasting process and their implication to source identification of downstream sediment in the Wanshan mercury mining area, SW China. Chemical Geology.

Yin, R. et al., 2013b. Mercury speciation and mercury isotope fractionation during ore roasting process and their implication to source identification of downstream sediment in the Wanshan mercury mining area, SW China. Chemical Geology, 336: 72-79.

Zheng, W., Hintelmann, H., 2009. Mercury isotope fractionation during photoreduction in natural water is controlled by its Hg/DOC ratio. Geochimica et Cosmochimica Acta, 73.

Zheng, W., Hintelmann, H., 2010a. Isotope fractionation of mercury during its photochemical reduction by low-molecular-weight organic compounds. The journal of physical chemistry. A, 114(12): 4246-4253.

Zheng, W., Hintelmann, H., 2010b. Nuclear field shift effect in isotope fractionation of mercury during abiotic reduction in the absence of light. The journal of physical chemistry. A, 114(12): 4238-4245.

Zheng, W., Liang, L., Gu, B., 2012. Mercury reduction and oxidation by reduced natural organic matter in anoxic environments. Environmental science & technology, 46(1): 292-299.

Zheng, W., Lin, H., Mann, B.F., Liang, L., Gu, B., 2013. Oxidation of Dissolved Elemental Mercury by Thiol Compounds under Anoxic Conditions. Environmental Science & Technology, 47(22): 12827-12834.

Chapter 5

Summary

Understanding the Hg cycle. The studies presented in this dissertation contribute to our understanding of Hg isotopes, which in turn will help us understand aspects of the Hg cycle (Figure 5.1). The studies range from using Hg isotope ratios as source tracers in a contaminated environment to identifying and quantifying chemical transformations in a contaminated creek to laboratory experiments testing the interaction between dissolved Hg(0) and Hg(II).

The study conducted in the Emory and Clinch Rivers in Tennessee, U.S.A was able to apportion the sources of Hg into the river system immediately after a contamination event released Hg into an already contaminated river system (Clinch River). All previous studies using Hg isotope ratios have only apportioned long-term sources of Hg (i.e. decommissioned mines) into the environment (Foucher et al., 2009; Feng et al., 2010; Perrot et al., 2010; Estrade et al., 2011; Gehrke et al., 2011; Liu et al., 2011; Day et al., 2012; Sherman et al., 2012; Wiederhold et al., 2013; Yin et al., 2013; Donovan et al., 2014; Li et al., 2014; Tsui et al., 2014). The Hg-source tracing study showed that the Hg present in coal ash is isotopically stable even once spilled into a river system in which methylation in the sediments is known to be taking place. This means we only need to measure the coal ash pile without needing to worry about the spilled ash becoming isotopically different from the starting pile over time. The sediment isotopic ratios also indicate that Hg appears to be isotopically stable in the shallow sediments (first 30cm) of large river systems. The ability to track the different sediments allowed for further investigation into the methylation potential of the Hg present in the coal ash (Deonarine et al., 2013).

The study presented in chapter 3 sought to use Hg isotope ratios to identify and quantify chemical transformations in a contaminated environment. This is the first study that attempts to quantify Hg chemical transformations in a contaminated creek. One of the very important findings of the study was that Hg that has gone through electrochemical processing does not have detectible isotopic fractionation. This suggests that Hg released from chlor-alkali plants will not be isotopically different than the Hg supplied to them. It is also observed that Hg isotope measurements of multiple sample types of Hg (sediments, water, and fish) can be used together to understand the biogeochemical conditions present in a contaminated system. Previous studies have shown fish have the potential to be proxies of the average biogeochemical conditions in an environment because they retain any mass independent fractionation of the Hg they uptake, and do not appear to fractionate the Hg isotopes during uptake (Bergquist and Blum, 2007; Kwon et al., 2012; Kwon et al., 2013). This study also presents an example of how fish can be used as proxies for the average conditions in an environment since they integrate Hg over time and therefore not affected by day-to-day shifts in conditions, which enabled us to identify and quantify the photochemical transformations present in the system.

The final study presented in this dissertation presents important findings regarding the potential behavior of Hg isotopes in the environment. As Hg goes through redox changes in the environment, both Hg(0) and Hg(II) may be present as dissolved species. This means they have the potential to exchange isotopes and evolve toward isotopic equilibrium, which will alter the kinetic isotopic fractionation associated with previous chemical transformations. The experimental results show that isotopic equilibrium between Hg(0) and Hg(II) in a simple NaCl solution matrix is approached within minutes, much faster than expected. Previous laboratory experiments regarding the kinetics of redox transformations of Hg did not detect this processes because the

studied reduction of Hg(II) to Hg(0), and immediately removed the Hg(0) product (Bergquist and Blum, 2007; Kritee et al., 2007; Kritee et al., 2008; Zheng and Hintelmann, 2009; Zheng and Hintelmann, 2010a; Zheng and Hintelmann, 2010b). These isotope exchange experiments are important if we want to apply Hg isotope measurements to the field and detect kinetic processes; if these species approach isotopic equilibrium, the resulting isotopic shifts have the potential to overprint previous kinetic fractionation. Accordingly, measured Hg isotope ratios could be dependent on the ligands present and the resulting Hg speciation, and not the chemical reactions taking place. Fortunately, exchange follows a mass dependent/nuclear volume fractionation regime, which will conserve photochemical mass independent isotopic values. Another factor that will affect the rate of isotopic exchange will be complexation of Hg(II), which is expected to hinder exchange; however, exchange rates with typical Hg speciation found in nature have not been measured yet.

Future directions. The field of Hg stable isotope geochemistry is still young. As mentioned in Chapter 1, we are beginning to understand different processes within the Hg cycle through laboratory experiments (Figure 5.1, Table 5.1) and the studies presented here. However, there are many aspects and processes we still do not fully understand. Transformations such as oxidation of Hg(0) to Hg(II) both abiotically and microbially, under dark conditions and exposed to light, are still needed. More studies need to be conducted regarding methylation since there are only two studies that currently exist about the process (Rodríguez-González et al., 2009; Jiménez-Moreno et al., 2013). Currently, we are unable to measure methyl-Hg isotope ratios in low concentration natural waters; developing separation and measurement methods of this species will be an important achievement in order get direct measurements of the methyl-Hg pool, the most toxic form of Hg. Lastly, isotopic exchange experiments containing more complex ligands, such as

thiols, need to be conducted in order for us to understand the interaction between Hg(0) and Hg(II) when strong ligands are present.

FIGURES AND TABLES

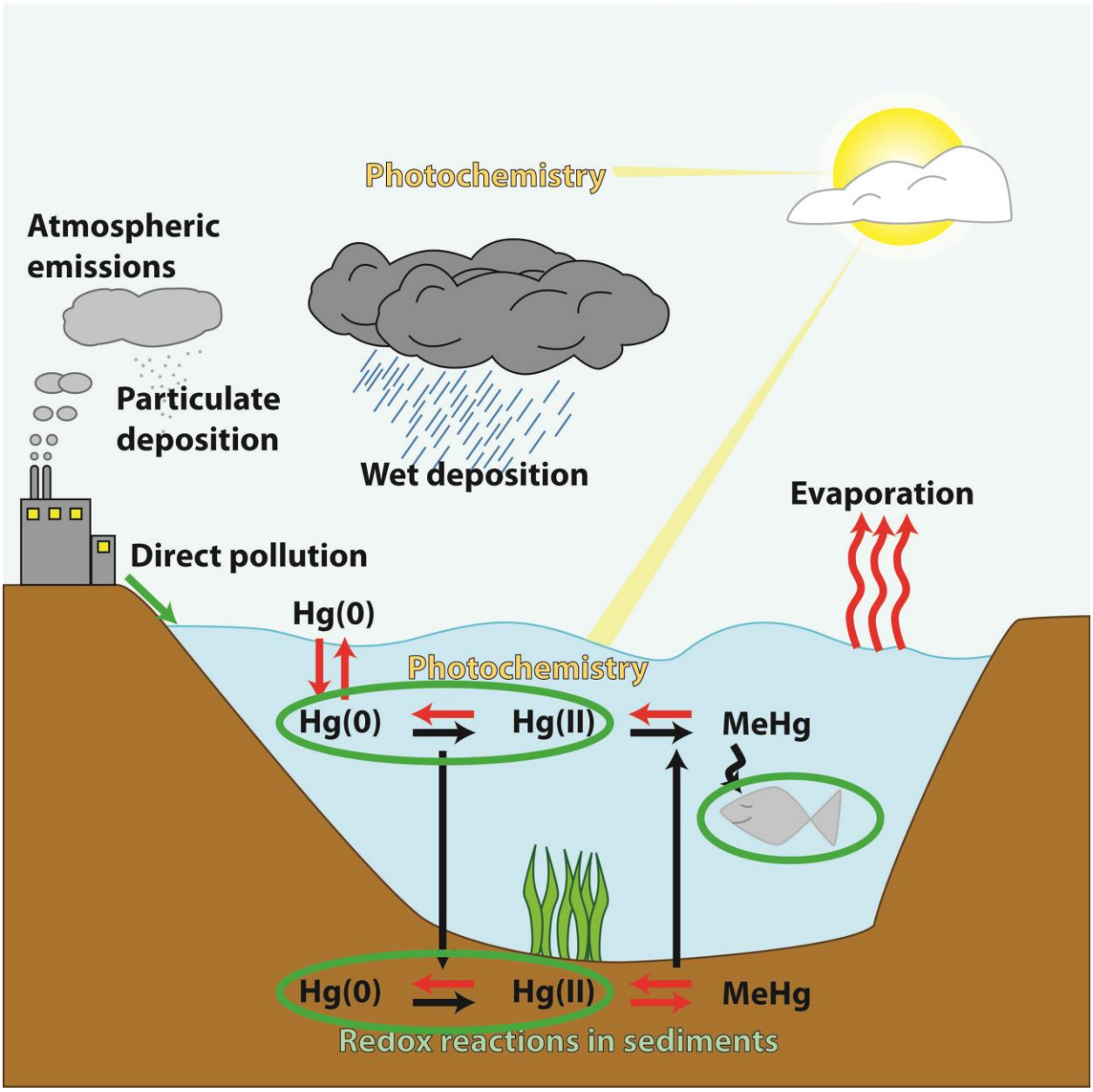

Figure 5.1. Generalized Hg cycle after being emitted to the environment. Not shown are natural emission sources such as volcanoes and biomass. Red arrows represent processes that have been studied, green arrows and circles represent processes and interactions studied in this dissertation.

Table 5.1. Isotopic shifts (reactant relative to product flux) induced by Hg transformations. Units are per mil (‰; parts per thousand)

Transformation	Mechanism	Magnitude of MDF (ordinary kinetic isotope effect)[a]	Magnitude of MIE (magnetic isotope effect)[b]	Reference
Hg(II) to Hg(0)	Photochemical	0.6‰	2.5‰	(Bergquist and Blum, 2007)
Hg(II) to Hg(0)	Photochemical, variable DOC	0.72–1.71‰	0.26–5.63‰	(Zheng and Hintelmann, 2009; 2010a)
Hg(II) to Hg(0)	Abiotic, non-photochemical	1.2–1.8‰	0.0‰	(Bergquist and Blum, 2007; Zheng and Hintelmann, 2010b)
Hg(II) to Hg(0)	Microbial	1.3–2.0‰	0.0‰	(Kritee et al., 2007; 2008)
Methyl-Hg breakdown	Photochemical	1.3‰	1.7‰	(Bergquist and Blum, 2007)
Methyl-Hg breakdown	Microbial	0.4‰	0.0‰	(Kritee et al., 2009)
Methylation	Microbial	2.6‰	0.0‰	(Rodríguez-González et al., 2009)
Methylation	Abiotic	4.0‰	0.0‰	(Jiménez-Moreno et al., 2013)
Hg(0) volatilization from solution	Diffusion	0.5–1.3‰	0.0‰	(Zheng et al., 2007; Ghosh et al., 2013)

[a]Isotopic fractionation driven by mass and nuclear volume difference; variation in the $^{202}Hg/^{198}Hg$ ratio.

[b]Additional isotopic fractionation effecting odd isotopes only; revealed in $^{199}Hg/^{198}Hg$ and $^{201}Hg/^{198}Hg$ ratios.

REFERENCES

Bergquist, B., Blum, J., 2007. Mass-dependent and -independent fractionation of Hg isotopes by photoreduction in aquatic systems. Science (New York, N.Y.), 318: 417-437.

Day, R. et al., 2012. Mercury stable isotopes in seabird eggs reflect a gradient from terrestrial geogenic to oceanic mercury reservoirs. Environmental Science & Technology, 46: 5327-5362.

Deonarine, A. et al., 2013. Environmental Impacts of the Tennessee Valley Authority Kingston Coal Ash Spill. 2. Effect of Coal Ash on Methylmercury in Historically Contaminated River Sediments. Environmental Science & Technology, 47(4): 2100-2108.

Donovan, P.M. et al., 2014. Identification of multiple mercury sources to stream sediments near Oak Ridge, TN, USA. Environmental Science & Technology, 48: 3666-3674.

Estrade, N., Carignan, J., Donard, O., 2011. Tracing and Quantifying Anthropogenic Mercury Sources in Soils of Northern France Using Isotopic Signatures. Environmental science & technology, 45: 1235–1242.

Feng, X. et al., 2010. Tracing mercury contamination sources in sediments using mercury isotope compositions. Environmental Science & Technology, 44: 3363-3371.

Foucher, D., Ogrinc, Hintelmann, H., 2009. Tracing Mercury Contamination from the Idrija Mining Region (Slovenia) to the Gulf of Trieste Using Hg Isotope Ratio Measurements. Environmental Science & Technology, 43.

Gehrke, G.E., Blum, J.D., Marvin-DiPasquale, M., 2011. Sources of mercury to San Francisco Bay surface sediment as revealed by mercury stable isotopes. Geochimica et Cosmochimica Acta, 75.

Ghosh, S., Schauble, E.A., Couloume, G.L., Blum, J.D., Bergquist, B.A., 2013. Estimation of nuclear volume dependent fractionation of mercury isotopes in equilibrium liquid–vapor evaporation experiments. Chemical Geology, 336.

Jiménez-Moreno, M., Perrot, V., Vladimir, N.E., Monperrus, M., Amouroux, D., 2013. Chemical kinetic isotope fractionation of mercury during abiotic methylation of Hg(II) by methylcobalamin in aqueous chloride media. Chemical Geology, 336: 26-36.

Kritee, K., Barkay, T., Blum, J.D., 2009. Mass dependent stable isotope fractionation of mercury during *mer* mediated microbial degradation of monomethylmercury. Geochimica et Cosmochimica Acta.

Kritee, K., Blum, J., Barkay, T., 2008. Mercury stable isotope fractionation during reduction of Hg(II) by different microbial pathways. Environmental Science & Technology, 42: 9171-9178.

Kritee, K., Blum, J., Johnson, M., Bergquist, B., Barkay, T., 2007. Mercury stable isotope fractionation during reduction of Hg(II) to Hg(0) by mercury resistant microorganisms. Environmental Science & Technology, 41: 1889-1984.

Kwon, S. et al., 2012. Absence of Fractionation of Mercury Isotopes during Trophic Transfer of Methylmercury to Freshwater Fish in Captivity. Environmental science & technology, 46(14): 7527-7534.

Kwon, S., Blum, J., Chirby, M., Chesney, E., 2013. Application of mercury isotopes for tracing trophic transfer and internal distribution of mercury in marine fish feeding experiments. Environmental toxicology and chemistry / SETAC.

Li, M. et al., 2014. Assessing sources of human methylmercury exposure using stable mercury isotopes. Environmental Science & Technology, 48: 8800-8806.

Liu, J., Feng, X., Yin, R., Zhu, W., Li, Z., 2011. Mercury distributions and mercury isotope signatures in sediments of Dongjiang, the Pearl River Delta, China. Chemical Geology, 287.

Tsui, M.T.-K. et al., 2014. Variation in Terrestrial and Aquatic Sources of Methylmercury in Stream Predators as Revealed by Stable Mercury Isotopes. Environmental Science & Technology, 48: 10128-10135.

Perrot, V. et al., 2010. Tracing sources and bioaccumulation of mercury in fish of Lake Baikal--Angara River using Hg isotopic composition. Environmental Science & Technology, 44: 8030-8037.

Rodríguez-González, P. et al., 2009. Species-specific stable isotope fractionation of mercury during Hg(II) methylation by an anaerobic bacteria (*Desulfobulbus propionicus*) under dark conditions. Environmental Science & Technology, 43: 9183-9191.

Sherman, L., Blum, J., Keeler, G., Demers, J., Dvonch, J., 2012. Investigation of local mercury deposition from a coal-fired power plant using mercury isotopes. Environmental science & technology, 46: 382-472.

Wiederhold, J. et al., 2013. Mercury Isotope Signatures as Tracers for Hg Cycling at the New Idria Hg Mine. Environmental science & technology.

Yin, R. et al., 2013. Mercury speciation and mercury isotope fractionation during ore roasting process and their implication to source identification of downstream sediment in the Wanshan mercury mining area, SW China. Chemical Geology, 336: 72-79.

Zheng, W., Foucher, D., Hintelmann, H., 2007. Mercury isotope fractionation during volatilization of Hg (0) from solution into the gas phase. Journal of Analytical Atomic Spectrometry, 22(9): 1097-1104.

Zheng, W., Hintelmann, H., 2009. Mercury isotope fractionation during photoreduction in natural water is controlled by its Hg/DOC ratio. Geochimica et Cosmochimica Acta, 73.

Zheng, W., Hintelmann, H., 2010a. Isotope fractionation of mercury during its photochemical reduction by low-molecular-weight organic compounds. The journal of physical chemistry. A, 114(12): 4246-4253.

Zheng, W., Hintelmann, H., 2010b. Nuclear field shift effect in isotope fractionation of mercury during abiotic reduction in the absence of light. The journal of physical chemistry. A, 114(12): 4238-4245.

APPENDIX A
SUPPORTING INFORMATION FOR CHAPTER 2

Environmental impacts of the Tennessee Valley Authority Kingston coal ash spill. 1. Source apportionment using mercury stable isotopes

Gideon Bartov[‡]*, *Amrika Deonarine*[§,†], *Thomas M. Johnson*[‡], *Laura Ruhl*[ǁ], *Avner Vengosh*[ǁ], *and Heileen Hsu-Kim*[§]

[‡] Department of Geology, 208 Natural History Building, University of Illinois at Urbana-Champaign, Urbana, Illinois 61801.

[§] Department of Civil and Environmental Engineering, 121 Hudson Hall, Box 90287, Duke University, Durham, North Carolina 27708.

[ǁ] Division of Earth and Ocean Sciences, Nicholas School of the Environment, 205 Old Chemistry Building, Box 90227, Duke University, Durham, North Carolina 27708

[†] Present address: U.S. Geological Survey, Reston, VA.

*Corresponding author: gbartov2@illinois.edu

MASS INDEPENDENT FRACTIONATION CALCULATIONS

Mass independent fractionation (MIF) is a deviation of a measured isotopic value from the calculated theoretical expectation based on the measured δ^{202}Hg. ^{199}Hg, ^{200}Hg, ^{201}Hg have been shown to exhibit MIF (Bergquist and Blum, 2007; Chen et al., 2012; Estrade et al., 2009; Gratz et al., 2010; Zheng and Hintelmann, 2010). These deviations are reported as Δ and are defined as:

$$\Delta^{199}Hg = 1000 * \left(\left[\ln\left(\left(\delta^{199}Hg/1000\right)+1\right)\right] - 0.252\left[\ln\left(\left(\delta^{202}Hg/1000\right)+1\right)\right]\right) \quad \text{(S1)}$$

$$\Delta^{200}Hg = 1000 * \left(\left[\ln\left(\left(\delta^{200}Hg/1000\right)+1\right)\right] - 0.502\left[\ln\left(\left(\delta^{202}Hg/1000\right)+1\right)\right]\right) \quad \text{(S2)}$$

$$\Delta^{201}Hg = 1000 * \left(\left[\ln\left(\left(\delta^{201}Hg/1000\right)+1\right)\right] - 0.752\left[\ln\left(\left(\delta^{202}Hg/1000\right)+1\right)\right]\right) \quad \text{(S3)}$$

MIXING MODEL CALCULATIONS

In order to solve the mixing model, we use these three general equations:

$$\delta^{202}Hg_{Mixture} = \frac{f_{Ash}\delta_{Ash}C_{Ash} + f_{ERM10}\delta_{ERM10}C_{ERM10} + f_{ERM12/CRM5.5}\,\delta_{ERM12/CRM5.5}C_{ERM12/CRM5.5}}{f_{Ash}C_{Ash} + f_{ERM10}C_{ERM10} + f_{ERM12/CRM5.5}C_{ERM12/CRM5.5}} \quad \text{(S4)}$$

$$C_{Mixture} = f_{Ash}C_{Ash} + f_{ERM10}C_{ERM10} + f_{ERM12/CRM5.5}C_{ERM12/CRM5.5} \quad \text{(S5)}$$

$$1 = f_{Ash} + f_{ERM10} + f_{ERM12/CRM5.5} \quad \text{(S6)}$$

Where f is the fraction of each component, C represents the concentration, and δ equals to the δ^{202}Hg value. Combining equation S6 and S5 gives us:

$$f_{ERM10} = \frac{C_{Mixture} - \left(f_{ERM12/CRM5.5} * \left[C_{ERM12/CRM5.5} - C_{Ash}\right] - C_{Ash}\right)}{C_{ERM10} - C_{Ash}} \quad \text{(S7)}$$

We iteratively solved equations S4, S6, and S7 simultaneously by guessing at the ERM 12 or CRM 5.5 components — depending on which river the sample came from.

In order to estimate the uncertainties in our model measurements, we chose the most extreme values of the end-members and augmented the measured sample's values within our uncertainties in order to minimize and maximize the contribution of coal ash. We tested multiple samples, one from each mile marker, in each River. For the two Emory samples that plotted within the Clinch River mixing field, we attempted to maximize the Clinch contribution in those samples in order to elucidate what is the maximum contribution of the Clinch sediments to the Emory River.

This exercise gave us total range of 23% (61–84%, mean 75%), and 14% deviation from the mean, for the ash in the Cove 1 sample from 8/09. Four other Emory River samples (One from each mile marker) gave smaller overall deviations from the mean. The two Emory River samples (ERM 1 and ERM 2) that plotted within the Clinch field gave a maximum range of 0–9% Clinch sediment using the extreme values; supporting our conclusion that the Clinch does not contribute to the Emory River samples.

The Clinch River samples had larger variations when trying to maximize and minimize the coal ash component of each location. Specifically CRM 2 that was sampled on 8/09 had the largest overall range of coal ash values at 70% (11–81%, mean 41%). This difference equates to a 40% uncertainty in the reported value. Again, it's important to note that this was only achieved using the most extreme values for the end-members.

This difference in uncertainties between the two rivers can possibly be explained by the fact that ERM 12 δ^{202}Hg values plot between the coal ash and ERM 10 values, which suppresses the effect of the coal ash member's scatter on the mixing field. Oppositely, the Clinch River mixing field does not have that luxury, and is more susceptible to the large range of coal ash δ^{202}Hg values.

FIGURES AND TABLES

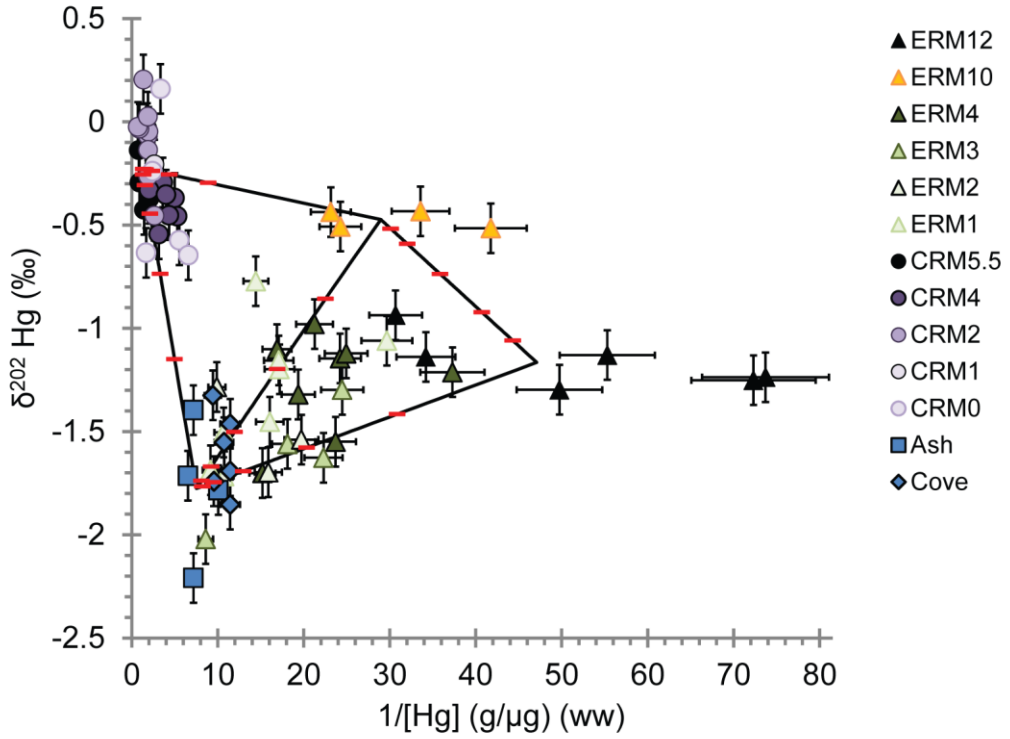

Figure A.1. δ^{202}Hg vs. inverse concentration. Ash samples are blue squares (□), cove samples are blue diamonds (◊), Clinch River sediments are purple circles (○), and Emory River sediments are green and orange triangles (Δ). Lighter colors indicate sites farther downstream. The black lines indicate mixing lines between pairs of end-members, and the red tick marks give mixing proportions at various points along those lines (10/90, 25/75, 50/50, 75/25, 90/10). All Emory River sediments, except two, plot between the Emory River and ash end-members. The Clinch River sediments are more complex and vary with time.

Table A.1. Geochemical data for Kingston coal ash and cove sediment samples

Site	Date Sampled (mm/yy)	Concentration[a] (ppm)	$\delta^{202}Hg$[b]	$\Delta^{199}Hg$[c]	$\Delta^{201}Hg$[d]	% Ash	% CRM 5.5	% ERM 12
Ash	02/09	0.153	-1.71	-0.21	-0.17	Not applicable		
	02/09[e]	0.139	-2.21	-0.23	-0.14			
	01/09	0.139	-1.40	-0.23	-0.16			
	09/09	0.099	-1.78	-0.17	-0.09			
Cove	06/09[f]	0.087	-1.85	-0.21	0.01	59	0	41
	06/09[e,f]	0.106	-1.32	-0.27	0.18	57	3	40
	08/09[f]	0.105	-1.74	-0.08	-0.09	75	0	24
	08/09[e]	0.087	-1.46	-0.20	-0.18	50	1	49
	09/09	0.093	-1.55	-0.22	-0.18	58	1	41
	09/09[e]	0.087	-1.69	-0.25	-0.22	58	0	34

[a] ±10% uncertainty

[b] ± 0.12‰ uncertainty

[c] ± 0.06‰ uncertainty

[d] ±0.07‰ uncertainty

[e] Separate sample from same day

[f] Mass independent fractionation values outliers and not considered due to analytical issues

Table A.2. Geochemical data for Emory River sediment samples

Site	Date Sampled (mm/yy)	Concentration[a] (ppm)	$\delta^{202}Hg$[b]	$\Delta^{199}Hg$[c]	$\Delta^{201}Hg$[d]	% Ash	% CRM 5.5	% ERM 12	% ERM 10
ERM 12	03/10	0.014	-1.25	-0.18	-0.15				
	04/10	0.014	-1.24	-0.24	-0.16				
	06/10	0.018	-1.13	-0.27	-0.16				
	06/10[e]	0.020	-1.30	-0.27	-0.20		Not applicable		
	08/10	0.033	-0.94	-0.13	-0.11				
	08/10[e]	0.029	-1.14	-0.18	-0.12				
ERM 10	6/11[e]	0.043	-0.44	-0.11	-0.13				
	6/11[e]	0.041	-0.51	-0.14	-0.12				
	6/11[e]	0.024	-0.52	-0.13	-0.17		Not applicable		
	6/11[e]	0.030	-0.43	-0.13	-0.16				
ERM 4	08/09	0.027	-1.21	-0.16	-0.19	4	0	88	8
	08/09[e,f]	0.052	-1.32	-0.16	-0.08	22	0	36	42
	09/09	0.042	-1.55	-0.24	-0.26	19	0	81	0
	09/09[e,f]	0.059	-1.10	-0.22	-0.03	25	0	0	75
	11/09[f]	0.041	-1.15	0.04	0.03	13	0	42	46
	04/10	0.047	-0.98	-0.28	-0.17	13	0	5	82
	06/10	0.040	-1.12	-0.25	-0.21	11	0	43	46
	08/10	0.066	-1.70	-0.22	-0.13	40	0	60	0
ERM 3	08/09	0.116	-2.02	-0.17	-0.15	85	0	15	0
	11/09	0.055	-1.56	-0.19	-0.17	29	0	62	9
	06/10	0.041	-1.30	-0.27	-0.18	14	0	59	26
	08/10	0.045	-1.63	-0.21	-0.13	21	0	79	0
ERM 2	11/09	0.101	-1.28	-0.15	-0.14	48	3	0	50
	06/10	0.051	-1.54	-0.23	-0.16	26	0	67	7
	08/10	0.063	-1.70	-0.24	-0.17	37	0	63	0
ERM 1	08/09	0.034	-1.06	-0.08	-0.09	7	0	56	38
	08/09[e,f]	0.069	-0.77	-0.25	0.48	6	4	0	91
	09/09	0.109	-1.69	-0.17	-0.15	76	0	3	21
	11/09	0.094	-1.50	-0.04	-0.08	60	0	0	40
	04/10	0.058	-1.20	-0.25	-0.07	24	0	1	74
	06/10	0.062	-1.45	-0.30	-0.22	33	0	32	36
	06/10[e]	0.059	-1.16	-0.16	-0.08	24	0	0	76
	08/10	0.093	-1.72	-0.23	-0.16	64	0	33	3

[a] ±10% uncertainty
[b] ± 0.12‰ uncertainty
[c] ± 0.06‰ uncertainty
[d] ±0.07‰ uncertainty
[e] Separate sample from same day
[f] Mass independent fractionation values outliers and not considered due to analytical issues

Table A.3. Geochemical data for Clinch River sediment samples

Site	Date Sampled (mm/yy)	Concentration[a] (ppm)	$\delta^{202}Hg$[b]	$\Delta^{199}Hg$[c]	$\Delta^{201}Hg$[d]	% Ash	% CRM 5.5	% ERM 12	% ERM 10
CRM 5.5	09/09	1.104	-0.29	-0.06	-0.10	Not applicable			
	09/09[e]	0.816	-0.10	-0.08	-0.05				
	11/09	0.558	-0.03	-0.04	-0.04				
	11/09[e]	1.209	-0.14	-0.07	-0.06				
	06/10	0.698	-0.43	-0.06	-0.06				
	08/10	0.491	-0.37	-0.08	-0.08				
CRM 4	08/09	0.200	-0.37	-0.18	-0.10	11	20	0	69
	09/09	0.277	-0.29	-0.09	-0.07	6	30	0	63
	04/10	0.189	-0.46	-0.10	-0.10	18	18	0	64
	04/10[e]	0.318	-0.54	-0.14	-0.08	33	21	0	46
	06/10	0.497	-0.33	-0.14	-0.10	57	36	0	16
	08/10	0.251	-0.35	-0.09	-0.08	13	26	0	61
	08/10[e]	0.230	-0.45	-0.11	-0.10	23	22	0	55
CRM 2	08/09	0.530	-0.07	-0.09	-0.06	0	58	0	42
	08/09[e]	0.380	-0.46	-0.14	-0.05	41	39	0	19
	09/09	0.739	0.20	-0.13	-0.08	0	89	0	11
	01/10	0.520	-0.26	-0.09	-0.07	8	61	0	31
	04/10	0.516	-0.05	-0.14	-0.09	0	56	0	44
	06/10	1.130	-0.03	-0.12	-0.10	0	100	0	0
	06/10[e]	1.388	-0.02	-0.10	-0.06	0	100	0	0
	08/10	0.529	0.02	-0.10	-0.10	0	58	0	42
	08/10[e]	0.526	-0.14	-0.10	-0.07	0	58	0	42
CRM 1	08/09	0.380	-0.21	-0.03	0.00	0	36	0	64
CRM 0	09/09	0.299	0.16	-0.16	-0.07	0	34	0	66
	04/10	0.597	-0.63	-0.04	-0.07	43	57	0	0
	06/10	0.416	-0.24	-0.07	-0.09	0	49	0	51
	08/10[f]	0.181	-0.57	-0.20	-0.12	28	15	0	57
	08/10[e]	0.152	-0.65	-0.14	-0.08	28	11	0	60

[a] ±10% uncertainty

[b] ± 0.12‰ uncertainty

[c] ± 0.06‰ uncertainty

[d] ±0.07‰ uncertainty

[e] Separate sample from same day

[f] Mass independent fractionation values outliers and not considered due to analytical issues

Table A.4. Average UM Almadén δ^{202}Hg, Δ^{199}Hg, Δ^{201}Hg values ± 2SD

	δ^{202}Hg	Δ^{199}Hg	Δ^{201}Hg	n
UM Almadén	−0.59±0.09‰	−0.05±0.08‰	0.00±0.15‰	8

REFERENCES

Bergquist, B., Blum, J., 2007. Mass-dependent and -independent fractionation of Hg isotopes by photoreduction in aquatic systems. Science (New York, N.Y.), 318: 417-437.

Chen, J., Hintelmann, H., Feng, X., Dimock, B., 2012. Unusual fractionation of both odd and even mercury isotopes in precipitation from Peterborough, ON, Canada. Geochimica et Cosmochimica Acta, 90.

Estrade, N., Carignan, J., Sonke, J.E., Donard, O.F.X., 2009. Mercury isotope fractionation during liquid–vapor evaporation experiments. Geochimica et Cosmochimica Acta, 73.

Gratz, L., Keeler, G., Blum, J., Sherman, L., 2010. Isotopic composition and fractionation of mercury in Great Lakes precipitation and ambient air. Environmental Science & Technology, 44(20): 7764-7770.

Zheng, W., Hintelmann, H., 2010. Nuclear field shift effect in isotope fractionation of mercury during abiotic reduction in the absence of light. The journal of physical chemistry. A, 114(12): 4238-4245.

APPENDIX B

SUPPORTING INFORMATION FOR CHAPTER 4

Mercury Isotope Exchange Between Dissolved Hg(0) and Hg(II)

FIGURES

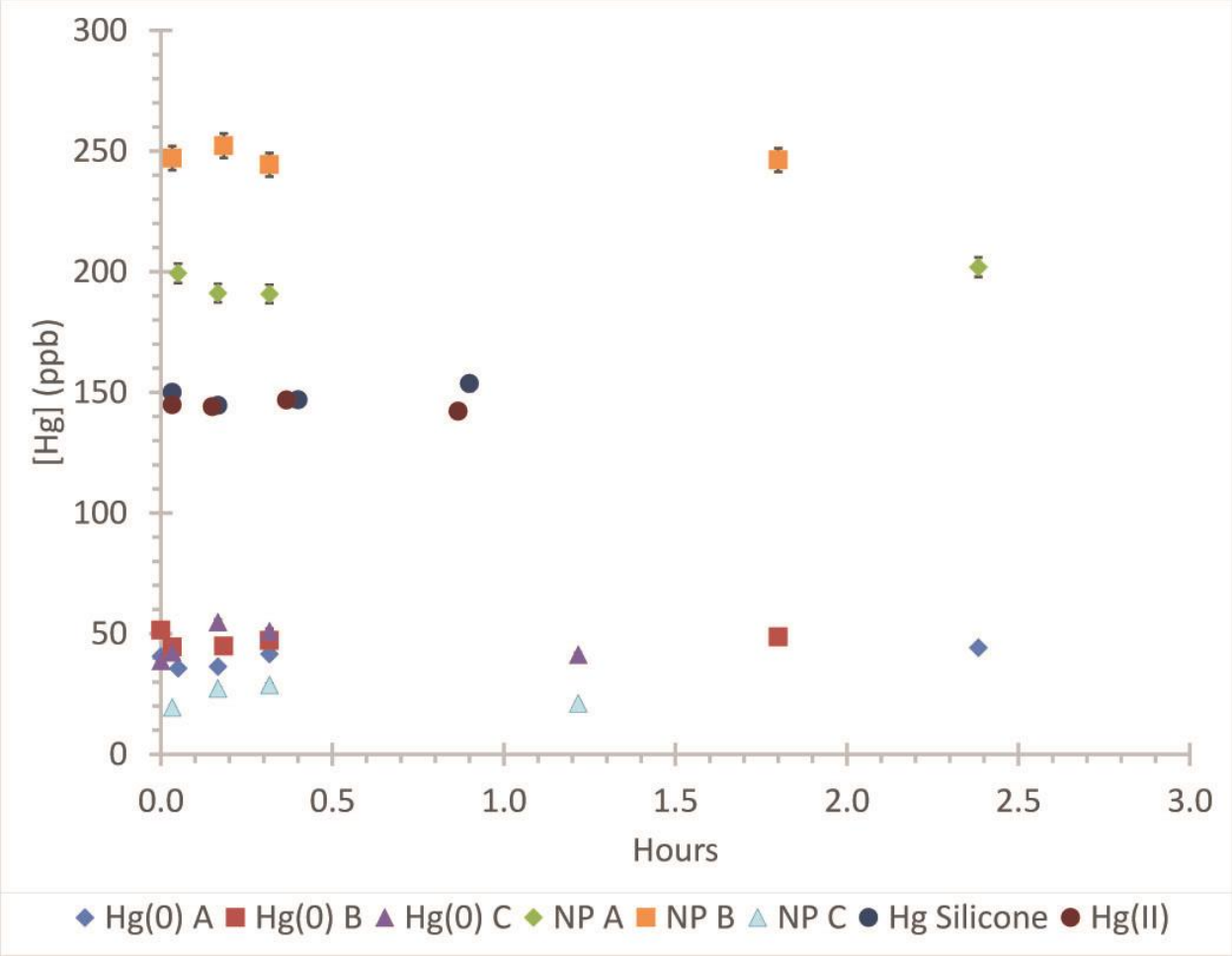

Figure B.1. Concentration of Hg versus time after Hg(II) injection (hours) in experiments A, B and Hg(II)-only controls, and after injection of an equal volume of N_2 gas in the Hg(0)-only control.

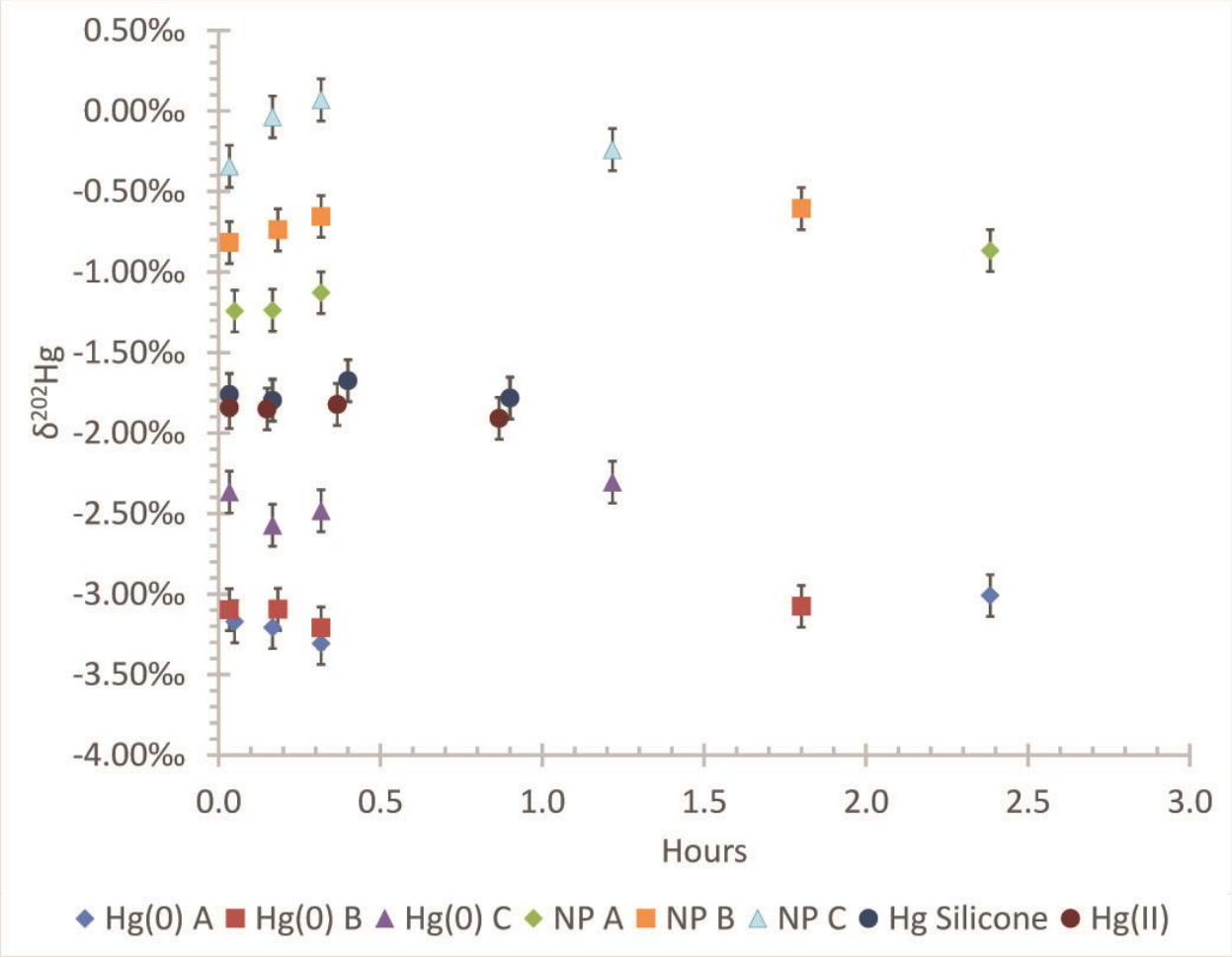

Figure B.2. δ^{202}Hg versus time after injection (hours).

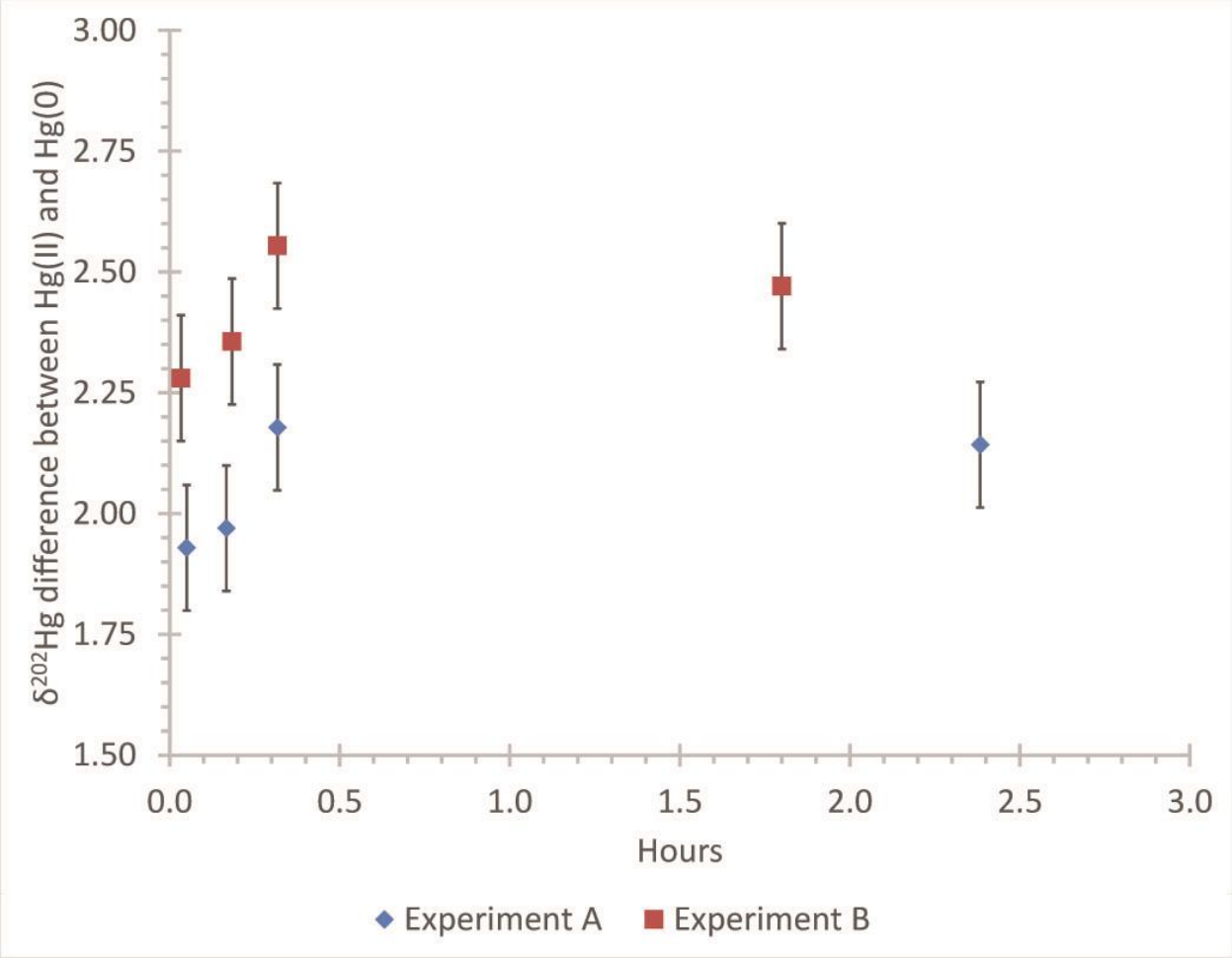

Figure B.3. Difference between the Hg(II) fraction and the Hg(0) in experiments A (diamonds) and B (squares) versus time post injection (hours).